Mechanistic modelling of heat and mass transfer in processing of solid and semi-solid foods

Rabeler, Felix

Publication date:
2020

Document Version
Publisher's PDF, also known as Version of record

DTU Food
National Food Institute

Mechanistic modelling of heat and mass transfer in processing of solid and semi-solid foods

Felix Rabeler

PhD Thesis

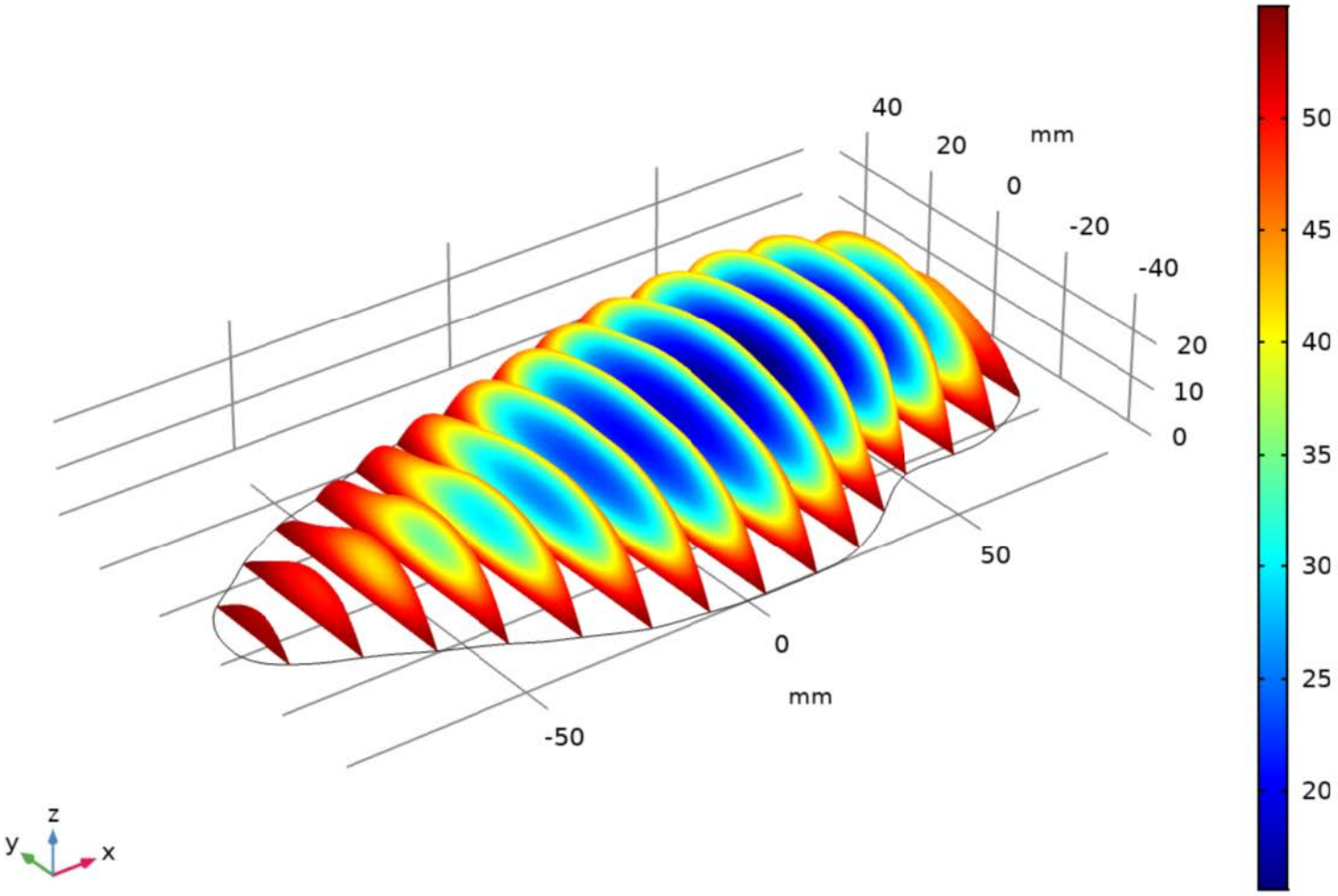

Mechanistic modelling of heat and mass transfer in processing of solid and semi-solid foods

PhD Thesis

Felix Lennart Rabeler

National Food Institute

Research Group for Food Production Engineering

Technical University of Denmark

March 2020

Title:	Mechanistic modelling of heat and mass transfer in processing of solid and semi-solid foods
Author:	Felix Lennart Rabeler
Affiliation:	National Food Institute Technical University of Denmark (DTU) Research Group for Food Production Engineering Søltofts Plads, 2800 Kgs. Lyngby, Denmark
E-mail:	felra@food.dtu.dk/ felix.rabeler@gmx.net
Principal Supervisor:	Associate Professor Aberham Hailu Feyissa
Second Supervisor:	Associate Professor Mohammad Amin Mohammadifar
Assessment committee:	Timothy John Hobley, PhD (Associate Professor, DTU) Dagbjørn Skipnes, PhD (Senior Scientist, Nofima, Norway) Bent Sarup, PhD (Vice President Global Sales, Edible Oil Systems, Alfa Laval Copenhagen A/S)
PhD enrollment:	01st of May 2017
Submitted:	13th of March 2020
Front Page:	Model prediction of the spatial texture (hardness) distribution inside a whole chicken breast after 10 min of roasting with hot air (T_{oven} = 200 °C, high fan speed).

Preface and acknowledgments

This PhD thesis is a synopsis of my PhD project, which I accomplished at the National Food Institute, Research Group for Food Production Engineering, Technical University of Denmark. I carried out my PhD project in the period from 1st of May 2017 to 13th of March 2020 under the supervision of Associate Professor Aberham Hailu Feyissa and Associate Professor Mohammad Amin Mohammadifar.

I would especially like to thank my supervisors Aberham and Amin for their support, guidance and advice throughout my whole PhD project. Without the countless discussions, brilliant ideas and numerous inspirations, this thesis would not have been possible. It was my deepest pleasure to work with both of you on that project.

I would further like to thank Jacob Lercke Skytte for helping me with the analysis of my data as well as creating great ideas for the project. Thanks to Nina Gringer for the highly appreciated help with the Danish translations in this work and the relaxed lunch times. Thanks also to all my other colleagues in the Division, especially in the research group for Food Production Engineering for the positive, supportive and inspiring atmosphere. It was a pleasure to work with all of you.

Finally, I would like to express my deepest gratitude to Mama, Papa, Chrissi and my fiancée Teresa for their great support as well as to my kids Maira and Eskil for putting a smile on my face even after the toughest days. I am so glad to have you in my life.

Copenhagen, March 2020

Felix Rabeler

Abstract

The heating of solid and semi-solid foods is a complex process that comprises coupled heat and mass transfer in a continuously changing porous medium. The irreversible changes in the composition, microstructure and other physical food properties during the heating process affect directly or indirectly the food quality such as texture, taste or appearance. In order to optimize existing heating processes and develop sustainable, healthy and high-quality food products, a quantitative knowledge about the mechanisms that lead to the physical and chemical changes is required.

The aim of my PhD project was to develop a mechanistic model of heat and mass transfer and couple it with kinetic models to predict the quality changes of solid and semi-solid foods during thermal processing.

Based on the conservation of mass and energy, we developed a mechanistic model of heat and mass transfer for the roasting of chicken breast meat from first principles, thoroughly considering the physical phenomena as well as natural variations in the chicken breast size and shape. A detailed description of the heat and mass transfer during the roasting process should include the dynamic changes of the chicken meat microstructure and physical properties. Therefore, we established semi-empirical correlations that describe the structural properties (i.e. storage modulus) and thermophysical properties (i.e. specific heat capacity and thermal conductivity) of chicken breast meat as function of the temperature and moisture content. This enabled us to predict precisely the temperature and moisture content profiles inside the chicken breast meat during the roasting process, which also agreed well with experimental data.

In order to predict the quality changes of chicken breast meat during roasting, we established kinetic models for the texture and color changes as function of the temperature and heating time by modifying the general rate law, taking the non-zero equilibrium of food quality attributes into account. Coupling the mechanistic model of heat and mass transfer with the kinetic models then enabled us to study the influence of the local temperature and moisture content changes on the spatial texture and color

development. Accordingly, the direct influence of the process parameters on the spatial quality changes was obtained.

This model of combined transport phenomena and quality kinetics provides a quantitative understanding of the phenomena that lead to the quality changes of chicken breast meat during the roasting process. It can be used as a knowledge-based decision tool to optimize the heating process with the aim of the highest possible food quality for the consumer.

Dansk Resumé

Opvarmning af faste og halvfaste fødevarer er en kompleks proces, der omfatter kombineret varme- og masseoverførsel i et konstant skiftende porøst medium. De irreversible ændringer i sammensætningen, mikrostrukturen og andre fysiske fødevareegenskaber under opvarmningsprocessen påvirker direkte eller indirekte fødevarekvaliteten, herunder struktur, smag og udseende. For at optimere eksisterende opvarmningsprocesser og udvikle bæredygtige, sunde fødevareprodukter af høj kvalitet, kræves en kvantitativ viden om de mekanismer der fører til de fysiske og kemiske ændringer.

Målet med mit ph.d.-projekt var derfor at udvikle en mekanistisk model for varme- og masseoverførsel og sammenkoble den med kinetiske modeller for at forudsige kvalitetsændringerne af faste og halvfaste fødevarer under termisk forarbejdning.

Baseret på bevarelse af masse og energi, udviklede vi en mekanistisk model for varme- og masseoverførsel til stegning af kyllingebrystkød ud fra de første principper, under grundig overvejelse af de fysiske fænomener såvel som naturlige variationer i kyllingebrystets størrelse og form. En detaljeret beskrivelse af varme- og masseoverførsel under stegeprocessen skal omfatte de dynamiske ændringer i mikrostrukturen af kyllingekødet og de fysiske egenskaber. Derfor etablerede vi semi-empiriske korrelationer, der beskriver de strukturelle egenskaber (dvs. reologiske parametre) og termofysiske egenskaber (dvs. specifik varmekapacitet og varmeledningsevne) af kyllingebrystkød som funktion af temperaturen og vandindholdet. Dette gjorde det muligt at forudsige de præcise temperatur- og vandindholdsprofiler inde i kyllingebrystkødet under stegningen, hvilket stemte godt overens med de eksperimentelle data.

For at forudsige ændringer i kvaliteten af kyllingebrystkød under stegning, etablerede vi kinetiske modeller for struktur- og farveændringer, som funktion af temperaturen og opvarmningstiden. Dette opnåede vi ved at ændre den generelle hastighedslov så den inkorporerede en ligevægt, forskellig fra nul, af forskellige fødevarekvalitetsparametre. Ved at kombinere den mekanistiske model for varme- og masseoverførsel med de

kinetiske modeller blev det muligt at undersøge påvirkningen af de lokale temperatur- og vandindholdsændringer på den rumlige struktur, samt at undersøge farveudviklingen. Herved opnåedes den direkte påvirkning af procesparametrene på de rumlige kvalitetsændringer.

Denne model af kombinerede transportfænomener og kvalitetskinetik giver en kvantitativ forståelse af de fænomener, der fører til kvalitetsændringer af kyllingebrystkød under stegning. Det kan bruges som et vidensbaseret beslutningsværktøj til at optimere opvarmningsprocessen med det formål at opnå den bedst mulige fødevarekvalitet for forbrugeren.

Table of contents

List of publications

Publication 1:

Rabeler, F., & Feyissa, A. H. (2018). Kinetic modeling of texture and color changes during thermal treatment of chicken breast meat. *Food and Bioprocess Technology*, *11*(8).

DOI: https://doi.org/10.1007/s11947-018-2123-4

Publication 2:

Rabeler, F., & Feyissa, A. H. (2018). Modelling the transport phenomena and texture changes of chicken breast meat during the roasting in a convective oven. *Journal of Food Engineering*, *237*.

DOI: https://doi.org/10.1016/j.jfoodeng.2018.05.021

Publication 3

Rabeler, F., & Feyissa, A. H. (2019). Modelling of food processes under uncertainty: Mechanistic 3D model of chicken meat roasting. *Journal of Food Engineering*, *262*, 49–59.

DOI: https://doi.org/10.1016/j.jfoodeng.2019.05.006

Publication 4

Rabeler, F., Skytte, J. L., & Feyissa, A. H. (2019). Prediction of thermal induced color changes of chicken breast meat during convective roasting: A combined mechanistic and kinetic modelling approach. *Food Control*, *104*.

DOI: https://doi.org/10.1016/j.foodcont.2019.04.018

Publication 5:

Rabeler, F., Skytte, J. L., & Feyissa, A.H. (2020). Mechanistic 3D modelling of solid foods with varying shape and size using statistical shape analysis: roasting of whole chicken breast meat. *Submitted to Food Engineering Reviews.*

Symbols and Abbreviations

A	Fitting parameter Arrhenius equation	
a_w	Water activity	
B	Fitting parameter Arrhenius equation	
$b(T)$	Weibull coefficient	1/s
C_{eq}	Equilibrium water holding capacity	kg/kg
C_i	Mass concentration	kg/kg
$c_{p,i}$	Specific heat capacity	J/(kg K)
D	Diffusion coefficient	m^2/s
E_a	Activation energy	J/mol
G'	Storage modulus	Pa
k	Reaction rate constant	$[Q]^{1-n}/s$
k_0	Pre-exponential factor	$[Q]^{1-n}/s$
k_i	Thermal conductivity	W/(m K)
M	Number of input parameters	
M_i	Molar mass	kg/mol
m	Fitting parameter Weibull equation	1/K
N	Number of samples	
n	Reaction order	
$n(T)$	Weibull coefficient	
p	Pressure	Pa
p_v	Water vapor partial pressure	Pa
Q	Quality attribute	[Q]

Q_v	Heat source or sink	W/m^3
r	Reaction rate	[Q]/s
R	Universal gas constant (8.314 J/(mol K))	J/(mol K)
R_i	Species source	
t	Time	s
T	Temperature	K
T_c	Fitting parameter Weibull equation	K
u	Fluid velocity	m/s

Greek symbols

β	Mass transfer coefficient	m/s
ε	Emissivity	
θ	Sample matrix	
κ	Permeability	m^2
μ	Dynamic viscosity	Pa s
ρ_i	Density	kg/m^3
ϕ_i	Volume fraction	

Subscripts

0	Initial condition (t = 0s)
air	Surrounding air
cm	Chicken breast meat
p	Product
surf	Surface

w	Water
wall	Oven wall

Abbreviations

FDM	Finite difference method
FEM	Finite element method
FVM	Finite volume method
LHS	Latin Hypercube sampling
OAT	One-at-a-time
ODE	Ordinary differential equation
PDE	Partial differential equation
WHC	Water holding capacity
SSM	Statistical shape model
SRC	Standardized regression coefficient
TPA	Texture profile analysis

1 Introduction

The thermal processing of solid and semi-solid foods is an essential step in domestic and professional kitchens as well as in the industrial scale production. The heating procedure ensures primarily the safety, palatability and digestibility of the food product, though it concomitantly has a direct influence on the quality of the final product (for example the texture or appearance) and with it on the acceptance by the consumer. Therefore, a detailed understanding of the heating process and the induced transformations of a food is crucial for optimizing the heating process and its productivity without compromising the food quality and safety (Datta, 2015).

However, especially the quality of cooked food products is still relying on the so-called cook-and-a-look approach and, thereby, on the knowhow of the cook or machine operator. This knowledge is mainly derived by empirical tests, from empirical databases or industrial handbooks, which are used to design, plan and control the process (Ivester, 2008). However, the experimental work that is needed to create this knowledge and/ or large databases is highly time consuming as well as technically and economically expensive. Furthermore, experimentation alone does not provide a detailed understanding of the different changes that food products undergo during the heat processing and how these are linked to the food quality (Datta, 2015). As a consequence, the development of new food products or processes is slowed down, which results in a lack of innovation in the food sector to fulfill the fast changing demands of the consumers for healthier, environmentally friendlier but yet tastier foods (Jousse, 2008).

The target of my PhD study was to use mathematical models to obtain the quantitative understanding of the phenomena that lead to the quality changes of solid and semi-solid food product during heating. I have used the convective roasting (with hot, dry air) of chicken breast meat as a representative case in my PhD project. This was done as the worldwide demand and consumption of chicken breast meat has been increasing considerably faster compared to other types of meat (OECD, 2020). Thus, optimized heating processes are necessary to ensure the highest possible quality for the consumer. Moreover, a first literature review revealed that there has not been

established a mechanistic model of chicken meat roasting with hot air and resulting quality changes, which made it a perfect food product for this study. However, the established framework can be applied to other meat products as well as to different other types of foods (**Chapter 8**).

In **Chapter 2** to **Chapter 4** I provide the background of my PhD thesis by reviewing and discussing the kinetic modelling of food quality changes during heating processes (**Chapter 2**), the formulation of physical based models of heat and mass transfer for the thermal processing of solid and semi-solid foods (**Chapter 3**) as well as the possibilities to evaluate the reliability of established models with uncertainty and sensitivity analysis (**Chapter 4**). The hypothesis and detailed objectives of my work are then given in **Chapter 5**. In **Chapter 6**, our own results from the PhD project are presented in the form of completed research publications (five in total), followed by the summary and general discussion of these in **Chapter 7**. Finally, the conclusion of my PhD project is given in **Chapter 8** together with the future perspective.

2 Kinetic modelling of quality changes

The thermal treatment of solid and semi-solid food has a direct impact on its quality. However, the quality of most food products is still relying on trial and error. Therefore, a more systematic way of studying the influence of the heating process and its parameters on the quality changes is necessary (Van Boekel, 2008). If a general understanding of the relationship between compositional and microstructural changes during heating and correlated quality degradation is achieved, a quantitative knowledge based process control and optimization would be possible. Mathematical models can provide this fundamental understanding and are therefore an essential tool to ensure the highest possible food quality and with it the satisfaction of the consumer (Ling et al., 2015).

In general, four different food quality factors can be distinguished (Bourne, 2002): the appearance (e.g. the color, shape or size), the flavor (e.g. taste and odor), the texture (e.g. physical touch, sight or sound) and nutritional value (e.g. composition, vitamins or minerals). In this study, I have focused on the appearance, specifically on the color, as well as the texture (**Publication 1**). This was done as the appearance of cooked foods is the first quality attribute that the consumer appraises (Guerrero-Legarreta and Hui, 2010), while the texture is rated as the overall most important quality attribute (Lawrie and Ledward, 2006).

Quality attributes of foods are usually changing with time. Kinetic models are therefore necessary to describe the quality degradation of foods during processing (Van Boekel, 2008). In this manner, kinetic modelling can provide a deeper understanding of the mechanisms that lead to the quality changes, predict the possible food quality outcome from the process settings as well as help to control and optimize the heating process by choosing the right process parameters (Haefner, 2005).

Kinetic models are applied to describe the time dependent quality changes due to chemical (e.g. Maillard reactions), biochemical (e.g. enzymatic reactions), microbial (e.g. growth or inactivation of microbes) or physical (e.g. texture degradation) reactions (Van Boekel, 2008). For the irreversible change of a quality attribute Q with

time, the so-called general rate law for a single reactant is most often used in food science (Eq. (1)):

$$r = -\frac{dQ}{dt} = kQ^n \quad (1)$$

With r the rate of the reaction ([Q]/s), Q the quality attribute ([Q]) at time t (s), k the reaction rate constant ([Q]$^{1-n}$/s) and n the reaction order.

Researchers most often assume zero-, first or second order kinetics to describe the change in food quality with time. For a zero-order reaction (n = 0) the integration of Eq. (1) leads to (Eq. (2)):

$$\frac{dQ}{dt} = -k \quad \Rightarrow \quad Q = Q_0 - kt \quad (2)$$

For a first order reaction (n = 1):

$$\frac{dQ}{dt} = -kQ \quad \Rightarrow \quad Q = Q_0 exp(-kt) \quad (3)$$

For a second order reaction (n = 2):

$$\frac{dQ}{dt} = -kQ^2 \quad \Rightarrow \quad Q = \frac{Q_0}{1+Q_0 kt} \quad (4)$$

with Q_0 the initial quality attribute at t = 0.

To proof that a reaction is following a first or second order, Eq. (3) and Eq. (4) are linearized using a logarithmic or inverse transformation, respectively, which leads to the following forms:

n = 1: $Q = Q_0 exp(-kt) \quad \Rightarrow \quad ln(Q) = ln(Q_0) - kt$ (5)

n = 2: $Q = \frac{Q_0}{1+Q_0 kt} \quad \Rightarrow \quad \frac{1}{Q} = \frac{1}{Q_0} + kt$ (6)

The plot of the transformed experimental data (ln(Q) or 1/Q for a first or second order, respectively) against the time should then follow a straight line. However, as

highlighted by Van Boekel (2008), the linearized forms should not be used to estimate the kinetic parameters, but for the visual check of the reaction order only. During the data transformation, the structure of the experimental error could be modified and consequently, the assumptions (error is normally distributed) that are made for the regression analysis could be violated. This could result in a bias during the parameter estimation and consequently to a prediction error (Van Boekel, 1996). Instead, the non-linear forms (Eq. (3) and Eq. (4)) or preferable the differential form (ordinary differential equation, ODE) of the reaction rate law (Eq. (1)) should be used for the parameter estimation. The latter has the advantage that the reaction order *n* can be estimated together with the other kinetic parameters, instead of relying on assumptions (Van Boekel, 2008).

The temperature dependency of the reaction is most often modelled using the Arrhenius equation (Peleg et al., 2002). It relates the reaction rate constant *k* in Eq. (1) directly to the absolute temperature (Eq. (7)):

$$k = k_0 \, exp\left(-\frac{E_a}{R\,T}\right) \tag{7}$$

with k_0 the pre-exponential factor, E_a the activation energy (J/mol), T the temperature (K) and R the universal gas constant (8.314 J/(mol K)). The activation energy can be interpreted as the minimum amount of energy that is needed to start the physical or chemical reaction. In this manner, it gives an indication of the temperature sensitivity of the reaction.

Similar to the first order reaction, the Arrhenius equation can be linearized using the natural logarithm (Eq. (8)):

$$ln(k) = ln(k_0) - \frac{E_a}{R\,T} \tag{8}$$

The linearized form can then be used to visually inspect if the Arrhenius equation can be used to describe the temperature dependency (the plot of ln(*k*) against 1/T should give a straight line). However, similar as before, the non-linear form of the Arrhenius equation (Eq. (7)) should be used for the parameter estimation (Van Boekel, 2008).

The combination of the reaction rate law (Eq. (1)) and the Arrhenius equation (Eq. (7)) leads then to (Eq. (9)):

$$\frac{dQ}{dt} = -k_0 \, exp\left(-\frac{E_a}{R\,T}\right) \, Q^n \tag{9}$$

For the estimation of the kinetic parameters E_a and k_0 it is beneficial to fit the data to the combined form (Eq. (9)) instead of using a two-step parameter estimation procedure (first k in Eq. (1) and afterwards E_a and k_0 in Eq. (7)) as normally a more precise prediction is achieved (Van Boekel, 2008).

Besides the Arrhenius equation, researchers proposed different modifications of it in the form of Eq. (10) (Van Boekel, 2008):

$$k = A \, exp\left(-\frac{B}{T}\right) \tag{10}$$

with A and B as fitting parameters without a direct physical meaning. These parameters are then described for example as function of moisture content or water activity to obtain a better description of the experimental data (Broyart et al., 1998; Purlis and Salvadori, 2009a).

Another possibility to describe the temperature dependency of quality degradation reactions in food science is the Weibull model, an empirical model that was supposed by Peleg et al., (2002) in the following form (Eq. (11)):

$$\frac{Q}{Q_0} = exp(-b(T) \, t^{n(T)}) \tag{11}$$

with the temperature dependent coefficients $b(T)$ and $n(T)$. Peleg et al. (2002) used an empirical relationship to describe the temperature dependency of $b(T)$ (Eq. (12)):

$$b(T) = ln\big(1 + exp\big(m(T - T_c)\big)\big) \tag{12}$$

where m and T_c are constant fitting parameters.

Researchers have successfully applied both Arrhenius type of equations (Eq. (7) or Eq. (10)) (e.g. Ovissipour et al. (2013) or Jobe et al. (2016)) as well as the Weibullian

power law (Eq. (11)) (e.g. Kong et al. (2007) or Halder et al. (2007)) to describe the temperature dependence of food quality changes. In general, the model that has the lowest number of coefficients (simplicity of the model) with the lowest deviation between the experimental observations and the model predictions should be chosen (Saguy and Karel, 1980). Furthermore, formulations which involve parameters with a physical meaning or relationship, such as the activation energy (E_a) in the Arrhenius equation (Eq. (7)), should be preferred compared to pure empirical equations, as a more fundamental understanding is obtained. This could also help to apply the kinetic model to other food products.

Compared to chemical reactions, most food products retain a measurable, non-zero degree of quality, such as texture or color, even after prolonged heating times (Rizvi and Tong, 1997). However, the common rate law as described by Eq. (1) does not consider this. To overcome this issue, Rizvi and Tong (1997) proposed the fractional conversion model for a first order kinetic in the following form (Eq. (13)):

$$ln(1-f) = ln\left(\frac{Q_t - Q_\infty}{Q_0 - Q_\infty}\right) = -k\,t \qquad (13)$$

where Q_∞ is the final non-zero equilibrium quality value after long heating times and f the quality index as defined by Eq. (14):

$$f = \frac{Q_0 - Q}{Q_0 - Q_\infty} \qquad (14)$$

In food science, different researchers showed that by using Eq. (13), an improved accuracy in describing the quality changes can be achieved (Kong et al., 2007; Rizvi and Tong, 1997; Thussu and Datta, 2012).

However, the reported fractional conversion form by Rizvi and Tong (1997) (Eq. (13)) to describe food quality changes with a non-zero equilibrium was not derived mathematically from the general rate law (Eq. (1)). It was instead proposed on the integrated rate law for a first order reaction (Eq. (3)) by substituting Q/Q_0 with $(1-f)$. For chemical reactions, where Q_∞ is 0, the fractional conversion form, also known as the extent of reaction, can be gained by substituting Q in the general rate law (Eq. (1)) in

terms of *f* (Atkins and de Paula, 2014). Conversely, most food quality changes retain a non-zero equilibrium ($Q_\infty \neq 0$) and, consequently, it is not possible to directly substitute *Q* in Eq. (3) in terms of *f* (from Eq. (14): $Q = Q_0 - f(Q_0 - Q_\infty)$) to obtain the desired fractional conversion form (Eq. (13)). Additionally, to transform the kinetic model from Eq. (3) to Eq. (13) the assumption has to be made that the random error associated with the data must be multiplicative and not additive (lack of variance homogeneity). However, for most cases it is difficult to distinguish the type of the random error associated with the experimental data (Van Boekel, 1996). Accordingly, if the error type (e.g. multiplicative or additive) is not clear, the transformation might be inappropriate and accordingly, the reliability of the fractional conversion model is questionable. Thus, another kinetic formulation that takes the non-zero equilibrium quality value of food products into account is necessary.

In summary, kinetic models can be a great tool to obtain the fundamental understanding of quality changes during the thermal treatment of foods. However, the handling of non-zero food quality equilibriums is still relying on assumptions made during the model development process, such as the order of the reaction. Thus, a more general description of quality changes with or without a non-zero equilibrium is needed to increase the accuracy and reliability of quality predictions (**Section 7.1.2**). Furthermore, the quality development is dependent on the entire temperature-time history. Therefore, a detailed knowledge about the spatial temperature distribution is necessary to predict the local quality changes as function of the process settings. However, this information cannot be gained by experimentation alone, where temperature measurements can be typically performed at a few specific points only (e.g. the geometric core). Therefore, a different approach is needed to enhance our knowledge about the mechanisms that lead to the spatial quality changes during thermal processing (**Section 7.1**).

3 Mechanistic modelling

The mathematical description of food processes is a continuously growing research field in food technology (Datta, 2008). In general two different types of models can be distinguished: 1) Empirical models and 2) Physics based models (Halder et al., 2011; Wedzicha and Roberts, 2006). Empirical or observation based models describe the direct relationship between inputs (e.g. process settings) and outputs (e.g. safety or quality), without attempting to relate the possible relationship to physical phenomena. Most often the experimental obtained data is fitted to a mathematical expression (e.g. polynomial equations) using appropriate statistical tools, treating the whole process as a black box. As no detailed knowledge about the physical processes is needed, observation based models can be developed in relative short times without a more specified training (compared to physical based models) (Sablani, 2008). This makes them also the most common type of models in the food industry, helping to characterize and control food process systems (Wedzicha and Roberts, 2006). However, observation based models are developed for specific processing conditions and food products. Therefore, they are only valid in the range of the used experimental data to build the model. Generalization or extrapolation to different other cases (e.g. other food products or process settings) is difficult and associated with high risks, restricting the use of observation based models (Erdogdu et al., 2017; Sablani, 2008).

In contrast, physics based models, also called mechanistic models, do not necessarily need experimental data as a starting point. Instead, they are based on fundamental physical laws, such as the conservation of mass, energy or momentum, capturing the observed physical phenomena as accurate as possible (Datta, 2008). Mechanistic models that describe the transport phenomena during food processing require typically the combination with empirical, yet, accepted universal rate laws, such as Fourier's and Darcy's law, why they are often referred as grey-box or hybrid models (Balsa-Canto et al., 2016; Datta, 2008). As mechanistic models are developed from first principles, they are more flexible than observation based models, allowing for example the assessment of different geometries, process conditions or product formulas (Trystram, 2012). At the same time, the model solutions are more reliable and

advances our understanding of the physical process, which cannot be gained by pure experimentation (Datta, 2008).

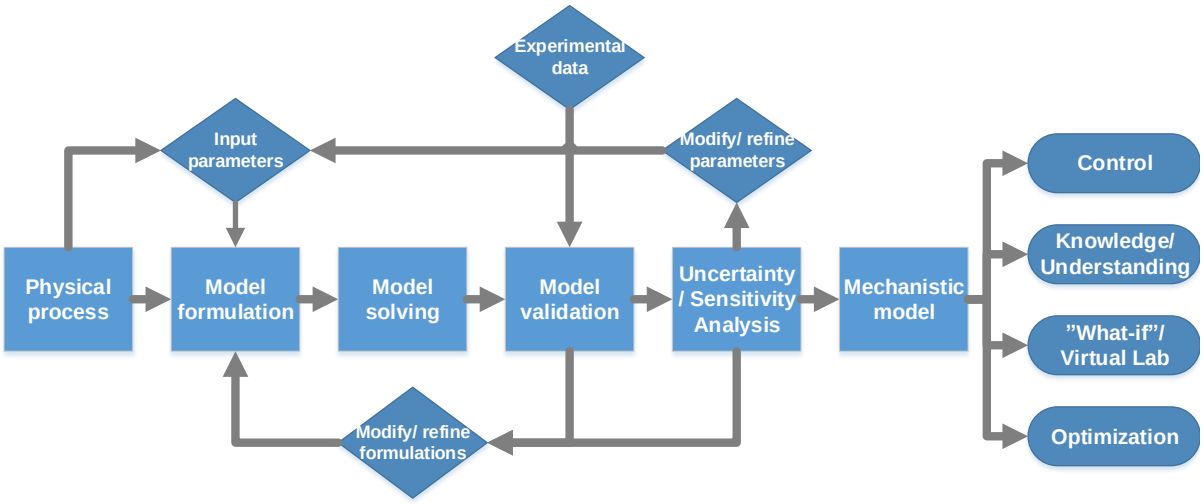

Figure 1: Framework of mechanistic modelling steps – From physical process observations to a validated mechanistic model

The first step during the development of mechanistic models is to observe the physical phenomena that occur during the process in order to obtain a qualitative understanding (see Figure 1). However, this is most often a challenging task for food processes, where not all phenomena are completely understood, yet (Trystram, 2012). The development time for mechanistic models is, therefore, typically much longer compared to observation based models and it usually requires specialized trainings (Datta, 2015; Sablani, 2008).

During the model formulation the observed physical processes are then expressed as a system of mathematical equations, often a set of coupled partial differential equations (PDEs) (see **Section 3.1**), which cannot be solved analytically. Instead, numerical methods such as the finite volume (FVM), finite difference (FDM) or finite element method (FEM) has to be used for solving the model. In engineering applications, including mathematical models, the latter one, FEM, is the most common and powerful technique to solve coupled PDEs numerical (Chaskalovic, 2008).

Before the established model can be further used, it should be validated using experimental data from varying processes conditions (Erdogdu et al., 2017) and the model formulations (e.g. model assumptions) modified or refined if necessary. Furthermore, uncertainty and sensitivity analysis should be integrated to ensure the reliability of the established model (see **Chapter 4**). Once established, physics based models allow the performance of “what-if” scenarios, reducing the time for experimental work and consequently speeding up the whole research and development process. Furthermore, modelling can increase the productivity due to enhanced process control and optimization possibilities, while at the same time maximizing the quality of the food product (Datta, 2008; Erdogdu et al., 2017). Overall, mechanistic models can increase the competiveness of food manufacturer as well as process designers by the development of highly automated and intelligent processing machines (Datta, 2015).

However, the use of mechanistic models in the food sector (e.g. research, education or industrial application) is still underdeveloped compared to other disciplines, such as chemical engineering, automotive or aerospace industry (Datta, 2015; Erdogdu et al., 2017). Reasons for this are the complexity of the physical phenomena that occur during the heating of food products, the biological variability of food materials as well as the drastic changes the food material properties (e.g. thermophysical and structural properties) go through during the heating. This also restricts the use of off-the-shelf simulation software for food process modelling as it is most often too specialized and unable to cope with the complexity of food processing (Datta, 2015).

Nevertheless, due to the considerable advantages, mechanistic models will take a keystone in the field of food engineering and should be the choice in the long term (Datta, 2008; Erdogdu et al., 2017). Therefore, I have also focused in my PhD project on the development of a mechanistic model for the convective roasting of chicken breast meat (see **Chapter 1**).

In the following sections, the basic mathematical description of the heat and mass transfer (governing equations) during heating processes is described (**Section 3.1**) as well as the importance of the used food geometry discussed (**Section 3.2**). For a detailed review of already established models as well as frameworks that can be

applied to describe the heat and mass transfer during food cooking processes, the reader is referred to Balsa-Canto et al. (2016), Datta (2015), Erdogdu et al. (2017) and Trystram (2012).

3.1 Heat and mass transfer

Thermal food processing, such as roasting, microwave heating, frying or drying, implicates coupled heat and mass transfer through a porous food product. The conservation of energy and mass are the basis to formulate the governing transport phenomena equations, while homogenization is typically applied to treat the food as continues material without information about the discrete pore size scale and distribution (Datta, 2015).

The conservation of energy leads to the governing equation of internal heat transfer, which is given by Eq. (15) (Bird et al., 2006):

$$\underbrace{c_{p,p}\,\rho_p\,\frac{\partial T}{\partial t}}_{accumulation} = \underbrace{\nabla\left(k_p\,\nabla T\right)}_{conduction} - \underbrace{\rho_w\,c_{p,w}\,u_w\,\nabla T}_{convection} \pm \underbrace{Q_v}_{generation} \tag{15}$$

with $c_{p,p}$ and $c_{p,w}$ the heat capacity (J/(kg K)) of the food product and water, respectively, ρ_p and ρ_w the density (kg/m^3) of the food product and water, respectively, k_p the thermal conductivity (W/(m K)) of the product, u_w the velocity (m/s) of the moving liquid (i.e. water) and Q_v is the heat source or sink (W/m^3).

The term on the left side of Eq. (15), the accumulation term, represents the rate at which the stored energy is changing. On the right side of Eq. (15), the first term (conduction term) represents the rate of energy transport due to conduction; the second term (convection term) describes the convective energy transport due to a fluid bulk motion (e.g. water) and the third term (generation term) represents the internal generation or dissipation of energy (e.g. evaporation/ condensation of water or conversion of electromagnetic energy in volumetric heating).

The thermophysical properties density (ρ), heat capacity (c_p) and thermal conductivity (k) in Eq. (15) are important parameters to describe the transport of heat through the porous food medium. However, during the heating process the physical food

properties are continuously changing due to changes in the compositions, structure and temperature (Choi and Okos, 1986), which need to be incorporated to ensure a realistic prediction (Datta, 2008). Different options exist to describe the development of physical food properties during processing and a recent review by Gulati and Datta (2013) gives a comprehensive summary of possible approaches.

The most common method to incorporate the dynamic changes of the thermophysical food properties is to describe them as function of temperature and composition in the following forms (Eq. (16) to Eq. (19)) (Choi and Okos, 1986; Gulati and Datta, 2013).

Density $\frac{1}{\rho_p} = \sum_i \frac{x_i}{\rho_i}$ (16)

Heat capacity $c_{p,p} = \sum_i x_i c_{p,i}$ (17)

Thermal conductivity $k_{p,\parallel} = \sum_i \phi_i k_i$ *(parallel model)* (18)

$\frac{1}{k_{p,\perp}} = \sum_i \frac{\phi_i}{k_i}$ *(perpendicular model)* (19)

with x_i and ϕ_i the mass and volume fraction of the individually components *i* (i.e. water, fat, protein, carbohydrates and ash), respectively. For the thermal conductivity, the parallel model as described by Eq. (18) ($k_{p,\parallel}$) represents the higher limit of the thermal conductivity, while the perpendicular model, given by Eq. (19) ($k_{p,\perp}$) gives the lower limit (Rao et al., 2014). However, as the property estimations are relying on empirical correlations reported by Choi and Okos, 1986, the thermophysical parameters should be taken into account for the uncertainty and sensitivity analysis (see **Chapter 4**).

The transfer of energy from the surrounding towards the products surface (boundary) depends on the used process and process settings. To describe the heat transfer boundary conditions, three mechanisms can be distinguished: conduction, convection and radiation. Conductive heat transfer describes the energy transport between two or more surfaces that are in direct contact with each other, for example in pan-frying. When a moving fluid (i.e. air) is surrounding the food, energy is transferred by convection to the surface. Radiative heat transfer describes the transport of

electromagnetic energy from one surface to another and the conversion to thermal energy (Bird et al., 2006).

The heat transfer by convection is typically described using Newton's law of cooling, while the Stefan-Boltzmann law describes the radiative heat transfer (Eq. (20)):

$$-n.\left(\nabla\left(k_p\,\nabla T\right)-\rho_w\,c_{p,w}\,u_w\,\nabla T\right)=\underbrace{h\left(T_{air}-T_{surf}\right)}_{Convection}+\underbrace{\varepsilon\sigma({T_{wall}}^4-{T_{surf}}^4)}_{Radiation} \qquad (20)$$

with h the heat transfer coefficient (W/(m^2 K)), T_{air} the temperature of the surrounding air (K), T_{surf} the temperature of the food surface (K), T_{wall} the temperature of the surrounding walls (K), ε the emissivity of the food and σ the Stefan-Boltzmann-constant (5.67x10^{-8} W/(m^2 K^4)).

For the convective roasting of foods using hot dry air, convection is the predominant heat transfer mechanism compared to radiation and conduction. Therefore, researchers often use an effective heat transfer coefficient in Eq. (20), which takes the radiative and/ or conductive heat transfer into account (Kondjoyan and Portanguen, 2008; Sakin-Yilmazer et al., 2012; Zhang and Datta, 2006).

The governing equation for the mass transfer inside the porous food medium is based on the conservation of mass in the following form (Eq. (21)) (Bird et al., 2006):

$$\underbrace{\frac{\partial C_i}{\partial t}}_{accumulation}=\underbrace{\nabla(D\nabla C_i)}_{diffusion}-\underbrace{u_w\nabla C_i}_{convection}\pm\underbrace{R_i}_{generatoin} \qquad (21)$$

where C_i is the concentration (kg/kg sample) of the component (e.g. water), D is the diffusion coefficient (m^2/s) and R_i is the species source (kg/(kg s)).

The term on the left side of Eq. (21), the accumulation term, describes the rate at which the concentration is changing. On the right side of Eq. (21), the first term, diffusion term, represents the transport due to diffusion, the second term, convection term, describes the mass transport due to the bulk motion of a fluid (e.g. water) and the third term, generation term, represents the generation or consumption rate of the component (e.g. evaporation or condensation of water).

For a porous food medium with small pores the velocity u_w of the fluid (i.e. water) in Eq. (15) and Eq. (21) can be described using Darcy's law (Eq. (22)):

$$u_w = \frac{\kappa}{\mu_w} \nabla p \tag{22}$$

with κ the permeability (m^2), μ_w the dynamic viscosity of the fluid (Pa s) and p the pressure (Pa).

For muscle foods, such as chicken breast meat, the pressure in Eq. (22) is the driving force for the liquid water transport. The heating of the meat reduces the water holding capacity (WHC), which results in a release of liquid water into the pore space between meat fibers. The deformation of the food matrix (shrinkage) causes an internal pressure gradient and the expulsion of liquid water towards the products surface (Godsalve et al., 1977). The Flory-Rehner theory, which has been applied to food gels and biological tissues to describe the moisture transport, was adapted by van der Sman (2007) to derive the pressure (so-called swelling pressure) inside of meat products in the following form (Eq. (23)):

$$p = G'(C - C_{eq}(T)) \tag{23}$$

with G' the storage modulus (Pa) and C_{eq} the equilibrium water holding capacity, which is a function of the temperature (van der Sman, 2013). The approach was then also applied to other food materials such as vegetables (van der Sman et al., 2013).

The mass flux at the surface (boundary) of the food product due to water evaporation or condensation is typically written as (Eq. (24)):

$$n.\nabla(D\nabla C_i) - u_w \nabla C_i) = \beta \frac{M_w}{R} (\frac{p_{v,surf}}{T_{surf}} - \frac{p_{v,air}}{T_{air}}) \tag{24}$$

where β is the mass transfer coefficient (m/s), M_w the molar mass of water (kg/mol) and $p_{v,surf}$ and $p_{v,air}$ the partial water vapor pressure (Pa) at the food surface and surrounding air, respectively. The mass transfer coefficient is usually calculated from the air properties and the heat transfer coefficient using the Chilton-Colburn analogy (see **Publication 2** in **Chapter 5**). However, as reported by different researchers this

approach can result in an overestimation of the mass loss by the model. This is mainly related to a crust formation at the food boundary, which results in an extra resistance to moisture evaporation (Purlis and Salvadori, 2009b; van der Sman, 2013). Thus, different modifications to the Chilton-Colburn analogy or simple empirical approximations are used to obtain a better match with the experimental data (Llave et al., 2016; Lucas et al., 2015; Mondal and Datta, 2010; Purlis and Salvadori, 2009b; van der Sman, 2013). This should, however, be taken into consideration in the uncertainty and sensitivity analysis of the established model (see **Chapter 4**).

3.2 Geometry of the food product

Most foods do not have a uniform shape but an irregular 3-dimensional geometry. When developing mechanistic models of heat and mass transfer, the description and incorporation of the actual food geometry is an important step, as it is greatly influencing the temperature and moisture content profiles during the heating process. This becomes even more critically for the prediction of quality attributes (e.g. texture or color), as they are mostly linked to the spatial development of the state variables (Goñi and Purlis, 2010). Thus, exact food geometries should be used in mechanistic models and the influence of natural variations in the shape on the model predictions considered to obtain realistic and useful model predictions (Uyar and Erdoğdu, 2009).

However, the most common approach in modelling studies is to simplify the actual, irregular geometry of the food product by using regular shapes, such as spheres, slabs, cones, cylinders or similar (Feyissa, 2011; Isleroglu and Kaymak-Ertekin, 2016; Kumar et al., 2016; Mabrouk et al., 2012; Rakesh et al., 2012; Rinaldi et al., 2017; van der Sman, 2007). This can be mainly related to the difficulties to obtain the actual, irregular food geometry. Even with computer-aided design (CAD) programs, such as SolidWorks, PTC Creo or AutoCAD, it is challenging to precisely reconstruct the actual irregular shape of most food products including all geometric features (Goñi et al., 2007). In contrast, most commercial modeling software allow the construction of simple geometries without detailed previous knowledge and the computational time is typically lower compared to models that include highly irregular food shapes.

Nevertheless, different techniques were applied to obtain irregular food geometries for mathematical models, such as computer vision systems (Goñi and Salvadori, 2010; Jancsók et al., 2001; Purlis and Salvadori, 2009b), magnetic resonance imaging (Goñi et al., 2008) or x-ray computed tomography (Schoeman et al., 2016; Warning et al., 2014). However, all these techniques require a detailed knowledge including specialized training and their implementation is normally time consuming as well as expensive (Datta, 2015; Uyar and Erdoğdu, 2009).

Another possibility to obtain the 3D geometry of food products is the use of 3D scanners (Fabbri et al., 2011; Siripon et al., 2007; van der Sman, 2013). Many different 3D scanners, such as structured light or laser line scanners, are nowadays commercially available, providing high accuracies and details at relative low costs (Bternardini and Rushmeier, 2002). Compared to the methods named before, the 3D scanning of irregular foods is a user-friendly technique that does not require any specific prior knowledge and the generation of ready to use 3D geometries can be automated up to a certain degree (Uyar and Erdoğdu, 2009). Furthermore, it is possible to estimate for example the surface area or volume of the food product from the obtained 3D model, which could be used in additional analysis of the model predictions.

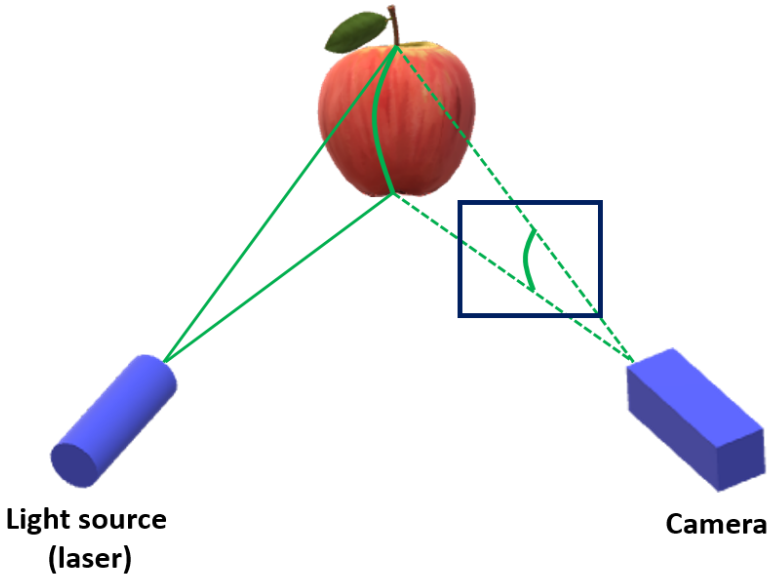

Figure 2: Principle description of a laser light triangulation system.

Most available 3D scanners are based on triangulation (see Figure 2). From a light source a spot, line or specific light pattern is projected on the object, from which the light is reflected. A detector, for example a CCD camera system, captures then the light reflection and, from the orientation and position of the lighting system, points in a 3D coordinate system are created. By rotating the object, for example with a turn table, points from all directions are detected and a 3 dimensional point cloud formed (Bernardini and Rushmeier, 2002). Afterwards, the point cloud can be meshed and finally imported into different software for further processing. As the entire scanning process is non-destructive, the scanned food object can be used afterwards, for example for validation trials.

Overall, mechanistic models enable a quantitative understanding of the heating process, which can be used for knowledge based process optimization instead of trial-and-error. As described before, a detailed understanding of the mechanisms that lead to the transfer of heat and mass through the food product is necessary to develop mechanistic models. However, for many food products, including the roasting of chicken breast meat, not all of these mechanisms are entirely explored, yet. Moreover, the physical parameters and their correlation with the observed phenomena are usually not available in the literature and need to be adapted from other food products or determined by experimentations. Additionally, the implementation of the complex and irregular shape of food products is important during the modelling development process. It can help to speed up the model developing process, leading to highly realistic model predictions. However, comprehensive studies that evaluate the influence of the food geometry on the model predictions is lacking. Furthermore, the shape and size of food products is not constant but it can varying considerably. The influence of this natural variation on the temperature, moisture content or quality distribution has not been taken into consideration, yet. 3D scanning combined with statistical tools could help to capture the shape variations of foods at relative low costs and consequently, the influence on the spatial model predictions could be studied (**Section 7.2**).

4 Uncertainty and sensitivity analysis

The uncertainty of mathematical models that describe any type food process is a critical issue that should be evaluated and addressed during the model development process (see Figure 1) (Datta, 2008; Feyissa, 2011). The uncertainty of a model can be divided into two groups: 1) uncertainty in the model formulation and 2) uncertainty in the model parameters (Sin et al., 2009). The first group is related to the assumptions and simplifications that are made during the development of the model, which are consequently influencing the overall structure of the model (e.g. which physical phenomena are included). This can directly result in a discrepancy between the model predictions and the experimental observations. By establishing the model from first principles, describing the observed physical phenomena as accurate as possible, the structural uncertainty can be reduced to a certain degree (Feyissa et al., 2012). Nevertheless, once the model is established, the assumptions and simplifications, made in the beginning of the modelling process, should be reviewed and if necessary changed to ensure the accuracy and reliability of the developed model (Figure 1).

The second group of uncertainty, the uncertainty in the model parameters, is especially in food science a major problem, due to the complexity and natural variability of foods (Feyissa et al., 2012). Most physical food properties are directly dependent on the temperature, composition (i.e. water, fat, protein, air), structure and state of the food (Datta, 2008). Even the foods origin (natural variability) and total processing history can have an influence. Thus, the experimental estimation of food properties is difficult, time expensive and the obtained values come usually with high variances (Gulati and Datta, 2013). Furthermore, with increasing complexity of the developed model, the amount of needed input parameters is increasing considerably (Feyissa, 2011). Not all of these parameters are readily available in literature or they have to be estimated from empirical correlations. The experimental variability as well as the lack of knowledge results finally in uncertainties in the model input parameters, which leads to an uncertainty of the model output (Feyissa et al., 2012). Consequently, it has a direct impact on the reliability of the established model.

To study the influence of the input uncertainty on the model output, different uncertainty analysis techniques are available, such as the Bayesian analysis (combined with optimization algorithms) or the Monte Carlo method (see **Section 4.1**) (Sin et al., 2009). These methods allow the identification of the uncertainty in the model predictions due to the variance in the model input parameters. However, no conclusion can be made, which uncertain input parameters contribute to the output uncertainty and to which degree (its magnitude). Thus, sensitivity analysis should be run in tandem with uncertainty analysis (Saltelli et al., 2007) (see **Section 4.2**). Sensitivity analysis techniques allow the determination of the relative impact of each input parameter uncertainty on the variance of the model outputs. Consequently, the key input parameters with the highest but also with the lowest relative influence on the model output can be identified and finally the input parameters ranked accordingly (Sin et al., 2009).

However, comprehensive uncertainty and sensitivity analyses of established models are lacking in the field of food process modelling (Datta, 2015; Feyissa et al., 2012). The following sections give an overview of different uncertainty and sensitivity analysis techniques as well as how these can benefit the modelling process.

4.1 Uncertainty analysis

The Monte Carlo method was established by Metropolis and Source (1949) and is a highly reliable and effective (computationally wise) uncertainty analysis method. Nowadays, it can be seen as the standard uncertainty analysis method in the field of engineering (Helton and Davis, 2003; Sin et al., 2009). Accordingly, I used it also in this project to evaluate the influence of the input uncertainty on the model output uncertainty. Following, the different steps of the Monte Carlo method are summarized. For a detailed description of the global uncertainty analysis method, the reader is referred to Feyissa et al. (2012); Helton (1993) or **Publication 3** in **Chapter 5**.

The Monte Carlo method includes 4 consecutive steps (Helton, 1993) and the workflow of the method is given in Figure 3 .

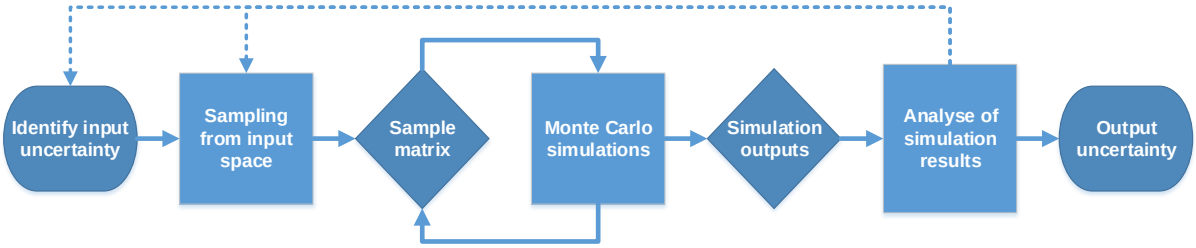

Figure 3: Workflow of the Monte Carlo method.

In the first step, the uncertain model input parameters are identified. Consequently, the range and distribution of the uncertainty for each input parameter is defined. One should be aware, that the choice of the input parameters as well as the corresponding uncertainty range is based on a subjective review process (experimental data, literature data as well as assumptions). Thus, an extra effort should be done to ensure that all uncertain input parameters are identified and their range is reasonable. Otherwise, the results of the analysis are difficult or not even possible to interpret (Helton, 1993; Saltelli et al., 2007).

In the second step, samples from the before defined input space are generated. Different sample techniques are readily available such as random sampling, Latin Hypercube sampling (*LHS*) or quasi-random sampling techniques, to name some (see Figure 4). For a large number of samples (*N*), no difference between the sampling methods should exist. However, with decreasing sample size, the coverage of the sample space is not the same for all sampling techniques. Random sampling normally results in the worst coverage of the sample space. Therefore, more samples are typically needed compared to for example the *LHS* method, which covers the input space better (see Figure 4). The most homogenous distribution is achieved by quasi-random sampling methods (Halton and Sobol sequence sampling in Figure 4). This shows that the sampling method could have an influence on the total number of samples needed for to ensure the reliability of the analysis. However, a comparison of sampling methods and their influence on the analysis is missing in the field of food process modeling.

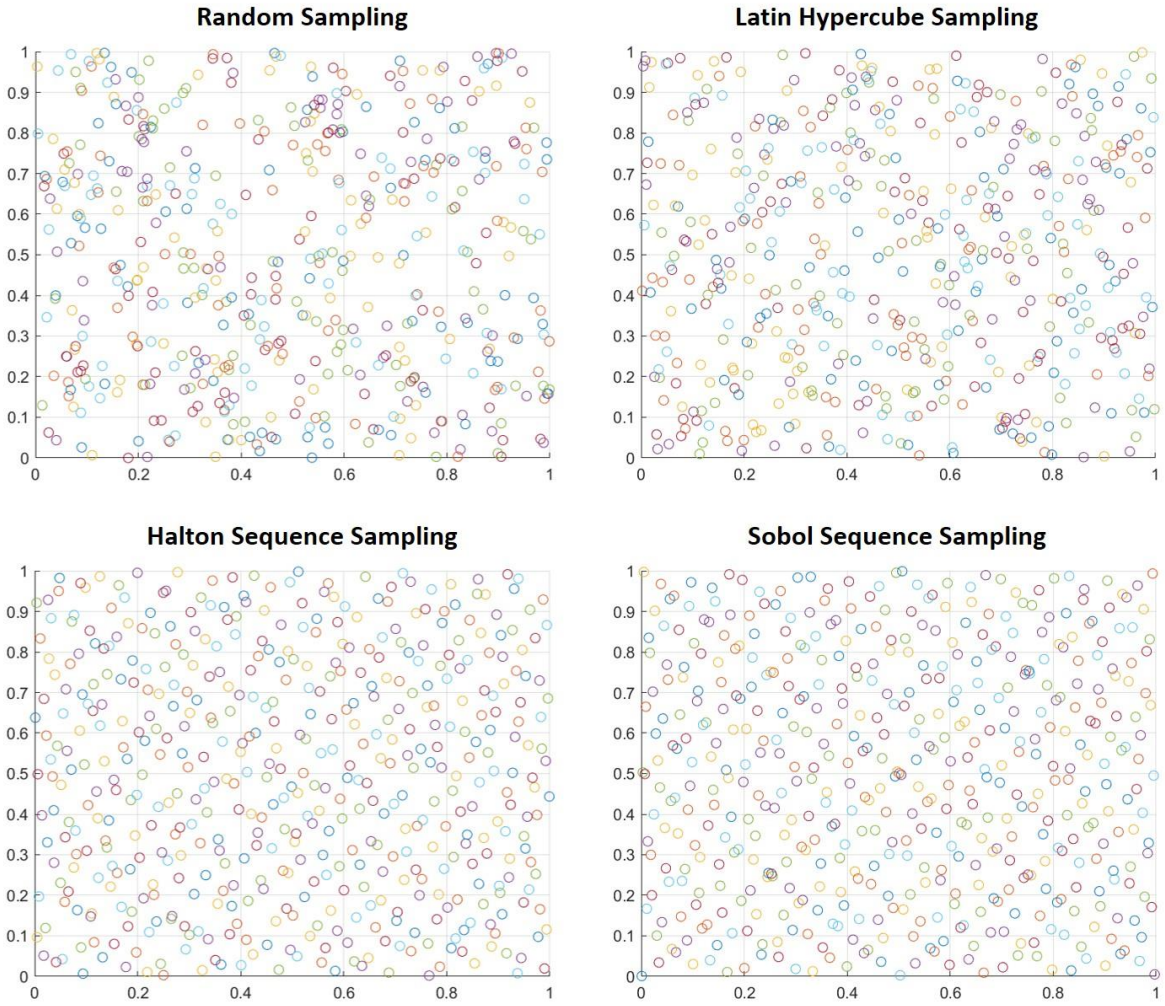

Figure 4: Comparison of different sampling techniques for a total of 500 samples with 12 input parameters: Random sampling, Latin Hypercube sampling, Halton sequence and Sobol sequence sampling.

In the third step, the sampling matrix θ_{NxM} from the second step is taken to perform *N* Monte Carlo simulations using the model (Feyissa et al., 2012). After each simulation step, the corresponding model outputs are stored for further processing.

In the fourth and last step, the results of the *N* simulation runs are evaluated. This can be done by simply plotting all the simulation runs (so-called spaghetti plots, (Sin et al., 2009)) and visually inspect them. Furthermore, the mean, the standard deviations as well as percentiles can be calculated and reviewed. If necessary, modifications of the

input parameter space (step 1) or sampling method (step 2) can be done and the whole analysis repeated (Figure 3).

Even though the Monte Carlo method is easy to implement in any type of software such as MATLAB® (The Mathworks Inc., Massachusetts, USA) or Python (Python Software Foundation (PSF), Delaware, USA), only few researchers in the field of food process modelling actually used it to study the uncertainty in their established models. For drying models, Defraeye et al. (2013) and Tanaka et al. (2008) for example used the Monte Carlo method to study the influence of varying or uncertain input parameters, highlighting the significant influence on the model predictions. Furthermore, Feyissa et al. (2012) evaluated the uncertainty of a 2D pancake-baking model, showing that the uncertainty in the model output is not constant but can vary with time. However, for convective roasting models that take the 3D geometry of the food product into account, a detailed uncertainty analysis is lacking. This is mainly due to the fact that computation times can be very long when the complexity of the model is increasing (Datta, 2015). Nevertheless, uncertainty analysis of the established model is a crucial step to ensure the safety and reliability of the model predictions. Thus, it should be included in the model development process (Figure 1).

4.2 Sensitivity analysis

Two types of sensitivity analysis can be distinguished: local and global techniques (Saltelli et al., 2007). The local sensitivity analysis method is based on first derivatives of a model output with respect to a model input. One uncertain input parameter is varied around its nominal value (typically, only small variations are used) and the corresponding impact on the model output is studied. As all other model input parameters are kept constant, this method is also called one-at-a-time analysis or short OAT-analysis (Dimov and Georgieva, 2010). OAT-methods require normally short computation times (i.e. only few model runs) and their integration is simple (Saltelli et al., 2007). However, local sensitivity methods, as the name already says, provide the user only information at the exact point where they are evaluated. Thus, the effect of other uncertain input parameters as well as their possible interaction effects on the model output are not explored (Czitrom, 1999; Dimov and Georgieva,

2010; Saltelli et al., 2007). Consequently, only limited information can be gained by performing local sensitivity analysis.

A better way to explore the sensitivity of all uncertain input parameters towards the model output are global methods. By taking the entire variations of all input parameters into account, a global and quantitative sensitivity measure can be obtained (Dimov and Georgieva, 2010). Furthermore, global sensitivity analysis techniques allow the detection of interactive effects between different uncertain input parameters. Thus, a comprehensive understanding of the model output sensitivity with respect to the input uncertainty is obtained. Examples of global sensitivity analysis methods are the Monte Carlo based regression analysis, which is also called standardized linear regression analysis method (SRC method) (Helton and Davis, 2003; Sin et al., 2009), analysis of elementary effects using Morris screening (Morris, 1991), derivative based global sensitivity analysis (Sobol and Kucherenko, 2009) or variance based sensitivity measure using Sobol's method (Saltelli et al., 2010). The choice of the analysis method depends on the structure of the established model as well as if the inputs are independent or correlated.

The results of the sensitivity analysis enables the user to identify critical factors as well as rank the input parameters according to their relative impact on the model output. Subsequently, further analysis and possible experimental setups can be prioritized, focusing on the most influential parameters. On the contrary, parameters with low impact can be fixed or the formulation simplified which results in an overall simpler model without losing important information and prediction accuracy (Saltelli et al., 2007, 2000; Sin et al., 2009).

Despite the advantages of global sensitivity methods, local or OAT-methods are still the most common used techniques in the field of food science modelling. Gulati and Datta (2016), Nicolas et al. (2017), Ousegui et al. (2010) or Purlis and Salvadori (2009b), to name only few, evaluated the influence of single uncertain model input parameters on the model outputs, without exploring the sensitivity of all uncertain model parameters or considering the possible interactions between them. In contrast, only few authors considered global sensitivity methods (Feyissa et al., 2012). Additionally, a comparison and adoption of the different sensitivity analysis techniques

already applied in other fields is missing. The identification of the right conditions and tools for the uncertainty and sensitivity analysis is especially for the food modelling community important. In this way, the method that requires the lowest computational time could be identified and adopted, as this is quite often the main limiting factor (Datta, 2015).

In summary, uncertainty and sensitivity analysis are crucial and should be integrated into the model development process (Figure 1). Consequently, the quality and reliability of the established model can be evaluated. For the industry, it is especially important to obtain a quantitative knowledge about the sensitivity of variations in the process settings and conditions on the final quality of the product. Accordingly, critical process parameters can be identified and controlled thoroughly (**Section 7.1**).

5 Objectives

Kinetic models can describe the rate at which food quality attributes are changing during thermal processing (see **Chapter 2**). However, the spatial distribution of the quality changes cannot be captured by kinetic models, as the entire history of the temperature and moisture content changes during processing is needed. Mechanistic models of heat and mass transfer, as described in **Chapter 3**, could provide the required knowledge about the spatial changes of the state variables. Consequently, a combination of kinetic and mechanistic modelling could enable not only the prediction of the spatial quality changes during thermal heating, but would also enhance our knowledge about the phenomena that lead to the quality changes.

However, the potential of coupling models of heat and mass transfer with models that describe the quality changes as function of the state variables (i.e. temperature and moisture content) is still not fully explored. Therefore, the working hypothesis of my PhD project has been that:

Mechanistic models of heat and mass transfer can be used to obtain a fundamental knowledge about the transformations a food undergoes during the heating process and how these are linked to the spatial quality changes of the food product.

In order to answer the working hypothesis, four specific objectives have been defined:

1) Describe essential chicken breast meat quality attributes as function of temperature, moisture content and heating time.
2) Develop and validate a mechanistic model of convective chicken breast meat roasting. Missing model parameters should be measured and/ or described as accurate as necessary to capture the dynamic changes of chicken breast meat during roasting. Furthermore, the model should include the irregular 3D geometry of the whole chicken breast to ensure realistic model predictions.

3) Combine the mechanistic model of heat and mass transfer with the kinetic models to study the influence of the process parameters on the spatial quality changes of chicken breast meat
4) Perform uncertainty and sensitivity analysis and identify the most influential model input parameters. Comparison of different analyses techniques should be included and their influence on the analysis results evaluated.

6 Own findings

The background given in the **Chapters 2, 3** and **4** shows that there is a possibility of combining kinetic and mechanistic models to predict the spatial quality degradation of foods during heating processes. In the following, our own findings are presented in the form of five completed research papers:

1. In Publication 1, we developed kinetic models that describe the texture and color changes of chicken breast meat during isothermal heating. A modified reaction rate law was proposed that takes the non-zero equilibrium of quality attributes into account, without the need of preliminary assumptions.
2. In Publication 2, we established a mechanistic model for the roasting of chicken breast meat from first principles. We then coupled the mechanistic model with the texture kinetic models developed in Publication 1, which enabled the prediction of the spatial texture changes as function of the process conditions.
3. In Publication 3, we evaluated the developed model in Publication 2 by using global uncertainty and sensitivity analysis. Furthermore, the influence of different sampling and global sensitivity analyses techniques are compared. Consequently, we proposed possibilities for model refinements and reductions.
4. In Publication 4, we developed a non-isothermal kinetic model for the surface browning of chicken breast meat and coupled it with the established mechanistic model in Publication 2. In combination with the kinetic models from Publication 1, this enabled us to predict the internal as well as surface color development as function of the temperature and water activity development during the roasting process.
5. Publication 5 aimed to evaluate the sensitivity of the chicken breast geometry on the temperature, moisture content and quality predictions. Therefore, we developed a statistical shape model (SSM) and combined it with the established mechanistic model in Publication 2. Subsequently, we studied the influence of the natural shape and size variation on the model predictions.

In **Chapter 7**, after the publications, I give a summary and general discussion of my own findings and in **Chapter 8** the main conclusions as well as future perspectives are presented.

Publication 1

Rabeler, F., & Feyissa, A. H. (2018). Kinetic modeling of texture and color changes during thermal treatment of chicken breast meat. *Food and Bioprocess Technology*, *11*(8).

DOI: https://doi.org/10.1007/s11947-018-2123-4

Due to merging of files, the inserted publication does not follow the page numbering of the overall document but instead the page numbering of the journal.

Food and Bioprocess Technology
https://doi.org/10.1007/s11947-018-2123-4

ORIGINAL PAPER

Kinetic Modeling of Texture and Color Changes During Thermal Treatment of Chicken Breast Meat

Felix Rabeler[1] · Aberham Hailu Feyissa[1]

Received: 22 January 2018 / Accepted: 23 May 2018

Abstract
Heat treatment is commonly applied as a primary method for ensuring the microbial safety of poultry meat and to enhance its palatability. Although texture and color of cooked chicken breast meat are important quality parameters for the consumers that need to be controlled during thermal processing, studies assessing the temperature-time-dependent quality changes during thermal treatment are lacking. This work aims to investigate the texture and color changes of chicken breast meat during thermal processing and to develop kinetic models that describe these changes. We studied the storage modulus changes of chicken breast meat as function of temperature. The storage modulus increases from 55 °C until leveling off in an equilibrium value above 80 °C, which was attributed to microstructure changes and described with a sigmoidal function. The changes in the texture (TPA) and color (CIE $L^*a^*b^*$) of chicken breast meat were measured as function of temperature and time. The texture and color parameters show a rise with heating time until reaching an equilibrium value, while the rate of change increased with temperature. Kinetic models that take the non-zero equilibrium into account were developed to describe the color (lightness) and texture (hardness, gumminess, and chewiness) changes with heating time and temperature. The kinetic models provide a deeper insight into the mechanisms of texture and color changes during thermal treatment. They can be used to predict the texture and color development of chicken breast meat during thermal processing and, thus, help to optimize the process.

Keywords Poultry meat · Quality changes · Rate law · Storage modulus · Texture profile analyses (TPA) · Thermal processing

Introduction

The worldwide consumption of poultry meat has increased more than 30% over the last 10 years (OECD 2018). Particularly, chicken breast meat is popular among consumers due to its relative low price compared to other meat products (e.g., beef and pork meat) and its low fat and high protein content (Guerrero-Legarreta and Hui 2010; Magdelaine et al. 2008).

To ensure the safe consumption of chicken meat, it should be heated at least to an internal temperature of 72 °C (Fsis 2000). The heating leads to changes in the microstructure, texture, and appearance of the chicken breast meat and may affect the acceptance by the consumers (Lawrie and Ledward 2006).

The convective roasting (using hot air) is the most common heating method for chicken meat in professional kitchens and the large-scale food industry, but also, contact frying/grilling or the cooking in hot water is often applied (Guerrero-Legarreta and Hui 2010; Lawrie and Ledward 2006). Different studies show that the heating methods have different impact on the texture and color of poultry meat. Barbanti and Pasquini (2005) reported that hot air roasting leads to tougher poultry meat samples compared to the steam cooked samples, whereas Zell et al. (2010) reported that there is no significant difference in the texture of samples prepared by ohmic heating and convectional heating. In these studies, the poultry meat samples were heated to different core temperatures and the change in the quality correlated with these temperatures. However, conventional heating methods (e.g., roasting in convection oven) lead to temperature gradients inside the meat, which results in a non-uniform texture and color development.

✉ Felix Rabeler
felra@food.dtu.dk

[1] Food Production Engineering, National Food Institute, Technical University of Denmark (DTU), Søltofts Plads, 2800 Kgs. Lyngby, Denmark

Published online: 01 June 2018

The heating of poultry meat above 55 °C leads to denaturation of myoglobin protein, which results in whitening of the meat (Guidi and Castigliego 2010). At higher temperatures, Maillard reactions take place, resulting in a browning of the surface and the formation of flavor components (Brunton et al. 2002). Heating also induces transversely shrinkage of the meat fibers leading to wider gabs between them, followed by longitudinal shrinkage of the fibers, solubilization of connective tissue, muscle protein aggregation, and gel formation (Tornberg 2005). This leads to changes in the microstructure (denser matrix with compact fiber arrangements) and, thus, to a toughening of the meat (Wattanachant et al. 2005). Additionally, the protein denaturation reduces the water-holding capacity, which results in water loss during the cooking process (Micklander et al. 2002).

If the main physical factors that influence the quality of chicken meat are known, the thermal processing can be optimized to achieve the best possible quality of the meat product for the consumer. In this manner, kinetic modeling can provide a deeper understanding of the changes that occur during thermal processing and help to control and optimize the food quality (Haefner 2005). For different muscle foods and vegetables, researchers showed that the quality degradation during thermal treatment can be described by a general rate law. The quality changes mainly follow a zero-, first-, or second-order kinetic (Ling et al. 2015; Van Boekel 2008). To describe the relationship between the temperature and the reaction rate constant, the common Arrhenius model is mostly used (Goncalves et al. 2007; Goñi and Salvadori 2011; Ko et al. 2007; Kong et al. 2007).

There have been no systematic studies of the thermal changes of chicken meat quality with time and related kinetic models. Therefore, the aim of this study is to investigate the changes of chicken meat quality (texture and color) with time and temperature in order to develop kinetic models that describe these changes. We here present the effect of temperature and time on the texture (texture profile analyses (TPA)) and color of chicken breast meat, as well as the effect of the temperature on the rheological properties of chicken breast meat.

Kinetic Modeling

The irreversible change of a quality attribute Q under isothermal condition can be described by the general rate law in the following form Eq. (1) (Levenspiel 1999; Van Boekel 1996):

$$\frac{\partial Q}{\partial t} = -kQ^n \tag{1}$$

where k is the reaction rate constant (min^{-1} $[\mathrm{Q}]^{1-\mathrm{n}}$), Q is the quality attribute at time t (min), and n is the reaction order.

The temperature dependence of the reaction rate is mostly described by the Arrhenius equation Eq. (2):

$$k = k_0 \exp\left(-\frac{E_a}{R\,T}\right) \tag{2}$$

where k_0 is the pre-exponential factor (min^{-1} $[\mathrm{Q}]^{1-\mathrm{n}}$), E_a is the activation energy (J/mol), R is the universal gas constant (8.314 J/(mol K)), and T is the temperature (°C).

Food quality changes are mostly reported to follow a zero-, first-, or second-order reaction. For isothermal conditions, integration of Eq. (1) gives (Steinfeld et al. 1999; Van Boekel 1996)

$$Q = Q_0 - k\,t \qquad \mathrm{n} = 0 \tag{3a}$$

$$\mathrm{Q} = Q_0{}^{*}\exp(-k\,t) \qquad \mathrm{n} = 1 \tag{3b}$$

$$Q = \left(k\,t + \frac{1}{Q_0}\right)^{-1} \qquad \mathrm{n} = 2 \tag{3c}$$

where Q_0 refers to the initial quality value.

The common rate law in the form of Eq. (1) is not taking into account that most foods retain a constant measurable (non-zero) degree of quality (for example, firmness and color) even after long heating times (Rizvi and Tong 1997). To account for this non-zero equilibrium, a modified rate law is used with the following forms:

Equation (4a) when the non-zero equilibrium is smaller than the initial quality value (e.g., softening of the texture):

$$\frac{\partial Q}{\partial t} = -k\,(Q - Q_\infty)^n \quad Q_0 \geq Q \geq Q_\infty \tag{4a}$$

and Eq. (4b) when the non-zero equilibrium is larger than the initial quality value (e.g., toughening of the texture):

$$\frac{\partial Q}{\partial t} = k\,(Q_\infty - Q)^n \quad Q_0 \leq Q \leq Q_\infty \tag{4b}$$

where Q_∞ is the final non-zero equilibrium quality value after long heating times.

For isothermal conditions, integration of Eq. (4b) for a first- and nth-order leads to Eqs. (5a) and (5b), respectively:

$$Q = Q_\infty - (Q_\infty - Q_0)*\exp(-k\,t) \qquad n = 1 \tag{5a}$$

$$Q = Q_\infty - \left[kt(n-1) + (Q_\infty - Q_0)^{1-n}\right]^{\frac{1}{1-n}} \qquad n \neq 1 \tag{5b}$$

For this study, Eq. (4b) is used to describe the quality changes (texture and color) of chicken breast meat. Therefore, only the integrated forms of this equation are shown here for clarity. For a first-order reaction (Eq. (5a)), the same form as the fractional conversion model (proposed by Rizvi and Tong (1997) for food quality changes) is obtained. Instead of assuming the order of the reaction, it

is, however, more appropriate to estimate the reaction order n together with the other kinetic parameters by solving and fitting the differential form of the kinetic model (Eq. (4a) or Eq. (4b)) to the experimental data set (see the "Parameter estimation" section).

Materials and Methods

Raw Material

Chilled (4 °C) chicken breast meat (without skin and bone) was obtained from a local supermarket (the same day as the experimental tests) and stored at 2 °C until preparation for the experiments.

Rheological Measurement

For the rheological measurement, the chicken meat was sliced along the fiber direction using an electrical meat slicer (AM 300, Minerva Omega group s.r.l., Italy), and circular samples with a height of 3 ± 0.5 mm and a diameter of 35 ± 1 mm were cut using a cork borer.

The rheological characteristics of whole chicken breast meat were measured using a controlled stress rheometer (Haake Mars Rheometer, Type 006–0572; Thermo Fisher Scientific, USA) equipped with a 35-mm parallel plate attachment. Both plates were serrated to prevent any unwanted slipping, and the rheometer was complemented with a temperature controller to precisely control (± 0.5 °C) and monitor the sample temperature. Dynamic rheological measurements were performed as described by Hashemi and Jafarpour (2016). One chicken disk sample was loaded between the plates, and the sample sides were covered with a thin layer of silicon oil to minimize the moisture evaporation with increasing temperature. The sample was held at 25 °C (starting temperature) for 5 min to ensure equilibrium. Afterwards, the sample temperature was increased stepwise from 25 to 85 °C with steps of 5 °C and holding times of 3 min at every temperature step before measurements (recording the data). The holding time was chosen as no further changes in the storage modulus were found for longer holding times (> 3 min). All dynamic oscillating analyses were performed with a gap of 3 mm between the plates, a constant stress of 6 Pa, and a constant frequency of 1 Hz. The constant value for the stress was chosen within the linear viscoelastic region that was determined by performing stress sweeps (0.1–1000 Pa). Changes in the storage modulus G' (elastic property), complex modulus G'' (viscous property), and phase angle (ratio of loss modulus to storage modulus) were recorded directly by the rheometer software (Haake RheoWin 4).

Texture and Color Measurements

For the texture and the color measurements, disk-shaped chicken meat samples with heights of 6 ± 0.5 mm and diameters of 21 ± 1 mm were prepared according to the "Rheological measurement" section. Thin samples were used to ensure a fast heating to the desired temperature and to achieve a uniform temperature within the chicken meat by reducing the time for internal heat transport. The samples were heated in a thermostatic water bath with circulating water (SW22, Julabo GmbH, Germany) at five different temperatures (50, 65, 75, 85, and 95 °C) with varying heating times (see Table 1). In order to control the sample temperature and moisture content, water as a heating medium was chosen, as it allows a fast heating of the samples and avoids water loss from the samples (the total moisture loss from the chicken meat was less than 6%) (Thussu and Datta 2012).

The water bath was filled with demineralized water and pre-heated for 30 min to achieve the desired temperatures and to ensure steady state conditions. The temperature of the water bath as well as the sample temperature was monitored during the heat treatment using thermocouples (type T). As the samples were thinly sliced, temperature equilibrium was reached for every time step. After heating the samples in the water bath, they were immediately placed in ice water for approximately 30 to 60 s to cool down the samples. Subsequently, excess moisture was removed with a filter paper. The samples were sealed in aluminum cups and stored for 2 h at room temperature prior to further analysis.

Texture Profile Analysis

The texture of raw and cooked chicken breast meat was analyzed using a TA.XTplus (Stable Micro Systems, UK) texture analyzer with a 30-kg load cell. Double compression tests (TPA) were performed according to the procedure described by Bourne (2002) with a cylindrical probe of 50-mm diameter at room temperature. The probe contact area for all samples was 350 mm^2, and the samples were compressed to a final strain of 40% with a test speed of 1 mm/s. The time interval between the first and the second stroke was 5 s. From the force-time plot of the double compression test, the TPA

Table 1 Heating the chicken meat samples at different water bath temperatures and cooking times

Water bath temperature (°C)	Cooking times (s)
50	200, 400, 600, 800, 1000, 1200
65	100, 200, 300, 400, 500, 600, 800, 1000
75	50, 100, 150, 200, 250, 300, 400, 600, 800
85	50, 100, 150, 200, 250, 300, 400
95	50, 100, 150, 200, 250, 300, 400

parameters hardness, cohesiveness, springiness, gumminess, and chewiness were calculated (Bourne 2002).

Color Measurements

The color of the chicken disk samples before and after cooking was measured using a hyperspectral imaging system (VidometerLab 2, Videometer A/S, Denmark), which allows measuring the color of the whole sample surface. The Videometer is widely used for imaging food samples, for example, for assessing the quality of minced beef after a frying process (Daugaard et al. 2010). The device was calibrated radiometrically using a diffuse white as well as dark target, and geometrical calibration was performed with a geometric target. The light setup of the device was then adjusted to chicken breast meat (Hansen 1999).

The sample was placed in a petri dish under the camera and an image was taken. Afterwards, the image was processed using the software package MATLAB (R2017a, The Mathworks Inc., MA, USA) and the color of the raw and cooked chicken meat samples was obtained in the $L^*a^*b^*$ system. The L^* defines the color lightness of the product (varies from 0 for white to 100 for black), a^* indicates the color degree between red and green (a negative value indicates green color and a positive value indicates red color), and b^* specifies the color degree between yellow and blue (negative values indicate blue colors and positive values yellow colors). The total color difference ΔE is defined by Eq. (6):

$$\Delta E = \sqrt{(L-L_0)^2 + (a^*-a^*_0)^2 + (b^*-b^*_0)^2} \quad (6)$$

with $L_0 = 66.95 \pm 1.62$, $a_0^* = 5.05 \pm 0.70$, and $b_0^* = 18.95 \pm 1.16$, the lightness, redness, and yellowness of the raw chicken meat, respectively.

Parameter Estimation

MATLAB (R2017a, The Mathworks Inc., MA, USA) was used to solve the ordinary differential equations that describe the quality changes (Eqs. (4a) and (4b)) and to estimate the kinetic parameters. The parameters were estimated using nonlinear least squares (*lsqnonlin* solver in MATLAB) (minimization of the sum of squared differences between the predicted ($Q_{predicted}$) and measured ($Q_{experiment}$) quality changes) and the bootstrap method with 1000 bootstrap samples (Efron 1979). A detailed description of the bootstrap method can be found in Sin and Gernaey (2016).

Statistical Analysis

The precision of the calculated parameters was assessed by confidence intervals at 95%. Furthermore, the residual randomness and normality was used to evaluate the quality of the regression. All experiments were repeated four times and the values from the rheological, texture, and color measurements presented as mean values ± 95% confidence intervals. One-way ANOVA analyses and Tukey multiple range tests were performed to evaluate the influence of the heating time and temperature on the texture and on the color changes of chicken breast meat. Chi-squared test was used to evaluate the goodness of fit. For all statistical analyses, a significance level of $P < 0.05$ was used.

Results and Discussion

Rheological Changes

The changes of the storage modulus G' and the phase angle γ as function of the sample temperature were recorded as shown in Fig. 1. In the range of 25 and 55 °C, the storage modulus does not change with the temperature. However, from 60 to 80 °C, G' increases sharply with increasing sample temperature, and reaches a maximum plateau (around 92 kPa) above 80 °C. The phase angle (the ratio of loss modulus to storage modulus) decreases over the whole temperature range, while an accelerated decrease is observed for sample temperatures above 50 °C.

Tornberg (2005) observed a similar behavior of the storage modulus for whole beef meat with rising temperature. However, the storage modulus for beef meat increases earlier (around 50 °C) and also the maximum value is slightly lower (around 80 kPa) than for the chicken breast meat (92 ± 2 kPa). The different behavior of chicken breast meat compared to whole beef meat could be explained by an overall higher protein quality and quantity in chicken or broiler meat (16% higher myofibrillar protein content) compared to beef meat (Montejano et al. 1984; Mudalal et al. 2014; Tornberg 2005).

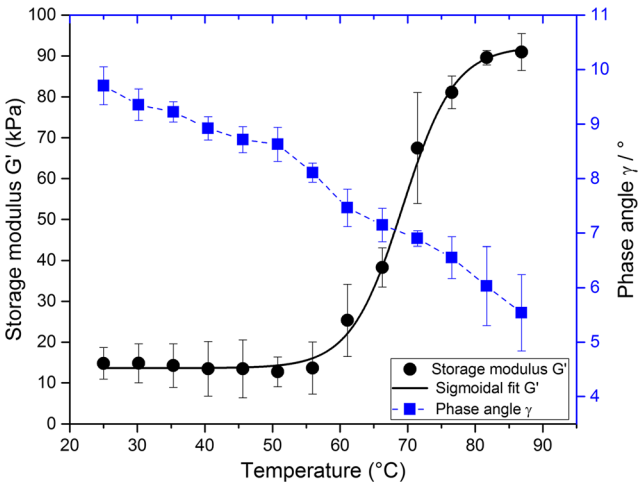

Fig. 1 Change of the storage modulus (kPa) and phase angle (deg) for chicken breast meat as function of sample temperature. Bars indicate the 95% confidence intervals ($n = 4$)

The storage modulus indicates the change in the meat microstructure due to protein denaturation that results in a toughening of the meat. Around a temperature of 62 °C, myosin starts to denature, followed by collagen at 70 °C and actin at 82 °C (Bircan and Barringer 2002). This leads to structural changes inside the meat by longitudinal and transversal shrinkage of meat fibers and solubilization of connective tissue. As a result, the meat becomes more compact and harder, leading to the increase of the storage modulus with rising temperature (Tornberg 2005).

The change of the storage modulus with temperature can be described as a sigmoidal curve (Fig. 1, solid line) with the following equation:

$$G' = G'_{max} + \frac{(G'_0 - G'_{max})}{1 + \exp\left(\frac{T - \overline{T}}{\Delta T}\right)} \quad (7)$$

where $G'_{max} = 92 \pm 2$ kPa refers to the maximum storage modulus for chicken meat and $G'_0 = 13.5 \pm 1.3$ kPa to the initial storage modulus. $\overline{T} = 69 \pm 1$ °C and $\Delta T = 4 \pm 0.6$ °C are fitting parameters that were estimated using the bootstrap method (see the "Parameter estimation" section).

Texture Changes

The TPA parameters hardness (*Ha*), gumminess (*Gu*), and chewiness (*Cw*) increase significantly ($P < 0.01$) with heating time (Fig. 2a–c). They all show a similar behavior with a steeper slope in the beginning, a gradually leveling off with increasing heating time until the texture parameters reach a constant value (equilibrium). The rate (slope) of the texture change is influenced by the temperature, with steeper slopes at higher temperatures. The changes of cohesiveness and springiness with temperature and time are summarized in Table 2. The cohesiveness shows an increase with time until reaching an equilibrium value, similar to hardness, gumminess, and chewiness. The springiness shows a decrease in the beginning (50–200 s), after which it is also reaching an equilibrium value. However, no significant influence of the temperature on the springiness was found.

Under thermal treatment, the meat proteins denature stepwise with different mechanisms for each temperature interval. In the temperature range from 40 to 50 °C, collagen fibers partially denature and straighten, leading to a first toughening of the meat (Lewis and Purslow 1989). Further temperature increase leads to denaturation and shrinkage of myofibrillar proteins as well as dehydration and shrinkage of actomyosin, resulting in a supplementary toughening of the meat (Christensen et al. 2000; Tornberg 2005). The rate of the protein denaturation increases with increasing temperature of the sample, resulting in a faster

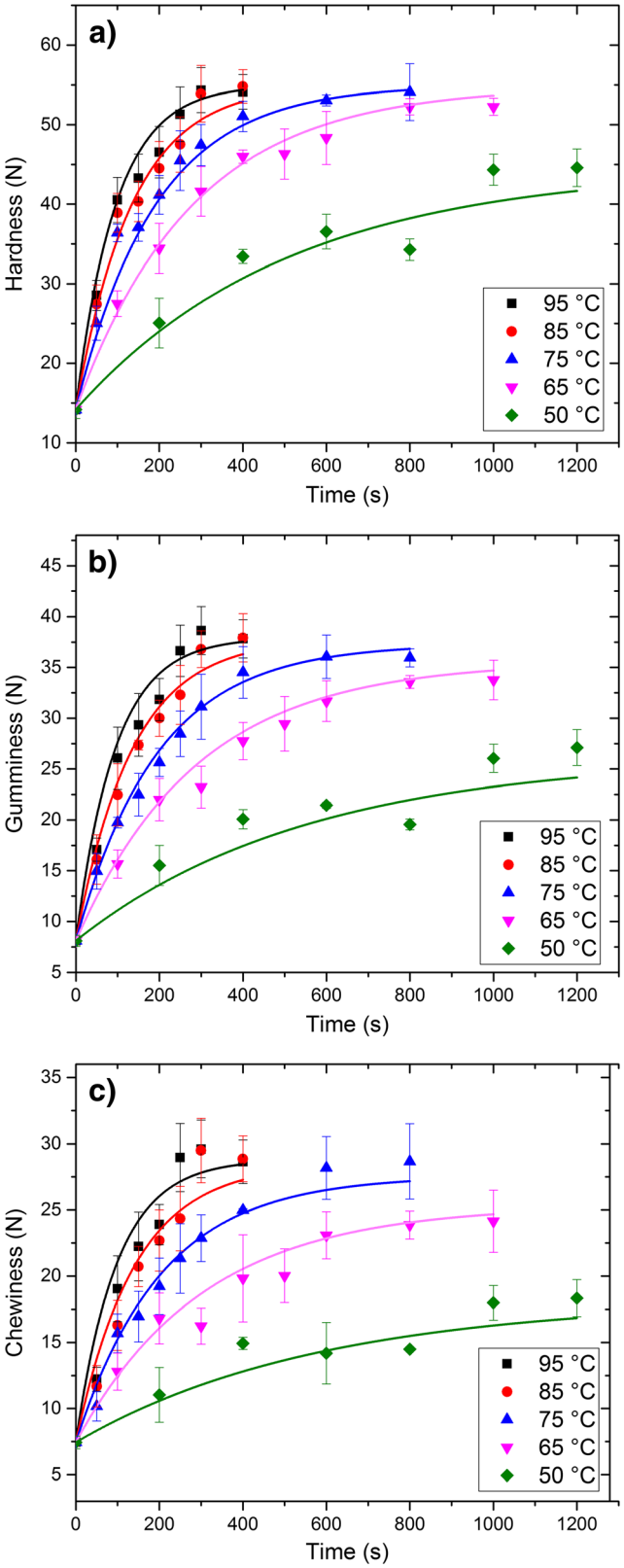

Fig. 2 Changes of the TPA parameters. **a** Hardness, **b** gumminess, and **c** chewiness with heating time and sample temperature fitted with the modified rate law. Symbols with bars indicate the experimental mean values with the 95% confidence intervals, and the solid lines indicate the model fit ($n = 4$)

Table 2 Measured values of the TPA parameters cohesiveness and springiness of chicken breast meat with time and temperature

Cohesiveness							Springiness					
Time (s)	Temperature (°C)						Temperature (°C)					
	50	65	75	85	95		50	65	75	85	95	
0	0.573 ± 0.038	0.573 ± 0.038	0.573 ± 0.038	0.573 ± 0.038	0.573 ± 0.038		91.98 ± 1.57	91.98 ± 1.57	91.98 ± 1.57	91.98 ± 1.57	91.98 ± 1.57	
50	–	–	0.596 ± 0.028	0.589 ± 0.021	0.598 ± 0.001		–	–	68.38 ± 5.37	72.80 ± 2.78	71.60 ± 0.94	
100	–	0.574 ± 0.015	0.543 ± 0.024	0.578 ± 0.038	0.644 ± 0.031		–	83.02 ± 1.55	79.32 ± 5.18	72.18 ± 3.59	73.08 ± 3.73	
150	–	–	0.606 ± 0.039	0.683 ± 0.046	0.675 ± 0.031		–	–	75.30 ± 3.53	75.71 ± 4.98	75.08 ± 5.18	
200	0.619 ± 0.013	0.599 ± 0.026	0.624 ± 0.011	0.676 ± 0.033	0.685 ± 0.038		70.72 ± 5.4	76.71 ± 3.02	74.91 ± 2.15	75.60 ± 5.64	75.24 ± 3.86	
250	–	–	0.626 ± 0.001	0.681 ± 0.036	0.714 ± 0.031		–	–	84.46 ± 3.92	75.20 ± 5.50	78.65 ± 3.62	
300	–	0.604 ± 0.060	0.642 ± 0.0113	0.740 ± 0.048	0.712 ± 0.042		–	66.56 ± 5.57	70.21 ± 6.32	81.14 ± 2.50	76.65 ± 3.84	
400	0.601 ± 0.038	0.623 ± 0.029	0.677 ± 0.021	0.692 ± 0.036	0.699 ± 0.035		74.45 ± 1.29	78.60 ± 0.74	82.52 ± 6.93	76.11 ± 3.00	71.71 ± 3.92	
600	0.587 ± 0.027	0.655 ± 0.023	0.695 ± 0.037	–	–		66.08 ± 6.95	72.98 ± 2.00	79.44 ± 7.34	–	–	
800	0.571 ± 0.007	0.652 ± 0.044	0.709 ± 0.013	–	–		74.07 ± 1.64	73.53 ± 3.98	76.62 ± 5.81	–	–	
1000	0.588 ± 0.021	0.646 ± 0.036	–	–	–		68.96 ± 1.43	69.02 ± 5.27	–	–	–	
1200	0.605 ± 0.015	–	–	–	–		78.59 ± 4.00	–	–	–	–	

toughening of the meat at higher temperatures (Bailey and Light 1989).

Wattanachant et al. (2005) investigated the change of the chicken meat microstructure at different core temperatures. They showed that the microstructure of chicken meat became denser with more compact fiber arrangements at increasing internal temperature. However, no further toughening of the texture above 80 °C was observed. Furthermore, the storage modulus of chicken breast meat, G', is reaching an equilibrium value for temperatures above 80 °C (see Fig. 1 and the "Rheological changes" section), indicating no further changes in the microstructure due to protein denaturation. These observations could explain why there is no significant difference between the slope as well as the equilibrium values of hardness ($P > 0.05$), gumminess ($P > 0.05$), and chewiness ($P > 0.05$) for sample temperatures of 85 to 95 °C.

For the TPA parameters hardness, gumminess, and chewiness (Fig. 2a–c), a small plateau is visible before reaching the equilibrium value especially at 50 and 65 °C. Feyissa et al. (2013) showed that the microstructure of meat is changing dramatically during the cooking. Protein denaturation leads to pore formation, decrease in the water-holding capacity (WHC), and water migration into the spaces between the muscle fibers. For chicken breast meat, Van der Sman (2013) showed that the WHC is a function of temperature. The unbound water could work as a plasticizer, leading to the small plateau before further denaturation results in the further toughening of the meat until the equilibrium is reached (Hughes et al. 2014).

Equation (4b) (Q_∞ is larger than the initial value Q_0) was used to model the changes in the TPA parameters hardness, gumminess, and chewiness with temperature and time. The Arrhenius equation (Eq. (2)) is used to describe the temperature dependence of the rate constant k. By solving and fitting Eq. (4b) to the experimental data set, the equilibrium values Q_∞, the activation energies E_a, the pre-exponential factors k_0, and the reaction orders n were estimated (see the "Parameter estimation" section).

The obtained individual equilibrium values for hardness (Ha_∞), gumminess (Gu_∞), and chewiness (Cw_∞) vary with temperature (see Fig. 2a–c) and are described by Eqs. (8a)–(8c):

$$\text{Hardness} \quad \mathrm{Ha}_\infty(\mathrm{T}) = Q_{max} + \frac{Q_0 - Q_{max}}{1 + \exp\left(\frac{T-\overline{T}}{\Delta T}\right)} \tag{8a}$$

$$\text{Gummies} \quad \mathrm{Gu}_\infty(\mathrm{T}) = Q_{max} + \frac{Q_0 - Q_{max}}{1 + \exp\left(\frac{T-\overline{T}}{\Delta T}\right)} \tag{8b}$$

$$\text{Chewiness} \quad \mathrm{Cw}_\infty(\mathrm{T}) = Q_{max} + \frac{Q_0 - Q_{max}}{1 + \exp\left(\frac{T-\overline{T}}{\Delta T}\right)} \tag{8c}$$

Table 3 Estimated parameters for Eqs. (8a)–(8c) to describe the equilibrium of hardness, gumminess, and chewiness of chicken meat as a function of temperature

	Q_{max} (N)	Q_0 (N)	$\overline{T}$ (°C)	ΔT (°C)
Hardness (Ha_∞)	55.2 ± 3.5	14 ± 1.4	45 ± 1.5	4 ± 1.1
Gumminess (Gu_∞)	38.6 ± 2.2	7 ± 1.1	47 ± 2.1	8 ± 1.4
Chewiness (Cw_∞)	28.5 ± 1.7	6.9 ± 1.5	50 ± 2.9	10 ± 2.1

where Q_{max}, $\overline{T}$, and ΔT are the fitting parameters. The corresponding parameters are presented in Table 3. The changes of the equilibrium values with temperature show a similar behavior as the change of the storage modulus with temperature (see Fig. 1). This indicates that the degree of structural changes due to protein denaturation is responsible for the change in the equilibrium value with temperature.

The results for the estimated activation energies E_a, pre-exponential factors k_0, and reaction orders n are summarized in Table 4 with the corresponding 95% confidence intervals. As shown in Fig. 2a–c, the developed kinetic models (solid lines) can describe the changes in hardness, gumminess, and chewiness with time and temperature ($X^2_{hardness} = 4.05$, $X^2_{gumminess} = 3.15$, $X^2_{chewiness} = 39.67$; $P > 0.05$).

The obtained activation energies E_a for hardness, gumminess, and chewiness are 39.3 ± 2.7, 35.9 ± 2.2, and 44.6 ± 3.5 kJ/mol, respectively. The values are in the same range as reported by other authors for textural changes of different foods (10–100 kJ/mol) (Ling et al. 2015): for example, mussels (65 kJ/mol) (Ovissipour et al. 2013), pumpkin (72 kJ/mol) (Goncalves et al. 2007), or mushrooms (15 kJ/kg) (Ko et al. 2007).

Color Changes

Figure 3a–d shows the changes of chicken meat color (CIE L^*, a^*, b^*) with heating time.

During thermal treatment in a moist surrounding, chicken breast meat becomes white, leading to significant changes in the color values compared to the raw chicken meat color. For temperatures of 75 to 95 °C, the values of lightness L^* and total color difference ΔE (Eq. (1)) rise rapidly until leveling off and reaching an equilibrium value of 87 ± 0.72 and 21 ± 0.67, respectively (Fig. 3a, b). However, for 85 and 95 °C, no significant difference ($P < 0.01$) was found between the slopes of the curves. For temperatures of 65 and 50 °C, the slope of the curve decreases significantly ($P < 0.01$). For 65 °C, the same equilibrium value is reached as for 95, 85, and 75 °C, while for 50 °C, the equilibrium value for the lightness L^* and total color change ΔE is at 82 ± 0.63 and 15 ± 0.57, respectively (Fig. 3a, b).

For temperatures of 65 to 95 °C, the a^* and b^* values decrease with time until reaching an equilibrium, while the slopes of the curves increase with rising temperature. At 50 °C, the a^* value first increases before it is decreasing and leveling off to an equilibrium value (Fig. 3c). The b^* value is first slightly decreasing at 50 °C until reaching an equilibrium which is just marginally beneath the b^* value for the raw sample (Fig. 3d).

During the heating, heme proteins (hemoglobin and myoglobin) denature, resulting in the whitening of the muscle. Hemoglobin and myoglobin are relatively heat stable and completely denature at temperatures around 65 to 80 °C, while the rate and degree of denaturation increases with temperature (Lawrie and Ledward 2006; Martens et al. 1982). For temperatures below the denaturation temperature of myoglobin (< 65 °C), the color change cannot be explained just by heme protein denaturation. However, structural changes, initiated from the denaturation of myofibrillar proteins and other structural proteins, could lead to a higher light scattering and optical masking of heme proteins causing a lighter product (Hughes et al. 2014; Martens et al. 1982).

The changes in the lightness L^* of chicken breast meat for the tested temperature (50–95 °C) and time range (50–1200 s) were modeled using Eq. (4b) (Q_∞ is larger than the initial value Q_0). The Arrhenius equation (Eq. (2)) is used to describe the temperature dependence of the rate constant. By solving and fitting Eq. (4b) to the experimental data set, the activation energy E_a, the pre-exponential factor k_0, and the reaction order n were estimated (see the "Parameter estimation" section). The estimated value for the activation energy, pre-exponential factor k_0, and reaction order n are 101.59 ± 7.83 kJ/mol, $2.65 \times 10^{15} \pm 1.97 \times 10^{14}$ min^{-1}, and 1.1 ± 0.06, respectively. The developed kinetic model (solid lines in Fig. 3a) can describe the change in lightness with time and temperature ($X^2_{lightness} = 1.29$; $P > 0.05$).

The obtained E_a value for the change in the lightness L^* (101.59 ± 7.83 kJ/mol) is within the same range reported for

Table 4 Obtained kinetic parameters for the change of the TPA parameters (hardness, gumminess, and chewiness) of chicken meat with time and temperature

Texture index	n	E_a (kJ/mol)	k_0 (min^{-1} $[Q]^{1-n}$) × 10^{-3}	X^2
Hardness (N)	1.12 ± 0.11	39.3 ± 2.7	196 ± 8.3	4.05
Gumminess (N)	0.98 ± 0.06	35.9 ± 2.2	64 ± 4.1	3.15
Chewiness (N)	1.01 ± 0.09	44.6 ± 3.5	773 ± 29	39.67

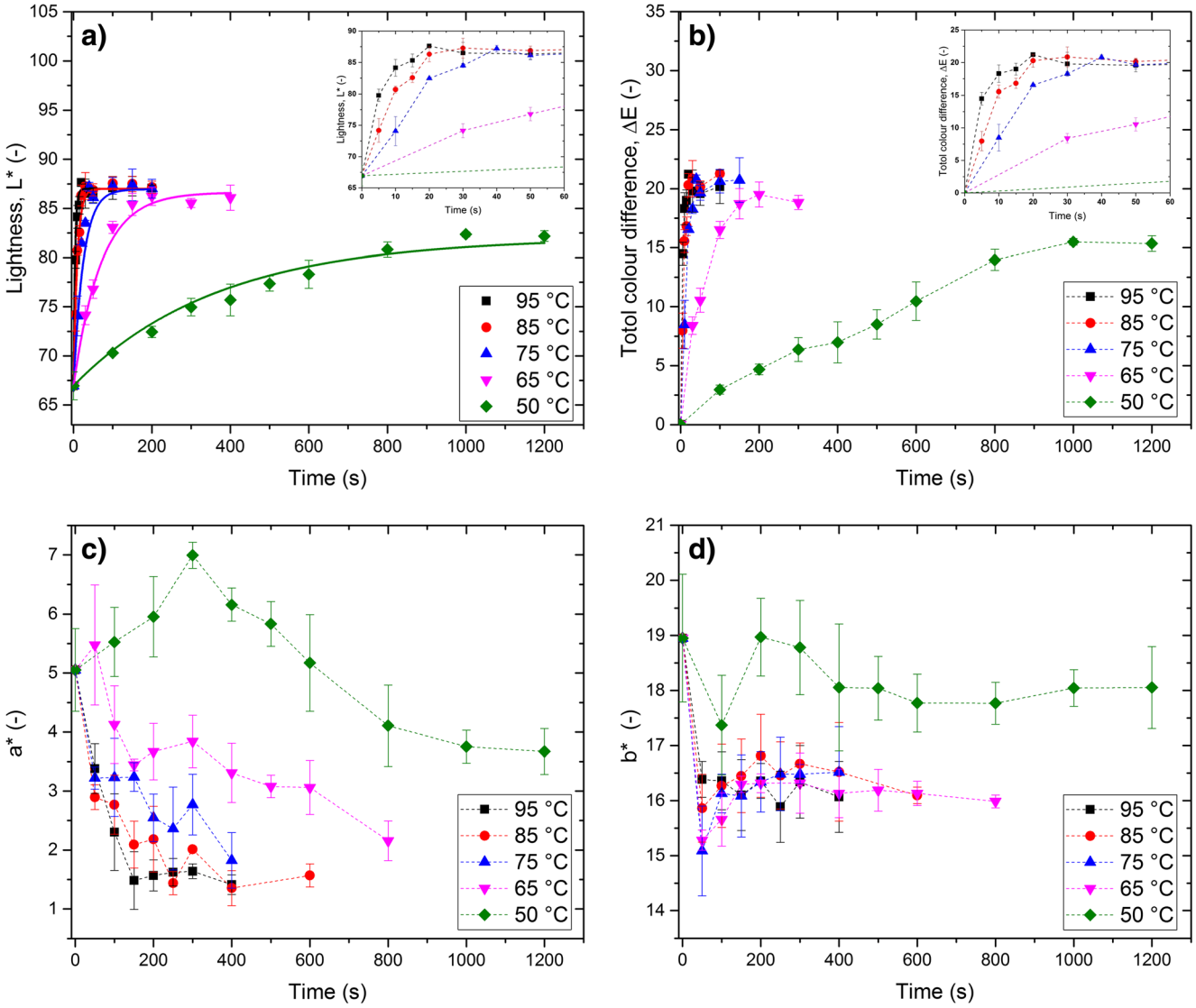

Fig. 3 Changes of the chicken meat color with heating time and sample temperature. **a** Lightness (L^*). **b** Total color difference (ΔE). **c** Redness (a^*). **d** Yellowness (b^*). Symbols with bars indicate the experimental mean values with the 95% confidence intervals ($n = 4$). The solid line in **a** shows the model fit

the color changes of different muscle foods and vegetables (80 to 120 kJ/mol) (Ling et al. 2015): salmon (88 kJ/mol) (Kong et al. 2007), beef (81 kJ/mol) (Goñi and Salvadori 2011), or pumpkin (120 kJ/mol) (Goncalves et al. 2007).

Conclusion

In this study, we developed kinetic models that describe the texture and color changes of chicken breast meat as function of temperature and heating time. The TPA parameters hardness, gumminess, and chewiness as well as the color parameter lightness increase with heating time until reaching an equilibrium value. The rate of the texture and color changes increases with temperature due to a faster protein denaturation. The color and texture changes were fitted to a modified rate law that takes the non-zero equilibrium into account. The resulting kinetic models well describe the measured quality changes. Moreover, the change in the storage modulus of chicken breast meat with temperature was evaluated and the development was well described with a sigmoidal function. The storage modulus increases sharply between 60 and 80 °C due to heat-induced protein denaturation, which leads to changes in the microstructure of the chicken meat.

Overall, the developed kinetic models and rheological properties provide a deeper understanding of the mechanism of the quality changes during the thermal processing of chicken breast meat. These can be coupled to physical-based models (such as heat and mass transfer) enabling the prediction of quality changes during thermal processing. This means that the spatial quality attributes can be predicted from the local temperature development with time, thus helping to

optimize the process settings for thermal treatments of foods to obtain the optimal quality for the consumer.

Nomenclature t, time (min); Q, quality attribute; T, temperature (°C); f, quality index (−); n, reaction order; k, reaction rate constant (min^{-1} $[Q]^{1-n}$); k_0, pre-exponential factor (min^{-1} $[Q]^{1-n}$); E_a, activation energy (J/mol); R, gas constant (8.314 J/mol K); L^*, a^*, b^*, color dimensions (−); ΔE, the total color difference (−); G', storage modulus (Pa); *Ha*, hardness (N); *Gu*, gumminess (N); *Cw*, chewiness (N)
Subscripts 0, initial value; ∞, equilibrium value

References

Bailey, A.J., Light, N.D., 1989. Connective tissue in meat and meat products. Elsevier applied science.

Barbanti, D., & Pasquini, M. (2005). Influence of cooking conditions on cooking loss and tenderness of raw and marinated chicken breast meat. *LWT- Food Science and Technology, 38*(8), 895–901. https://doi.org/10.1016/j.lwt.2004.08.017.

Bircan, C., & Barringer, S. a. (2002). Determination of protein denaturation of muscle foods using the dielectric properties. *Journal of Food Science, 67*(1), 202–205. https://doi.org/10.1111/j.1365-2621.2002.tb11384.x.

Bourne, M.C., 2002. Principles of objective texture measurement. Food texture viscosity: concept measurement. 2nd Ed.

Brunton, N. P., Cronin, D. A., & Monahan, F. J. (2002). Volatile components associated with freshly cooked and oxidized off-flavours in Turkey breast meat. *Flavour and Fragrance Journal, 17*(5), 327–334. https://doi.org/10.1002/ffj.1087.

Christensen, M., Purslow, P. P., & Larsen, L. M. (2000). The effect of cooking temperature on mechanical properties of whole meat, single muscle fibres and perimysial connective tissue. *Meat Science, 55*(3), 301–307. https://doi.org/10.1016/S0309-1740(99)00157-6.

Daugaard, S. B., Adler-Nissen, J., & Carstensen, J. M. (2010). New vision technology for multidimensional quality monitoring of continuous frying of meat. *Food Control, 21*(5), 626–632. https://doi.org/10.1016/j.foodcont.2009.09.007.

van der Sman, R. G. M. (2013). Modeling cooking of chicken meat in industrial tunnel ovens with the Flory-Rehner theory. *Meat Science, 95*(4), 940–957. https://doi.org/10.1016/j.meatsci.2013.03.027.

Efron, B. (1979). Bootstrap methods: another look at the jackknife. *The Annals of Statistics, 7*(1), 1–26.

Feyissa, A. H., Gernaey, K. V., & Adler-Nissen, J. (2013). 3D modelling of coupled mass and heat transfer of a convection-oven roasting process. *Meat Science, 93*(4), 810–820. https://doi.org/10.1016/j.meatsci.2012.12.003.

Fsis, U., 2000. Chicken from farm to table 1–8.

Goncalves, E. M., Pinheiro, J., Abreu, M., Brandão, T. R. S., & Silva, C. L. M. (2007). Modelling the kinetics of peroxidase inactivation, colour and texture changes of pumpkin (Cucurbita maxima L.) during blanching. *Journal of Food Engineering, 81*(4), 693–701. https://doi.org/10.1016/j.jfoodeng.2007.01.011.

Goñi, S. M., & Salvadori, V. O. (2011). Kinetic modelling of colour changes during beef roasting. *Procedia Food Science, 1*, 1039–1044. https://doi.org/10.1016/j.profoo.2011.09.155.

Guerrero-Legarreta, I., Hui, Y.H., 2010. Handbook of poultry science and technology, volume 2: ed. John Wiley & Sons, Inc. doi:https://doi.org/10.1002/9780470504475.

Guidi, A., & Castigliego, L. (2010). Poultry meat color. *Handb. Poult. Sci. Technol, 2*(2), 359–388. https://doi.org/10.1002/9780470504475.ch25.

Haefner, J. W. (2005). *Modeling biological systems: principles and applications*. New York: Springer-Verlag. https://doi.org/10.1007/b106568.

Hansen, J. F. (1999). *On chromatic and geometrical calibration*. Denmark: Technical University.

Hashemi, A., & Jafarpour, A. (2016). Rheological and microstructural properties of beef sausage batter formulated with fish fillet mince. *Journal of Food Science and Technology, 53*(1), 601–610. https://doi.org/10.1007/s13197-015-2052-4.

Hughes, J. M., Oiseth, S. K., Purslow, P. P., & Warner, R. D. (2014). A structural approach to understanding the interactions between colour, water-holding capacity and tenderness. *Meat Science, 98*(3), 520–532. https://doi.org/10.1016/j.meatsci.2014.05.022.

Ko, W. C., Liu, W. C., Tsang, Y. T., & Hsieh, C. W. (2007). Kinetics of winter mushrooms (Flammulina velutipes) microstructure and quality changes during thermal processing. *Journal of Food Engineering, 81*(3), 587–598. https://doi.org/10.1016/j.jfoodeng.2006.12.009.

Kong, F., Tang, J., Rasco, B., & Crapo, C. (2007). Kinetics of salmon quality changes during thermal processing. *Journal of Food Engineering, 83*(4), 510–520. https://doi.org/10.1016/j.jfoodeng.2007.04.002.

Lawrie, R.A., Ledward, D.A., 2006. Lawrie's meat science.

Levenspiel, O. (1999). Chemical reaction engineering. *Industrial and Engineering Chemistry Research, 38*(11), 4140–4143. https://doi.org/10.1021/ie990488g.

Lewis, G. J., & Purslow, P. P. (1989). The strength and stiffness of perimysial connective tissue isolated from cooked beef muscle. *Meat Science, 26*(4), 255–269. https://doi.org/10.1016/0309-1740(89)90011-9.

Ling, B., Tang, J., Kong, F., Mitcham, E. J., & Wang, S. (2015). Kinetics of food quality changes during thermal processing: a review. *Food and Bioprocess Technology, 8*(2), 343–358. https://doi.org/10.1007/s11947-014-1398-3.

Magdelaine, P., Spiess, M. P., & Valceschini, E. (2008). Poultry meat consumption trends in Europe. *World's Poultry Science Journal, 64*(01), 53–63. https://doi.org/10.1017/S0043933907001717.

Martens, H., Stabursvik, E., & Martens, M. (1982). Texture and color changes in meat during cooking related to thermal-denaturation of muscle proteins. *Journal of Texture Studies, 13*(3), 291–309.

Micklander, E., Peshlov, B., Purslow, P. P., & Engelsen, S. B. (2002). NMR-cooking: monitoring the changes in meat during cooking by low-field 1H-NMR. *Trends in Food Science and Technology, 13*(9-10), 341–346. https://doi.org/10.1016/S0924-2244(02)00163-2.

Montejano, J. G., Hamann, D. D., & Lanier, T. C. (1984). Thermally induced gelation of selected comminuted muscle systems-rheological changes during processing, final strengths and microstructure. *Journal of Food Science, 49*(6), 1496–1505. https://doi.org/10.1111/j.1365-2621.1984.tb12830.x.

Mudalal, S., Babini, E., Cavani, C., & Petracci, M. (2014). Quantity and functionality of protein fractions in chicken breast fillets affected by white striping. *Poultry Science, 93*(8), 2108–2116. https://doi.org/10.3382/ps.2014-03911.

OECD, 2018. Meat consumption (indicator). doi:https://doi.org/10.1787/fa290fd0-en.

Ovissipour, M., Rasco, B., Tang, J., & Sablani, S. S. (2013). Kinetics of quality changes in whole blue mussel (Mytilus edulis) during pasteurization. *Food Research International, 53*(1), 141–148. https://doi.org/10.1016/j.foodres.2013.04.029.

Rizvi, A. F., & Tong, C. H. (1997). Fractional conversion for determining texture degradation kinetics of vegetables. *Journal of Food Science, 62*(1), 1–7. https://doi.org/10.1111/j.1365-2621.1997.tb04356.x.

Sin, G., & Gernaey, K. (2016). Data Handling and parameter estimation. In M.C.M. van Loosdrecht, P.H. Nielsen, C.M. Lopez-Vazquez, & D. Brdjanovic (Eds.), *Experimental Methods in Wastewater Treatment* (pp. 201–234). Chapter 5. IWA Publishing Company.

Steinfeld, J. I., Francisco, J. S., & Hase, W. L. (1999). *Chemical kinetics and dynamics*. Upper Saddle River: Prentice Hall.

Thussu, S., & Datta, A. K. (2012). Texture prediction during deep frying: a mechanistic approach. *Journal of Food Engineering, 108*(1), 111–121. https://doi.org/10.1016/j.jfoodeng.2011.07.017.

Tornberg, E. (2005). Effects of heat on meat proteins—implications on structure and quality of meat products. *Meat Science, 70*(3), 493–508. https://doi.org/10.1016/j.meatsci.2004.11.021.

Van Boekel, M. A. J. S. (1996). Statistical aspects of kinetic modeling for food science problems. *Journal of Food Science, 61*(3), 477–485. https://doi.org/10.1111/j.1365-2621.1996.tb13138.x.

Van Boekel, M. A. J. S. (2008). Kinetic modeling of food quality: a critical review. *Comprehensive Reviews in Food Science and Food Safety, 7*(1), 144–158. https://doi.org/10.1111/j.1541-4337.2007.00036.x.

Wattanachant, S., Benjakul, S., & Ledward, D. A. (2005). Effect of heat treatment on changes in texture, structure and properties of Thai indigenous chicken muscle. *Food Chemistry, 93*(2), 337–348. https://doi.org/10.1016/j.foodchem.2004.09.032.

Zell, M., Lyng, J.G., Cronin, D.A., Morgan, D.J., (2010). Ohmic cooking of whole turkey meat - Effect of rapid ohmic heating on selected product parameters. *Food Chem 120*, 724–729. https://doi.org/10.1016/j.foodchem.2009.10.069.

Publication 2

Rabeler, F., & Feyissa, A. H. (2018). Modelling the transport phenomena and texture changes of chicken breast meat during the roasting in a convective oven. *Journal of Food Engineering*, *237*.

DOI: https://doi.org/10.1016/j.jfoodeng.2018.05.021

Due to merging of files, the inserted publication does not follow the page numbering of the overall document but instead the page numbering of the journal.

Journal of Food Engineering 237 (2018) 60–68

Contents lists available at ScienceDirect

Journal of Food Engineering

journal homepage: www.elsevier.com/locate/jfoodeng

Modelling the transport phenomena and texture changes of chicken breast meat during the roasting in a convective oven

Felix Rabeler, Aberham Hailu Feyissa*

Food Production Engineering, National Food Institute, Technical University of Denmark (DTU), Denmark

ARTICLE INFO

Keywords:
COMSOL multiphysics
Heat and mass transfer
Poultry meat
Quality prediction
Thermal processing
Transport phenomena in porous media

ABSTRACT

A numerical 3D model of coupled transport phenomena and texture changes during the roasting of chicken breast meat in a convection oven was developed. The model is based on heat and mass transfer coupled with the kinetics of temperature induced texture changes of chicken breast meat. The partial differential equations of heat and mass transfer as well as the ordinary differential equations that describe the kinetics of the texture changes were solved using COMSOL Multiphysics® 5.2a. The predicted temperature, moisture and texture (hardness, chewiness and gumminess) profiles were validated using experimentally values. The developed model enables the prediction of the texture development inside the chicken meat as function of the process parameters. The model predictions and measured values show the clear effect of changing process settings on the texture profiles during the roasting process. Overall, the developed model provides deep insights into the local and spatial texture changes of chicken breast meat during the roasting process that cannot be gained by experimentation alone.

1. Introduction

Heat treatment of chicken breast meat is a crucial processing step in households, professional kitchens and large-scale food industries to achieve a safe and high quality product. Roasting of chicken meat in a convection oven is a common process that involves simultaneous heat and mass transfer. However, the roasting affects the microstructure (Feyissa et al., 2013; Wattanachant et al., 2005), texture (Wattanachant et al., 2005) and appearance (Fletcher et al., 2000) of the product and, consequently, its acceptance by the consumer.

The texture of the chicken meat is the highest rated quality attribute for the consumer during consumption (Lawrie and Ledward, 2006) and it is mainly influenced by protein denaturation which leads to fiber shrinkage and straightening (Tornberg, 2005; Wattanachant et al., 2005). Consequently, the microstructure is becoming denser with compact fiber arrangements which results in the toughening of the chicken meat during the heating (Christensen et al., 2000; Lewis and Purslow, 1989; Wattanachant et al., 2005). Moreover, the protein denaturation leads to a reduction of the water holding capacity (WHC) of the chicken breast meat. The unbound water migrates into the spaces between the meat fibers which leads to a toughening of the meat and to the loss of water during the roasting process (Micklander et al., 2002; Tornberg, 2005).

The quality of the final product is mainly controlled by the chef or operator through adjustments of the process settings. However, this is still based on the cook-and-look approach, which relies on the experience and skills of the chef or operator. A number of researchers measured experimentally the texture change of poultry meat with temperature (Barbanti and Pasquini, 2005; Wattanachant et al., 2005; Zell et al., 2010) and Rabeler and Feyissa (2018) developed kinetic models to describe these changes with time. However, to gain the relationship between the process conditions and the texture development inside the chicken meat, the spatial temperature and time history during the roasting process is needed.

Mechanistic models of heat and mass transfer (based on fundamental physical laws) are able to predict the temperature and moisture distribution during the cooking process of meat (Feyissa et al., 2013; van der Sman, 2007), beef meat (Kondjoyan et al., 2013; Obuz et al., 2002) or poultry meat (Chang et al., 1998; van der Sman, 2013). However, for the roasting of chicken breast meat only a limited number of mathematical models are available.

Chen et al. (1999) developed a model of heat and mass transfer for convection cooking of chicken patties. In their model they described the transport of moisture inside the chicken patties by diffusion, which is a common approach for modelling mass transfer (Huang and Mittal, 1995; Isleroglu and Kaymak-Ertekin, 2016; Kassama et al., 2014). However, the moisture transport during the cooking process cannot be explained adequately by pure diffusion models (Feyissa et al., 2013; van

* Corresponding author. Søltofts Plads, 2800, Kgs. Lyngby, Denmark.
E-mail address: abhfe@food.dtu.dk (A.H. Feyissa).

https://doi.org/10.1016/j.jfoodeng.2018.05.021
Received 3 January 2018; Received in revised form 1 May 2018; Accepted 22 May 2018
Available online 22 May 2018
0260-8774/

der Sman, 2007). Roasting of chicken breast meat leads to protein denaturation, the shrinkage of the protein network and the reduction of the water holding capacity. This induces a pressure gradient inside the meat and the expulsion of the excess moisture to the surface of the meat.

This approach was used by van der Sman (2013) to model the cooking of chicken breast meat in an industrial tunnel oven. The author showed that the model is able to predict the temperature and moisture development inside the chicken meat for cooking temperatures below the boiling point. However, the presented cooking temperatures (45–100 °C) and times (up to 160 min) are not common settings for the roasting of chicken meat in industrial convection ovens, where hot dry air with more than 150 °C is employed (Chen et al., 1999; Guerrero-Legarreta and Hui, 2010).

Thussu and Datta (2012) showed that by coupling texture kinetics with physical based models of heat and mass transfer, the texture development during the frying of potato stripes can be predicted. However, for chicken breast meat or other muscle foods no attempt was made to couple kinetic models for textural changes with mechanistic models of heat and mass transfer to predict the local and spatial texture changes.

Therefore, the aim of this study is to first develop a mechanistic model to predict the temperature and moisture profiles of chicken breast meat during the roasting in a convection oven. Our hypothesis is then that by coupling the developed model for heat and mass transfer with the kinetic models of heat induced textural changes for chicken meat, the texture profile during the roasting process can be predicted as function of process parameters. Afterwards, the model predictions will be validated against experimental values.

2. Modelling of transport phenomena and texture changes

2.1. Process description and model formulation

Roasting in a convection oven is a thermal process, where the product is heated at high temperatures (150–300 °C) by circulated hot air. The main mechanisms during the roasting of chicken breast meat in a convective oven are illustrated in Fig. 1. Heat is transferred mainly through convection from the surrounding circulated hot air while a conductive heat flux comes from the roasting tray (bottom of chicken breast). The surrounding oven walls are made of polished stainless steel, thus, the effect of radiation is small compared to the convective transport (see section 3.2.1) (Feyissa et al., 2013). The effect of radiation was included in the model by using an estimated effective heat transfer coefficient (combined convective and radiative heat transfer coefficient, see section 3.2.1) (Kondjoyan and Portanguen, 2008; Sakin-Yilmazer et al., 2012; Zhang and Datta, 2006). The heat is then internally transferred by conduction and convection.

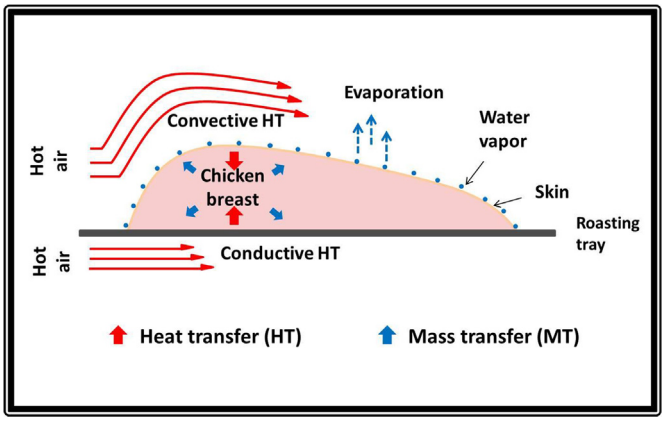

Fig. 1. Schematic illustration of the main mechanisms during the roasting of chicken breast meat in a convection oven.

Water migration within the product takes place by diffusion and convection mechanisms. The latter is a result of the heat induced protein denaturation and shrinkage of the protein network, which results in the decrease of the water holding capacity and a pressure gradient inside the chicken meat. This so called swelling pressure is the driving force for the convective water transport inside the meat and can be described by Darcy's law for flow through porous media (van der Sman, 2007). Liquid water that is expelled to the product surface is then evaporated to the surrounding hot air.

From the measured temperature profiles inside the chicken meat we observed that the temperature stays below the evaporation temperature and only a thin crust is formed during the roasting. Thus, internal evaporation of water was neglected in this study. Furthermore, the following basic assumptions are made to formulate the governing equations for the coupled heat and mass transfer: fat transport inside the chicken meat is negligible (since the fat content is less than 1% in chicken breast meat), evaporated water consists of pure water (no dissolved matter, measured similar to Feyissa et al. (2013)) and no internal heat generation.

2.2. Governing equations

2.2.1. Heat transfer

The heat transfer within the chicken breast meat is given by Eq. (1) (Bird et al., 2007)

$$c_{p,cm}\,\rho_{cm}\,\frac{\partial T}{\partial t} = \nabla(k_{cm}\,\nabla T) - \rho_w\,c_{p,w}\,u_w\,\nabla T \tag{1}$$

where $c_{p,cm}$ and $c_{p,w}$ are the specific heat capacities of chicken meat and water (J/(kg K)), respectively, ρ_{cm} and ρ_w are the densities of chicken meat and water (kg/m^3), respectively, k_{cm} is the thermal conductivity of chicken breast meat (W/(m K)), u_w the velocity of the fluid (m/s), T is the temperature (K) and t is the time (s).

2.2.2. Mass transfer

The governing equation for water transport is based on the conservation of mass and is given by Eq. (2) (Bird et al., 2007)

$$\frac{\partial C}{\partial t} = \nabla(-D\,\nabla C + C\,u_w) \tag{2}$$

where C is the moisture concentration (kg of water/kg of sample) and D is the moisture diffusion coefficient (m^2/s).

Darcy's law gives the relationship between moisture transport and pressure gradient inside a porous medium (in this case meat) and the velocity of the fluid inside the chicken meat can be expressed as

$$u_w = \frac{-\kappa}{\mu_w}\nabla p \tag{3}$$

where κ is the permeability of the chicken meat (m^2), μ_w is the dynamic viscosity of the fluid (Pa s) and ∇p is the pressure gradient vector (Pa/m). The swelling pressure is given by Eq. (4) (Barrière and Leibler, 2003; van der Sman, 2007)

$$p = G'(C - C_{eq}) \tag{4}$$

with G' the storage modulus and C_{eq} the water holding capacity of chicken breast meat.

By inserting the expression for the swelling pressure (Eq. (4)) into Eq. (3) the following expression results for the fluid velocity u_w:

$$u_w = \frac{-\kappa\,G'}{\mu_w}\nabla(\,C - C_{eq}) \tag{5}$$

The storage modulus varies with temperature and was described by with a sigmoidal function (Eq. (6)) (Rabeler and Feyissa, 2018):

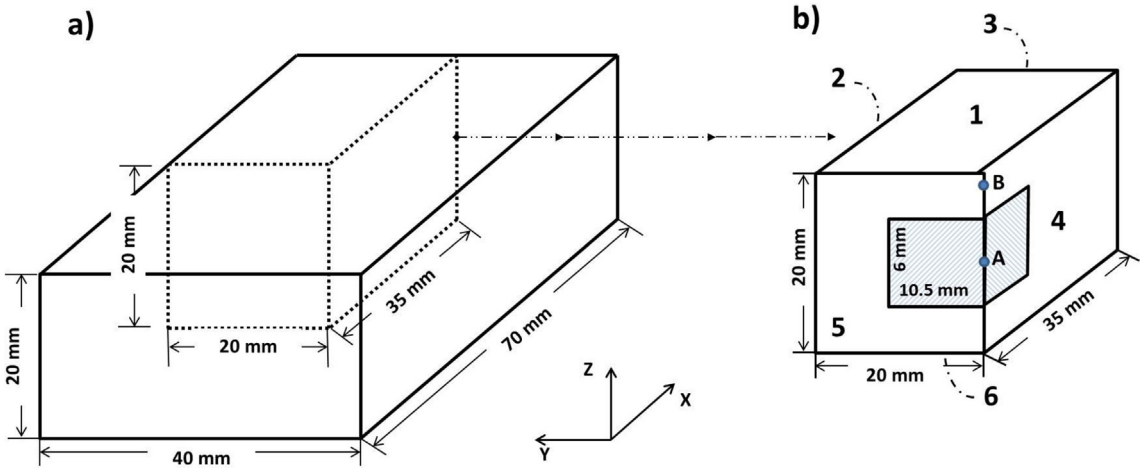

Fig. 2. Schematic illustration of (a) the rectangular chicken meat sample and (b) the geometry used in the developed model. The points: A (0, 0, 10 mm) and B (0, 0, 19 mm) indicate the position of the two thermocouples and the striped part shows the domain for the texture validation.

$$G' = G'_{max} + \frac{(G'_0 - G'_{max})}{1 + \exp\left(\frac{T - \overline{T}}{\Delta T}\right)} \tag{6}$$

with $G'_{max} = 92$ kPa (the maximum value of the storage modulus for chicken meat), $G'_0 = 13.5$ kPa (the initial value of the storage modulus), $\overline{T} = 69$ °C and $\Delta T = 4$ °C.

The change in the water holding capacity with temperature is described by Eq. (7) (van der Sman, 2013):

$$C_{eq(T)} = y_{w0} - \frac{a_1}{1 + a_2 \exp(-a_3(T - T_\sigma))} \tag{7}$$

where $y_{w0} = 0.77$ is the initial water content of raw chicken meat, $T_\sigma = 315$ K, $a_1 = 0.31$, $a_2 = 30.0$ and $a_3 = 0.17$.

2.3. Initial and boundary conditions

We assume a uniform initial temperature (Eq. (8)) and moisture distribution (Eq. (9)) throughout the whole sample domain (Fig. 2b):

$$T(x, y, z, 0) = T_0 \tag{8}$$

$$C(x, y, z, 0) = C_0 \tag{9}$$

2.3.1. Heat transfer boundary condition

The boundaries 1, 2 and 3 (see Fig. 2) are exposed to the hot air and the heat flux is given by Eq. (10):

$$-k_{cm} \nabla T = h_{eff} (T_{oven} - T_{surf}) \tag{10}$$

where k_{cm} is the thermal conductivity of the chicken breast meat (W/(m K)), h_{eff} is the effective heat transfer coefficient (W/(m^2 K)), which is the sum of both the convective and radiative heat transfer (Sakin et al., 2009) (see section 3.2.1), T_{oven} is the oven temperature (K) and T_{surf} is the surface temperature (K) of the chicken breast meat.

At boundary 6 the chicken meat is in contact with the roasting plate and a heat flux at this boundary is given by Eq. (11):

$$-k_{cm} \nabla T = h_{bot} (T_{oven} - T_{bot}) \tag{11}$$

with the heat transfer coefficient h_{bot} and bottom surface temperature T_{bot} (W/(m^2 K)).

Boundaries 5 and 4 are symmetry boundary conditions.

2.3.2. Mass transfer boundary condition

The water evaporation at the boundaries 1, 2, 3 and 6 is given by Eq. (12):

$$-D \nabla C + C u_w = \beta_{tot} (C_{surf} - C_{oven}) \tag{12}$$

where β_{tot} is the mass transfer coefficient (m/s), C_{surf} is the water vapor concentration at the surface of the meat (kg/kg) and C_{oven} the water vapor concentration in the air flow inside the oven.

van der Sman (2013) reported that the top layer (epimysium connective tissue) of the chicken breast meat becomes glassy during the roasting which results in an increased resistance against water evaporation. To take this into account the author formulated a mass transfer coefficient β_{skin} (Eq. (13)) which is dependent on the local moisture content at the surface of the chicken breast meat.

$$\beta_{skin} = \beta_1 y_w^b \tag{13}$$

where β_1 and b are 0.040 [m/s] and 4.0, respectively (van der Sman, 2013).

The total mass transfer coefficient is then given by Eq. (14):

$$\frac{1}{\beta_{tot}} = \frac{1}{\beta_{ext}} + \frac{1}{\beta_{skin}} \tag{14}$$

where β_{ext} refers to the external mass transfer coefficient which is calculated using the Lewis relation (Eq. (15)):

$$\beta_{ext} = \frac{h}{\rho_a c_{p,a} Le^{2/3}} \tag{15}$$

Boundaries 5 and 4 are symmetry boundary conditions.

2.4. Thermo-physical properties

The thermo-physical properties of chicken breast meat were described as function of composition and temperature (including the effect of fiber direction) (Choi and Okos, 1986). For the thermal conductivity we assume that all fibers are oriented along the x-axis (see Fig. 2) of the chicken breast. The thermal conductivity parallel to the fibers ($k_{cm,\parallel}$) is calculated using the parallel model (Eq. (16)) and for the thermal conductivity perpendicular to the fibers ($k_{cm,\perp}$), we assume the serial model (Eq. (17)).

$$k_{cm,\parallel} = \sum k_i \phi_i \tag{16}$$

$$\frac{1}{k_{cm,\perp}} = \sum \frac{\phi_i}{k_i} \tag{17}$$

where k_i and ϕ_i are the thermal conductivities (W/(m K)) and volume fractions of the each component i (water, protein, fat and ash), respectively.

The specific heat capacity (J/(kg K)) of chicken meat is calculated using Eq. (18)

$$c_{p,\,cm} = \sum y_i\, c_{p,\,i} \tag{18}$$

where y_i and $c_{p,i}$ are the mass fraction and specific heat capacity of each component i (water, protein, fat and ash), respectively.

2.5. Kinetic model for texture changes

A modified reaction rate law, which is taking into account that foods retain a non-zero equilibrium even after long heating times, was used to describe the texture (hardness, gumminess and chewiness) changes of chicken breast meat with temperature and time (for details see (Rabeler and Feyissa, 2018)) (Eq. (19)):

$$\frac{\partial Q}{\partial t} = k\,(Q_\infty - Q)^n \tag{19}$$

where Q is the quality attribute, Q_∞ is the final non-zero equilibrium quality value after long heating times, k is the reaction rate constant (min^{-1} $[Q]^{1-n}$) and n the reaction order.

The temperature dependence of the reaction rate constant is described by the Arrhenius equation as followed (Eq. (20)):

$$k = k_0 e^{-\frac{E_a}{R\,T}} \tag{20}$$

with k_o the pre-exponential factor (min^{-1} $[Q]^{1-n}$), E_a the activation energy in J/mol, R is the universal gas constant (8.314 J/(mol K)) and T is the temperature in K.

The modified reaction rate law is coupled with the model for heat and mass transfer (section 2.4), allowing the prediction of the texture parameters hardness, gumminess and chewiness from the local temperature development with time. The estimated activation energies, pre-exponential factors and reaction orders by Rabeler and Feyissa (2018) were used to solve Eqs. (19) and (20).

2.6. Model solution

The coupled PDEs of heat and mass transfer (equations described in section 2.4) and the kinetic models (ODEs) that describe the quality changes (hardness, gumminess and chewiness) (section 2.5) were implemented and solved using the finite element method (FEM) in the commercial software, COMSOL Multiphysics 5.2a. The model input parameters are shown in Table 1. A rectangular geometry with the dimensions illustrated in Fig. 2b was built in COMSOL and meshed. Mesh sensitivity analysis was conducted, where the mesh size was decreased in a series of simulations until it had no further impact on the model solution (Kumar and Dilber, 2006).

3. Materials and methods

3.1. Sample preparation and oven settings

Chicken breast meat (skinless and boneless) was purchased from a local supermarket the same day as the experiments and stored in plastic bags at 4 °C until it was used. For all roasting experiments, the chicken breasts were cut into rectangular blocks with the dimensions of 0.04 m × 0.02 m x 0.07 m and a weight of 63 g ± 2 g. The fiber direction for all samples was along the x-axis (see Fig. 2).

A professional convection oven with roasting chamber dimensions of 0.45 m × 0.50 m x 0.65 m was used for the roasting experiments. Dry hot air was circulated inside the roasting chamber by a fan, while the fan speed (air speed) could be adjusted. The oven temperature was controlled by the oven thermostat and additionally two thermocouples were placed at different positions in the oven to measure the oven temperature continuously. The measured oven temperature was stable around the set point with a standard deviation of ± 3 °C. Before each experimental run, the oven was preheated to the desired temperature for 30 min to ensure steady state conditions. The following process settings were used to show the effect of process conditions on the temperature, moisture and texture profile and to validate the developed model:

Setting I: T_{oven} = 170 °C, high fan speed (HF)
Setting II: T_{oven} = 230 °C, high fan speed (HF)
Setting III: T_{oven} = 230 °C, low fan speed (LF)

3.2. Experimental data

3.2.1. Heat transfer coefficient

The combined heat transfer coefficient, which is the sum of the radiative and convective heat transfer coefficient, was estimated using the lumped method (Sakin et al., 2009). The oven was preheated for 30 min before the experiments to ensure steady state conditions. Polished silver and black painted aluminum blocks (rectangular) were placed in the oven and heated for 20 min at 200 °C. The temperature in the center of the blocks was recorded continuously by using a thermocouple. As the Biot number was smaller than 0.1 the lumped heat transfer method was used and the combined heat transfer coefficient estimated as described by Feyissa et al. (2013). Only minor differences

Table 1
Model input parameters.

Parameter	Symbol	Value	Unit	Source
Density				
chicken meat	ρ_{cm}	1050	kg/m^3	Calculated from (Choi and Okos, 1986)
water	ρ_w	998	kg/m^3	
Diffusion coefficient	D	3×10^{-10}	m^2/s	(Ngadi et al., 2006)
Permeability	κ	3×10^{-17}	m^2	(Datta, 2006)
Viscosity water	μ_w	0.988×10^{-3}	Pa s	
Initial composition				
Water	y_{w0}	0.76	kg/kg	Measured
Protein	y_{p0}	0.22	kg/kg	(Barbanti and Pasquini, 2005)
Fat	y_{f0}	0.01	kg/kg	(Barbanti and Pasquini, 2005)
Ash	y_{a0}	0.01	kg/kg	(Barbanti and Pasquini, 2005)
Latent heat of vaporization of water	H_{evap}	2.3×10^6	J/kg	
Initial meat temperature	T_0	6	°C	Measured
Initial moisture concentration	C_0	0.76	kg/kg	Measured
Water vapor concentration in ambient air	C_{air}	0.05	kg/kg	Measured
Heat transfer coefficient				
High fan speed	h_{eff}	44	W/(m^2 K)	Measured
	h_{bot}	59	W/(m^2 K)	
Low fan speed	h_{eff}	21	W/(m^2 K)	Measured
	h_{bot}	41	W/(m^2 K)	

(less than 5%) between the estimated heat transfer coefficients for the black and polished aluminum block was found. This means that the radiative heat transfer from the oven walls is small compared to the convective heat transfer. Furthermore, the heat flux by radiation (assuming T_{oven} = 200 °C, $\varepsilon_{chicken}$ = 0.8, T_{surf} = 100 °C) is small (≈2% of the total flux) compared to the convective heat flux. In the model the estimated effective heat transfer coefficient, which includes the radiative effect, was used as described by Kondjoyan and Portanguen (2008), Sakin-Yilmazer et al. (2012) or Zhang and Datta (2006).

3.2.2. Local temperature

In order to measure the temperature profile inside the chicken meat sample, two thermocouples were placed at the center (point A, Fig. 2b)) and close to surface (point B, Fig. 2b) of the sample. One sample was then placed centrally on the roasting tray and the tray positioned in the middle of the oven. The temperature development was measured as function of time with sample intervals of 5 s for 15 min (for setting II, see section 3.1) and 20 min (for setting I and III).

3.2.3. Moisture content

To compare the predicted and measured moisture content at different time steps, roasting experiments were performed with different times: 1, 3, 5, 7, 10 and 15 min for all process settings. For setting I and III (see section 3.1), an additional sample was taken at 20 min of roasting. The samples were taken out of the oven after the corresponding roasting time, sealed in plastic bags and placed in ice water to stop further water loss from the surface. The average moisture content of the whole chicken meat sample was then measured using the oven drying method (Bradley, 2010). The samples were minced, weighed in aluminum cups and dried for 24 h at 105 °C. From the weight difference before and after the drying, the moisture content of the chicken meat samples was calculated.

3.2.4. Texture measurements

To validate the predicted texture development, roasting experiments were conducted at different time steps: 3, 5, 7, 10, 15 and 20 min (20 min only for Settings I and III, see section 3.1). After the roasting process, the samples were immediately placed in ice water for 4 min to cool them down quickly. The samples were then stored at room temperature for 2 h in sealed aluminum cups before the texture measurements.

To measure the textural changes of chicken breast meat, double compression tests (TPA) were performed according to the procedure described by Rabeler and Feyissa (2018). A cylindrical probe with a height of 6 mm ± 0.5 and a diameter of 21 mm ± 1 was cut out of the middle of the roasted chicken samples using a cork borer. The same sample dimension as in Rabeler and Feyissa (2018) were used for the TPA measurements. The samples were compressed to a final strain of 40%, setting the test speed to 1 mm/s with time interval of 5s between the first and second stroke. The TPA parameters hardness, gumminess and chewiness were then calculated from the recorded force-time plot (Bourne, 2002).

3.3. Statistical analysis

The chi-square test was used to evaluate the goodness-of-fit between the model predictions and the experimental data for the temperature, moisture and texture (Eq. (21)) (Taylor, 1997):

$$\chi^2 = \sum_{i=1}^{n} \frac{(\hat{\theta}_i - \theta_i)^2}{\sigma_i^2} \tag{21}$$

with $\hat{\theta}$ the predicted value, θ the measured value and σ the standard deviation. A significance level of $P < 0.05$ was used.

Furthermore, the root mean squared error (RMSE) was calculated by using Eq. (22):

$$RMSE = \sqrt{\frac{\sum_{i=1}^{n} (\hat{\theta}_i - \theta_i)^2}{n}} \tag{22}$$

where n is the total number of samples.

4. Results and discussion

4.1. Temperature and moisture predictions

Fig. 3 presents the predicted core (at position A, Fig. 2b) and surface (at position B. Fig. 2b) temperature as well as the predicted average moisture content as function of the roasting time for the different process settings (Fig. 3a for setting I, Fig. 3b for setting II, and Fig. 3c for setting III). A good agreement between the measured (symbols) and predicted (solid lines) temperature profiles at the core (*RMSE* = 1.85, 0.83 and 0.99 °C for setting I, II and III, respectively) and close to the surface (*RMSE* = 3.76, 2.69 and 2.6 °C for setting I, II and III, respectively) was found for all tested process settings. Furthermore, the model showed a high accuracy in the prediction of the average moisture content development of the chicken meat sample with *RMSE* values of 1.15, 1.39 and 0.91% for setting I, II and III, respectively (χ^2 = 4.78, 4.66 and 3.97, respectively, $P > 0.05$) (see also Fig. 3a and c).

The process conditions have an influence on the temperature and moisture content profile during the roasting process. Chicken breast meat should be heated to a core (coldest point) temperature of 75 °C to ensure a safe product for the consumers (Fsis, 2000). The time needed to reach this temperature in the core varies with the process settings: 12.5 min, 10 min and 13 min roasting time for setting I (T_{oven} = 170 °C and high fan speed, Fig. 3a), setting II (T_{oven} = 230 °C and high fan speed, Fig. 3b) and setting III (T_{oven} = 230 °C and low fan speed, Fig. 3c), respectively.

The higher temperature and fan speed for setting II compared to setting I and III, respectively, leads to an increased heat flux from the surrounding hot air to the sample surface. Consequently, the surface temperature is rising faster, which also leads to a faster increase of the core temperature. However, the high surface temperature for setting II results in an increased evaporation of moisture from the chicken meat surface. Therefore, a lower average moisture content is reached for setting II ($C_{av}(t = 10min) \approx 66\%$, Fig. 3b) compared to setting I ($C_{av}(t = 12.5\,min) \approx 69\%$, Fig. 3a) and setting III ($C_{av}(t_{75°C} = 13\,\text{min}) \approx 70\%$).

Setting I and III show a similar temperature and moisture content development with roasting time (Fig. 3a and c, respectively). This is reasonable as the heat flux from the surrounding hot air to the chicken meat surface is comparable for the two settings ($\dot{q}$ = 3080, 5720 and 2730 W/m^2 for setting I, II and III, respectively) (see Eqs. (12) and (13)). Thus, the times to reach 75 °C in the core as well as the moisture contents at this time step are comparable.

4.2. Prediction of texture changes

By coupling the model for heat and mass transfer with the kinetics for textural changes, it is possible to predict the spatial and local texture change inside the chicken meat from the local temperature development. Fig. 4 presents the simulated temperature and texture distributions inside the chicken meat during the roasting in the convection oven (for setting II, T_{oven} = 230 °C and high fan speed) for 5 min (Fig. 4a and c) and 10 min (Fig. 4b and d). The results illustrate that the development of the texture parameter hardness, but also the development of the other studied texture parameters (gumminess and chewiness, not shown here), is following the temperature changes. The high heat flux from the surrounding hot air is leading to a fast temperature increase of the chicken meat surface (see also Fig. 3b). This subsequently, results in a fast hardening of the chicken meat at the surface. On the contrary, the internal heat transfer is slow (Bi = 1.1 > 0.1), which leads to a

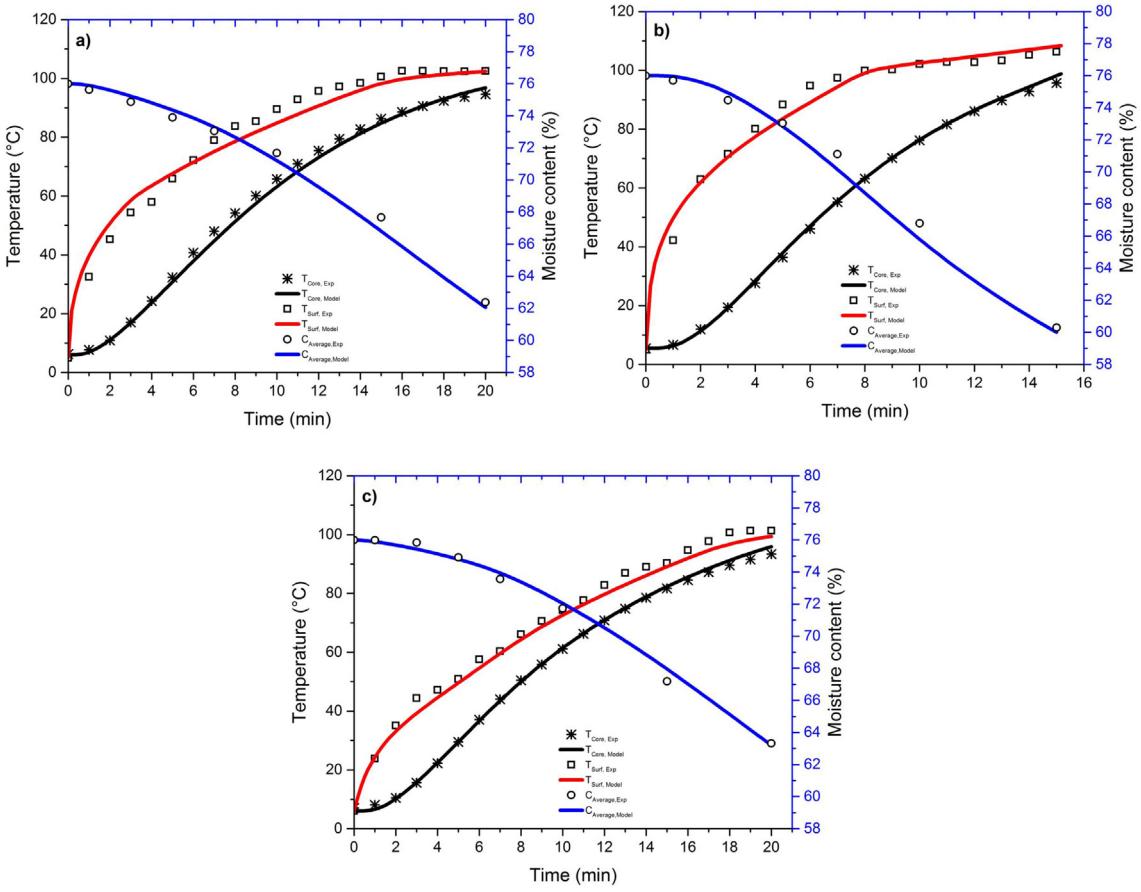

Fig. 3. Comparison between the predicted and measured temperature (core and surface) and moisture development of the chicken meat sample with varying air temperature and fan speed: a) Setting I: T_{oven} = 170 °C, high fan speed; b) Setting II: T_{oven} = 230 °C, high fan speed; c) Setting III: T_{oven} = 230 °C, low fan speed.

delayed heat up towards the center of the chicken meat. Accordingly, the hardness at the center is changing slower compared to the surface.

Overall, it becomes obvious that the non-uniform temperature development of the chicken meat sample results in the non-uniform texture profiles. The developed model is, therefore, a strong tool to predict the spatial texture development as function of the process conditions and roasting time which is difficult or even not possible to obtain by experimentation alone.

4.3. Effect of process parameters on the texture profile and model validation

In order to study the influence of the oven settings on the texture development of chicken breast meat and to validate the developed model, simulations with two different oven temperatures (230 °C and 170 °C) and fan speeds were compared (see process settings in section 3.1). The predictions of the texture development with roasting time were validated against experimental values that were obtained according to section 3.2.4. Fig. 5a and c shows that a good agreement between the predicted (solid lines) and experimental measured texture changes (hardness, gumminess and chewiness) (symbols) of chicken breast meat was found for all tested process settings. The *RMSE* and χ^2 values for hardness, gumminess and chewiness are summarized in Table 2. The results further show that the model is able to accurately predict the texture changes of chicken breast meat during roasting for all tested process settings.

The oven temperature has a high influence on the texture (hardness, gumminess and chewiness) profiles (Fig. 5a and c). A higher value of T_{oven} leads to an increased heat flux from the surrounding hot air to the chicken meat surface (see Eq. (10) and Eq. (11)) which results in a faster heat up of the sample (see also Fig. 3a and b). Therefore, the texture parameters (that are a function of the local temperature development with time) start to rise earlier for the oven temperature of 230 °C (red line) compared to 170 °C (black line) (setting II and I, respectively).

A higher fan speed results in a higher heat transfer coefficient (h_{eff} and h_{bot}, see Table 1) which leads to an increased heat flux to the chicken meat surface (see Eq. (10) and Eq. (11)). Accordingly, the texture parameter rise earlier for the high fan speed (black lines, Fig. 4) compared to the low fan speed (blue lines).

However, only a slight difference in the predicted profiles for hardness, gumminess and chewiness was found between the oven settings I and III (see section 3.1). This is reasonable as a similar temperature development of the two different oven settings was found (compare Fig. 3a with 3c), which results in the similar texture changes.

The predicted changes of the storage modulus with heating time for the tested process settings are presented in Fig. 6. A similar trend between the storage modulus and the TPA parameters hardness, gumminess and chewiness development with time was found for all tested process settings (compare Fig. 6 with Fig. 5a–c). Setting II (230 °C, high fan speed) leads to an earlier rise of the storage modulus compared to the lower oven temperature (setting I) and lower fan speed (setting III). Similar to the TPA parameters development only slight differences in the storage modulus development was observed between setting I and III (see Fig. 6). However, we found that the storage modulus starts to rise later (around 55 °C) compared to the texture parameters hardness, gumminess and chewiness (around 45 °C) (compare Fig. 6 with Fig. 5a–c). This earlier increase of the TPA parameters could be due to the earlier decrease of the water holding capacity at around 40 °C which leads to a water release into the pore spaces between the meat fibers (Micklander et al., 2002; van der Sman, 2013). Consequently, parts of

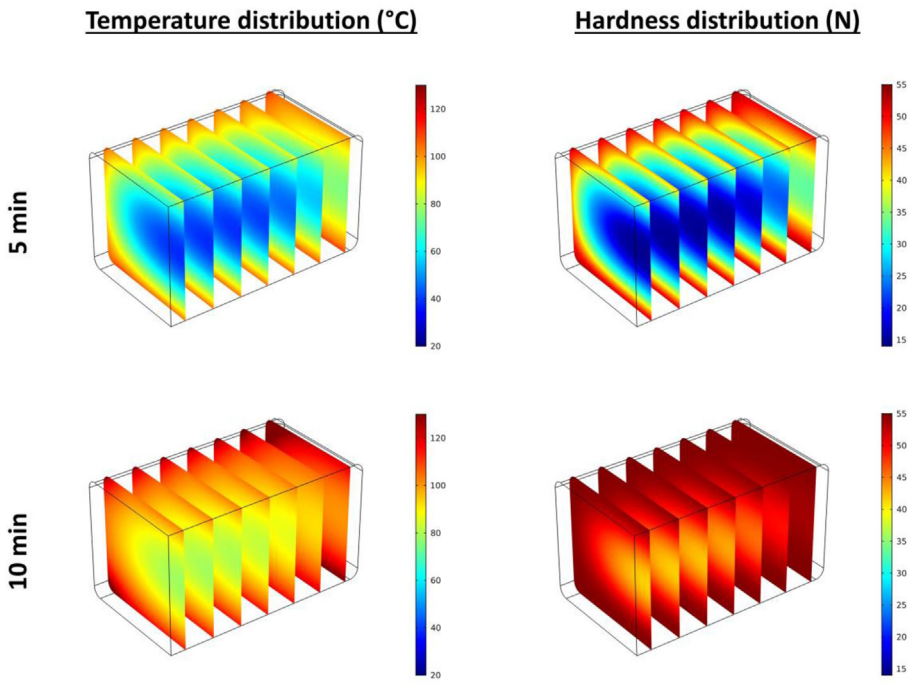

Fig. 4. Visualization of the simulated temperature and hardness distribution during the roasting process: a) temperature profile at $t = 5$ min; b) temperature profile at $t = 10$ min; c) hardness profile at $t = 5$ min; d) hardness profile at $t = 10$ min. Setting II: $T_{oven} = 230$ °C, high fan speed.

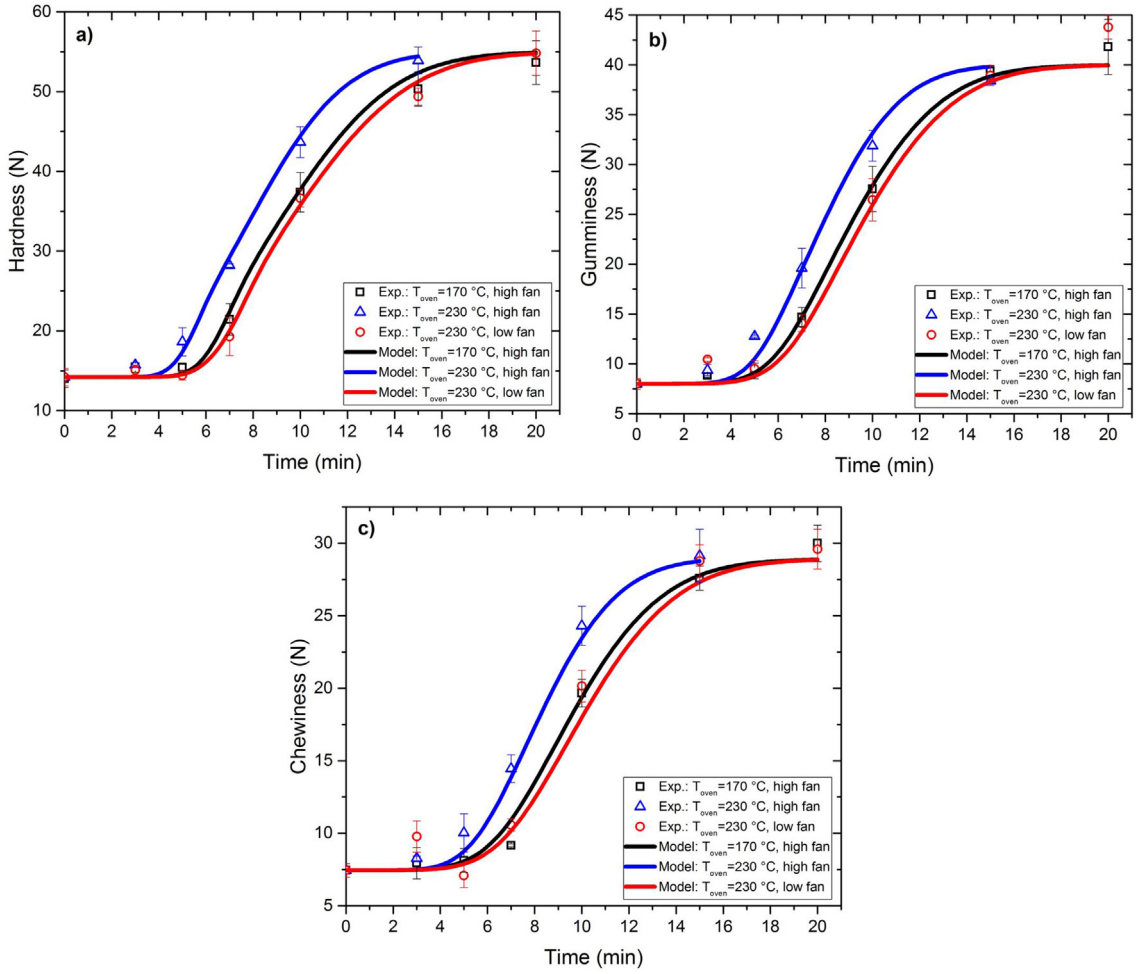

Fig. 5. Effect of process settings on the texture changes of chicken breast meat and comparison between predicted (lines) and experimental values (symbols): a) hardness (N), b) gumminess, c) chewiness. Bars indicate the standard deviation (n = 3).

Table 2
RMSE and χ^2 values for hardness, gumminess and chewiness for process setting I, II, and III.

	Hardness		Gumminess		Chewiness	
	RMSE	χ^2	*RMSE*	χ^2	*RMSE*	χ^2
Setting I	2.06 N	7.12	1.79 N	2.35	2.12 N	7.50
Setting II	1.70 N	2.90	2.11 N	5.12	2.11 N	3.63
Setting III	2.25 N	6.20	2.08 N	6.33	2.73 N	7.17

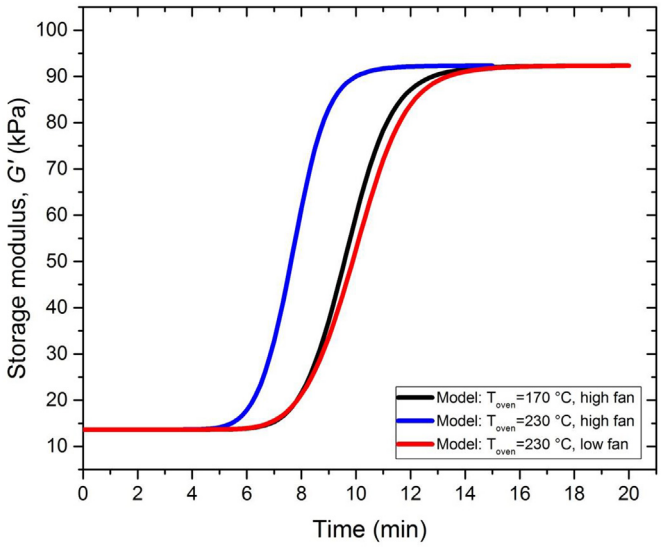

Fig. 6. Predicted storage modulus (*G′*) development with time for the oven settings I (black line), II (blue line) and III (red line). (For interpretation of the references to colour in this figure legend, the reader is referred to the Web version of this article.)

the compression energy (TPA measurements) could be dissipated as a result of the viscous flow of the fluid in the pore space which results in a toughening of the meat (Tornberg, 2005). However, deeper analyses of the heat induced changes in the microstructure of chicken breast meat are necessary to obtain a clear relationship between the storage modulus and the TPA parameters hardness, gumminess and chewiness.

Overall, the results show that by adjusting the oven settings, the texture of the chicken meat sample can be influenced. Consequently, the developed model can be used to control the quality (texture) of the product and to optimize the roasting process to obtain a safe final product with the highest quality for the consumer.

5. Conclusion

In this study, a mechanistic model of heat and mass transfer was developed for the roasting of chicken breast meat in a convection oven. The developed model was then coupled with the kinetics for heat induced texture changes. This enabled the prediction of the spatial and local texture development as function of the process parameters. The simulation results were validated against experimental obtained values. The developed model provides a more detailed understanding of the process mechanisms during roasting chicken breast meat.

We showed that the non-uniform temperature distribution inside the chicken meat sample during the roasting process, leads to a non-uniform texture profile. Furthermore, the clear effect of changing roasting parameters on the texture development was obtained. The developed model enables, thus, a deep insight into the effects of the process conditions on the texture changes of chicken breast meat that is difficult or even not possible to obtain by experimentation alone.

Nomenclature

a_w	water activity
C	mass concentration (kg/kg)
c_p	specific heat capacity (J/(kg K))
Cw	chewiness
D	diffusion coefficient (m^2/s)
E_a	activation energy (J/mol)
G'	storage modulus (Pa)
Gu	Gumminess
h	heat transfer coefficient (W/(m^2 K))
Ha	hardness (N)
k	reaction rate constant (1/min)
k_0	pre-exponential factor (1/min)
k_i	thermal conductivity (W/(m K))
M_w	molar weight of water (0.018 kg/mol)
n	number of samples
p	swelling pressure (Pa)
Q	quality attribute
R	universal gas constant (8.314 J/mol K)
T	temperature (K)
t	time (s)
u	velocity (m/s)
y	mass fraction
TPA	texture profile analyses
Bi	Biot number
RMSE	Root-mean-squared-error

Greek symbols

α	pre-factor (−)
β	mass transfer coefficient (m/s)
κ	permeability (m^2)
μ	dynamic viscosity (Pa s)
ρ	density (kg/m^3)
ϕ	volume fraction
$\widehat{\theta}_i$	predicted value (*T, C, Ha, Gu, Cw*)
θ_i	measured value (*T, C, Ha, Gu, Cw*)
σ	standard deviation
χ^2	chi-square value

Subscripts

a, f, p, w	ash, fat, protein, water
bot	bottom
cm	chicken meat
eff	effective
eq	equilibrium
ext	external
surf	surface
sat	saturation
tot	total
0	initial (t = 0)

References

Barbanti, D., Pasquini, M., 2005. Influence of cooking conditions on cooking loss and tenderness of raw and marinated chicken breast meat. LWT - Food Sci. Technol. (Lebensmittel-Wissenschaft -Technol.) 38, 895–901. http://dx.doi.org/10.1016/j.lwt.2004.08.017.

Barrière, B., Leibler, L., 2003. Kinetics of solvent absorption and permeation through a highly swellable elastomeric network. J. Polym. Sci., Part B: Polym. Phys. 41, 166–182. http://dx.doi.org/10.1002/polb.10341.

Bird, R.B., Stewart, W.E., Lightfoot, E.N., 2007. In: Wiley & Sons, John, Inc (Eds.), Transport Phenomena, 2n. ed. Revised.

Bourne, M.C., 2002. Principles of Objective Texture Measurement. Food Texture Viscosity Concept Meas, second ed. .

Bradley, R.L.J., 2010. Food analysis. In: Nielsen, S.S. (Ed.), Food Analysi. S. Springer-Verlag, West Lafayette, IN, USA, pp. 85–104.

Chang, H.C., Carpenter, J.A., Toledo, R.T., 1998. Modeling heat transfer during oven roasting of unstuffed turkeys. J. Food Sci. 63, 257–261. http://dx.doi.org/10.1111/j.

1365-2621.1998.tb15721.x.
Chen, H., Marks, B.P., Murphy, R.Y., 1999. Modeling coupled heat and mass transfer for convection cooking of chicken patties. J. Food Eng. 42, 139–146. http://dx.doi.org/10.1016/S0260-8774(99)00111-9.
Choi, Y., Okos, M.R., 1986. Effects of temperature and composition on the thermal properties of foods. Food Eng. Process Appl. 93–101.
Christensen, M., Purslow, P.P., Larsen, L.M., 2000. The effect of cooking temperature on mechanical properties of whole meat, single muscle fibres and perimysial connective tissue. Meat Sci. 55, 301–307. http://dx.doi.org/10.1016/S0309-1740(99)00157-6.
Datta, A.K., 2006. Hydraulic permeability of food tissues. Int. J. Food Prop. 9, 767–780. http://dx.doi.org/10.1080/10942910600596167.
Feyissa, A.H., Gernaey, K.V., Adler-Nissen, J., 2013. 3D modelling of coupled mass and heat transfer of a convection-oven roasting process. Meat Sci. 93, 810–820. http://dx.doi.org/10.1016/j.meatsci.2012.12.003.
Fletcher, D.L., Qiao, M., Smith, D.P., 2000. The relationship of raw broiler breast meat color and pH to cooked meat color and pH. Poultry Sci. 79, 784–788. http://dx.doi.org/10.1093/ps/79.5.784.
Fsis, U., 2000. Chicken from Farm to Table 1–8.
Guerrero-Legarreta, I., Hui, Y.H., 2010. In: In: Wiley & Sons, John, Inc (Eds.), Handbook of Poultry Science and Technology, vol. 2http://dx.doi.org/10.1002/9780470504475.
Huang, E., Mittal, G.S., 1995. Meatball cooking - modeling and simulation. J. Food Eng. 24, 87–100. http://dx.doi.org/10.1016/0260-8774(94)P1610-A.
Isleroglu, H., Kaymak-Ertekin, F., 2016. Modelling of heat and mass transfer during cooking in steam-assisted hybrid oven. J. Food Eng. http://dx.doi.org/10.1016/j.jfoodeng.2016.02.027.
Kassama, L.S., Ngadi, M.O., Campus, M., 2014. Pore development and moisture transfer in chicken meat during deep-fat frying. Dry. Technol. http://dx.doi.org/10.1081/DRT-200054239. 3937.
Kondjoyan, A., Oillic, S., Portanguen, S., Gros, J.B., 2013. Combined heat transfer and kinetic models to predict cooking loss during heat treatment of beef meat. Meat Sci. 95, 336–344. http://dx.doi.org/10.1016/j.meatsci.2013.04.061.
Kondjoyan, A., Portanguen, S., 2008. Prediction of surface and “under surface” temperatures on poultry muscles and poultry skins subjected to jets of superheated steam. Food Res. Int. 41, 16–30. http://dx.doi.org/10.1016/j.foodres.2007.07.006.
Kumar, A., Dilber, I., 2006. Fluid flow and its modeling using computational fluid dynamics. In: Sablani, S., Datta, A., Shafiur Rehman, M., Mujumdar, A. (Eds.), Handbook of Food and Bioprocess Modeling Techniques, Food Science and Technology. CRC Press. http://dx.doi.org/10.1201/9781420015072.
Lawrie, R.A., Ledward, D.A., 2006. Lawrie's Meat Science.
Lewis, G.J., Purslow, P.P., 1989. The strength and stiffness of perimysial connective tissue isolated from cooked beef muscle. Meat Sci. 26, 255–269. http://dx.doi.org/10.1016/0309-1740(89)90011-9.
Micklander, E., Peshlov, B., Purslow, P.P., Engelsen, S.B., 2002. NMR-cooking: monitoring the changes in meat during cooking by low-field 1H-NMR. Trends Food Sci. Technol. 13, 341–346. http://dx.doi.org/10.1016/S0924-2244(02)00163-2.
Ngadi, M., Dirani, K., Oluka, S., 2006. Mass transfer characteristics of chicken nuggets. Int. J. Food Eng. 2. http://dx.doi.org/10.2202/1556-3758.1071.
Obuz, E., Powell, T.H., Dikeman, M.E., 2002. Simulation of cooking cylindrical beef roasts. LWT - Food Sci. Technol. (Lebensmittel-Wissenschaft -Technol.) 35, 637–644. http://dx.doi.org/10.1006/fstl.2002.0940.
Rabeler, F., Feyissa, A.H., 2018. Kinetic modelling of texture and color changes during thermal treatment of chicken breast meat. Food Bioprocess Technol in press.
Sakin-Yilmazer, M., Kaymak-Ertekin, F., Ilicali, C., 2012. Modeling of simultaneous heat and mass transfer during convective oven ring cake baking. J. Food Eng. 111, 289–298. http://dx.doi.org/10.1016/j.jfoodeng.2012.02.020.
Sakin, M., Kaymak-Ertekin, F., Ilicali, C., 2009. Convection and radiation combined surface heat transfer coefficient in baking ovens. J. Food Eng. 94, 344–349. http://dx.doi.org/10.1016/j.jfoodeng.2009.03.027.
Taylor, J.R., 1997. An Introduction to Error Analysis: the Study of Uncertainties in Physical Measurements, second ed. University Science Books.
Thussu, S., Datta, A.K., 2012. Texture prediction during deep frying: a mechanistic approach. J. Food Eng. 108, 111–121. http://dx.doi.org/10.1016/j.jfoodeng.2011.07.017.
Tornberg, E., 2005. Effects of heat on meat proteins - implications on structure and quality of meat products. Meat Sci. 70, 493–508. http://dx.doi.org/10.1016/j.meatsci.2004.11.021.
van der Sman, R.G.M., 2013. Modeling cooking of chicken meat in industrial tunnel ovens with the Flory-Rehner theory. Meat Sci. 95, 940–957. http://dx.doi.org/10.1016/j.meatsci.2013.03.027.
van der Sman, R.G.M., 2007. Moisture transport during cooking of meat: an analysis based on Flory-Rehner theory. Meat Sci. 76, 730–738. http://dx.doi.org/10.1016/j.meatsci.2007.02.014.
Wattanachant, S., Benjakul, S., Ledward, D.A., 2005. Effect of heat treatment on changes in texture, structure and properties of Thai indigenous chicken muscle. Food Chem. 93, 337–348. http://dx.doi.org/10.1016/j.foodchem.2004.09.032.
Zell, M., Lyng, J.G., Cronin, D.A., Morgan, D.J., 2010. Ohmic cooking of whole Turkey meat - effect of rapid ohmic heating on selected product parameters. Food Chem. 120, 724–729. http://dx.doi.org/10.1016/j.foodchem.2009.10.069.
Zhang, J., Datta, A.K., 2006. Mathematical modeling of bread baking process. J. Food Eng. 75, 78–89. http://dx.doi.org/10.1016/j.jfoodeng.2005.03.058.

Publication 3

Rabeler, F., & Feyissa, A. H. (2019). Modelling of food processes under uncertainty: Mechanistic 3D model of chicken meat roasting. *Journal of Food Engineering*, *262*, 49–59.

DOI: https://doi.org/10.1016/j.jfoodeng.2019.05.006

Due to merging of files, the inserted publication does not follow the page numbering of the overall document but instead the page numbering of the journal.

Journal of Food Engineering 262 (2019) 49–59

Contents lists available at ScienceDirect

Journal of Food Engineering

journal homepage: www.elsevier.com/locate/jfoodeng

Modelling of food processes under uncertainty: Mechanistic 3D model of chicken meat roasting

Felix Rabeler, Aberham Hailu Feyissa*

Food Production Engineering, National Food Institute, Technical University of Denmark (DTU), Denmark

ARTICLE INFO

Keywords:
Heat and mass transfer
Monte Carlo method
Morris screening
Standardized regression coefficients
Transport phenomena in porous media
Global uncertainty and sensitivity analysis

ABSTRACT

Mathematical models that describe the transport phenomena and quality changes of foods during processing contain several uncertain model input parameters which result in uncertain model predictions. The objective of this study was to evaluate the impact of uncertain input parameters on the model predictions of the mechanistic 3D model of chicken meat roasting and to identify as well as rank the most important model parameters. We found that the uncertainty in the model output variables varies with roasting time, but also among the different output variables, by using the Monte Carlo method. To decompose the variance with respect to the input parameters, the method of standardized regression coefficients (SRC), a global sensitivity analysis method, was used. Consequently, the uncertain input parameters were ranked according to their relative impact. The results of the SRC method were compared with the Morris screening, a one-step-at-a-time (OAT) global sensitivity analysis method. The comparison of the two applied sensitivity methods showed that the ranking of the input parameters is similar, while the Morris screening is more efficient computational wise. Finally, we illustrate how the results of the analyses can be used for model refinement as well as to highlight parameters and areas where further research is necessary.

1. Introduction

The development of mathematic models to predict the heat and mass transfer during the baking or cooking of foods became an essential research field in food engineering. Models enable enhanced process control and make the scale-up easier. Additionally, the physics and mechanisms inside the foods during processing can be studied in a way that is not possible by experimentation alone (Datta, 2015).

However, mechanistic models that predict the transport phenomena during roasting processes of food products are rather complex. This is due to the highly coupled mechanisms of heat and mass transfer and the resulting physical-chemical changes. These are for example the evaporation of water and the following internal pressure increase, the chemical reactions leading to a browning of the surface or the denaturation of proteins causing a change in the microstructure of the food product. Detailed explanations of different roasting models are given for example by Feyissa et al. (2013) (pork meat roasting); Goñi and Salvadori (2011) (beef meat roasting); Jha (2005) (grain roasting); Rabeler and Feyissa (2018a) (chicken meat roasting) or van der Sman (2007) (beef meat roasting). To model these complex mechanisms many model input parameters and variables are necessary.

In a recent study we presented a mechanistic 3D model for the roasting of chicken breast meat in a convective oven, where the texture profile inside the chicken meat was predicted from the local temperature development with time (Rabeler and Feyissa, 2018a). To describe the transport phenomena and quality changes, approximately 130 input parameters and variables are needed. For chicken breast meat, however, not all input parameters are available that are necessary to describe the heat and mass transfer during the roasting or the values come with a large inherit uncertainty. This is due to the natural variation of the chicken meat tissue, but also from the fact that many phenomena that happen during the roasting are not fully understood. The uncertainties in the input parameters, however, affect the accuracy of the developed model, leading to uncertainties in the model predictions.

Uncertainty analysis techniques allow the evaluation of the propagation of uncertainty in the developed model. The impact of the uncertain input parameters on the model predictions can be determined and, consequently, the reliability of the model studied. Sensitivity analysis allows then the decomposition of the obtained variance in the model output in respect to the input parameters. In details, the contribution of each studied input parameter to the output variance is obtained and the parameters can be ranked according to their relative influence on the model output. By running both methods in tandem, the robustness of the developed model can be determined and a

* Corresponding author. Søltofts Plads, 2800, Kgs, Lyngby, Denmark.
E-mail addresses: felra@food.dtu.dk (F. Rabeler), abhfe@food.dtu.dk (A.H. Feyissa).

https://doi.org/10.1016/j.jfoodeng.2019.05.006
Received 31 October 2018; Received in revised form 16 March 2019; Accepted 7 May 2019
Available online 11 May 2019
0260-8774/

Nomenclature

a_w	water activity
b	evaporation parameter
C	mass concentration (kg/kg)
c_p	specific heat capacity (J/(kg K))
Cw	chewiness (N)
D	diffusion coefficient (m^2/s)
EE	Elementary Effect
F	distribution of Elementary Effects
G'	storage modulus (Pa)
h	heat transfer coefficient (W/(m^2 K))
Ha	hardness (N)
k	thermal conductivity (W/(m K))
T	temperature (K)
t	time (min)
u	velocity (m/s)
sY	output variable (vector)

Greek symbols

β	mass transfer coefficient (m/s)
ε_{im}	the error of the regression model
κ	permeability (m^2)
ρ	Density (kg/m^3)
θ	uncertain input parameters (vector)
μ	Mean of observed Elementary Effects
σ	Standard deviation of Elementary Effects
Δ	perturbation factor

Subscripts

0	initial condition (at t = 0 min)
bot	bottom
cm	chicken meat
eq	equilibrium
ext	external
i	index of Monte Carlo simulations (vector)
j	index of the parameter vector
m	index of output vector
surf	surface
w	water
eff	effective

fundamental understanding of the relationships between the input parameters and output variables can be achieved (Saltelli, 2006; Sin et al., 2009). Furthermore, the obtained information from the uncertainty and sensitivity analysis can be used in the following ways: prioritization of further research and experimental work by focusing efforts on parameters that mainly influence the model output; refinement and reduction of the model by describing the most influencing parameters as accurate as possible while fixing parameters with low impact; and for optimization of the studied process by concentrating on the most influencing process settings (Saltelli, 2006; Saltelli et al., 2007).

In food science mainly local sensitivity analysis techniques are applied to study the influence of one uncertain input parameter with small variations around their nominal value on the model predictions (Gulati and Datta, 2016; Ousegui et al., 2010; Purlis and Salvadori, 2009). Local sensitivity analyzing techniques vary only one input parameter at a time (one-factor-at-a-time, OAT), while the other parameters are kept constant at their nominal value. The corresponding changes of the output variables are then evaluated (Dimov and Georgieva, 2010). This requires relatively low computational effort and is most of the time easy to implement (Feyissa et al., 2012). However, as local sensitivity analysis varies only one parameter at a time, it is not possible to evaluate the effect of the whole uncertain input parameter space on the model predictions or to detect possible interactions between 2 or more uncertain input parameters (Czitrom, 1999).

Global sensitivity techniques, on the contrary, vary all uncertain input parameters at a time. Thus, the impact of all uncertain input parameters, with their corresponding uncertainty range, on the model predictions can be studied (Dimov and Georgieva, 2010). This means, however, that the implementation often takes more time and the computational burden is higher.

In food science only a few authors studied the global uncertainty and sensitivity of mathematical models (e.g. 2D modelling of contact baking process (Feyissa et al., 2012)), while it already became a common routine in other disciplines like for environmental models (Campolongo and Saltelli, 1997), ecological models (Cariboni et al., 2007), wastewater treatment (Sin et al., 2011) or risk assessment (Gargalo et al., 2016).

The objective of this work is, therefore, to study the impact of the uncertain model input parameters on the predictions (temperature, moisture and texture) of the mechanistic 3D model of chicken meat roasting in a convective oven and to identify the parameters with the highest relative impact. Different global sensitivity analysis methods are compared and the impact of the sampling method and size on the sensitivity analysis is studied. The results of the analyses are then discussed in terms of model refinement and reduction as well as possibilities for process optimization.

2. Methodology

2.1. Modelling the roasting of chicken breast meat

The roasting of chicken breast meat in a convection oven involves coupled heat and mass transfer, with a convective heat flux from the surrounding hot air to the sample surface, internal transfer of the heat by convection and conduction, water migration within the product by diffusion and convection, and evaporation of liquid water from the surface to the surrounding hot air (Rabeler and Feyissa, 2018a).

The governing equations for heat and mass transfer are given by Eq. (1) and Eq. (2), respectively (Bird et al., 2007):

$$\text{Heat transfer: } c_{p,cm}\,\rho_{cm}\frac{\partial T}{\partial t} = \nabla(k_{cm}\,\nabla T) - \rho_w\,c_{p,w}\,u_w\,\nabla T \tag{1}$$

$$\text{Mass transfer: } \frac{\partial C}{\partial t} = \nabla(-D\,\nabla C + C\,u_w) \tag{2}$$

where $c_{p,i}$ is the specific heat capacity (J/(kg K)), ρ_i the density (kg/m^3), k_i is the thermal conductivity (W/(m K)), T is the temperature (K), u_w the fluid velocity (m/s), C the moisture content (kg of water/kg of product), D the water diffusion coefficient (m^2/s) and t the time (s).

The main moisture transport inside the chicken breast meat results from a pressure gradient due to protein denaturation and shrinkage of the protein network and is given by Darcy's law in the following form (Eq. (3)) (Rabeler and Feyissa, 2018a):

$$u_w = \frac{-\kappa}{\mu_w}\nabla \mathrm{P} \tag{3}$$

with the permeability κ (m^2), the dynamic viscosity of water μ_w (Pa s) and the swelling pressure P (Pa). The boundary conditions for the heat and mass transfer at the boundaries 1, 2, 3 and 6 (see Fig. 1) are described in Eqs. (4) and (5):

$$-k_{cm}\nabla T = h\,(T_{air} - T_{surf}) \tag{4}$$

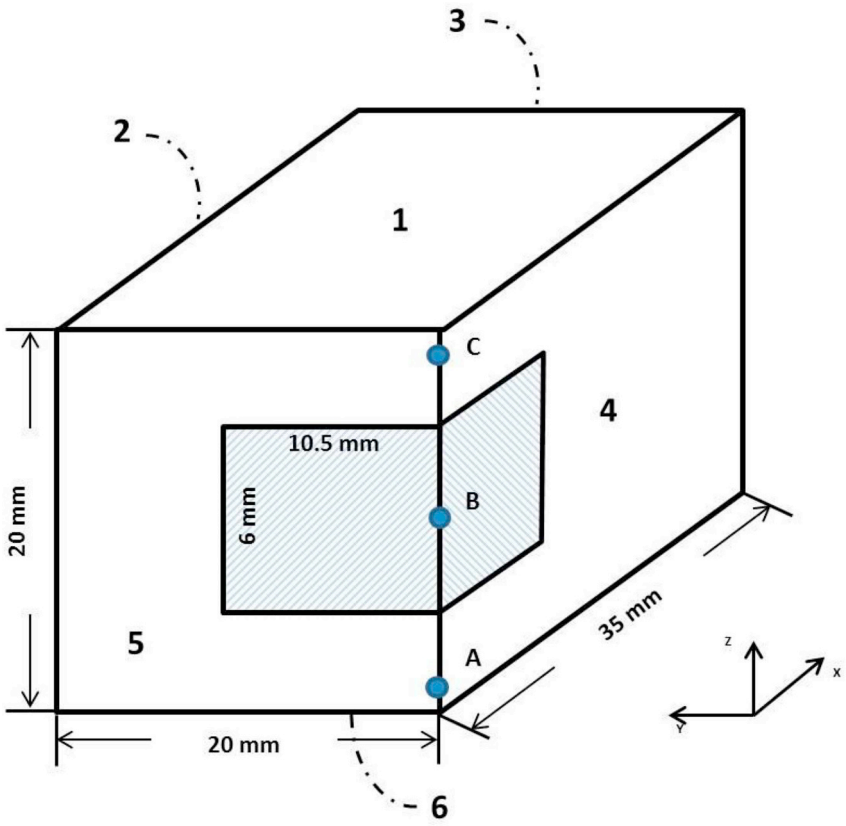

Fig. 1. Schematic illustration of the geometry that was used in the model.

$$-D\,\nabla C + C\,u_w = \beta_{tot}\,(C_{surf} - C_{air}) \tag{5}$$

The heat transfer coefficient (h) at the boundaries 1, 2 and 3 is h_{eff} (combined convective and radiative heat transfer) and at boundary 6 the heat transfer coefficient is h_{bot}. The mass transfer coefficient β_{tot} is described by Eq. (6):

$$\frac{1}{\beta_{tot}} = \frac{1}{\beta_{ext}} + \frac{1}{\beta_{skin}} \text{ with } \beta_{skin} = \beta_1\,C^b \tag{6}$$

where β_{ext} is the eternal mass transfer coefficient (m/s), which is calculated with the Lewis relation (Rabeler and Feyissa, 2018a) and β_{skin} is a mass transfer coefficient that depends on the moisture content (C) and the two fitting parameters β_1 and b.

The boundaries 4 and 5 are symmetry boundary conditions. For a detailed description of the developed model, the reader is referred to Rabeler and Feyissa (2018a).

The texture changes (hardness and chewiness) of chicken breast meat with temperature and roasting time were described with a modified rate law (Rabeler and Feyissa, 2018b) (Eq. (7)):

$$\frac{\partial Q}{\partial t} = k\,(Q_\infty - Q)^n \tag{7}$$

with the quality attribute Q, the non-zero equilibrium value Q_∞, the reaction order n and the reaction rate constant k ($\text{min}^{-1}\,[\text{Q}]^{1-\text{n}}$). The temperature dependency of the reaction rate constant was described with the common Arrhenius equation (Rabeler and Feyissa, 2018b). A detailed description of the model can be found in Rabeler and Feyissa (2018b).

2.2. Model output variables

In total 8 output variables were taken into consideration for the uncertainty and sensitivity analyses as described in section 2.4 and 2.5. The temperature was evaluated at 3 different positions inside the chicken meat sample (see Fig. 1): position A(0,0,1 mm) the bottom temperature (T_A), position B(0,0,10 mm) the core temperature (T_{core}) and position C(0,0,19 mm) the top surface temperature (T_C). Besides the temperature, the volume average moisture content (C_{av}), the moisture content at point A (C_A) and the moisture content at point B (C_B) of chicken meat sample was evaluated as well as the volume average of the texture parameters hardness (Ha) and chewiness (Cw) (Rabeler and Feyissa, 2018b). All the selected output variables are represented by the vector Y as: $Y = [T_A, \text{T}_{\text{core}}, T_C, C_{av}, C_A, C_C, Ha, Cw]$.

2.3. Model input variables

In total 12 uncertain model input parameters were identified, where only a limited amount of data is available, or the values have a large uncertainty. The variation in those uncertain parameters was taken into consideration for the uncertainty and sensitivity analyses. The uncertain input parameters are associated with the following: (1) Initial conditions (T_0 and C_0), (2) boundary conditions (T_{air}, h_{eff}, h_{bot}, C_{air} and b), (3) chicken meat properties (ρ_{cm}, $c_{p,cm}$ and k_{cm}) and (4) transfer coefficients (D and κ). The vector θ represents all the uncertain input parameters, where $\theta = [T_0, C_0, T_{air}, h_{eff}, h_{bot}, C_{air}, b, \rho_{cm}, c_{p,cm}, k_{cm}, D, \kappa]$.

2.4. Uncertainty analysis

The well-established Monte Carlo technique was used in this study to determine the uncertainty in the model outputs resulting from the uncertainty in the model input (Helton, 1993; Metropolis and Source, 1949). The method was chosen as it is computationally effective and reliable (Helton and Davis, 2003; Sin et al., 2009). The Monte Carlo method consists of three steps: (1) identification of uncertain input parameters and specification of the input uncertainty, (2) generation of samples from the input space and (3) model evaluation with sampled

input uncertainty with statistical analysis of the results (Feyissa et al., 2012). The individual steps are described in detail in the following sections.

2.4.1. Step 1: specifying uncertainty in input parameters

The first step, the selection of the uncertainty range of the uncertain input parameters, is the most important step in the Monte Carlo procedure. The uncertainty range was selected after a subjective expert review process of the literature data, experimental data and expert assumptions (Table 1). For the experimental gained input parameters (marked with *) the range from the measurements was taken. For the remaining uncertain input parameters three classes with low, medium and high uncertainties were defined with 5, 15 and 30% variability around the mean value, respectively. For the permeability (κ) of meat products only limited knowledge is available in literature. Consequently, the broader range as reported by Datta (2006) and Feyissa et al. (2013) was chosen (see Table 1). For all input parameters a uniform probability distribution within the specified range was assumed.

2.4.2. Step 2: sampling

Three different sampling methods, the Halton sequence, the Latin hypercube sampling as well as the Sobol sequence were used in this study to evaluate the influence of the sampling method on the standardized regression coefficients (see section 2.5.1). A detailed description of the Halton sequence and Sobol sequence is given by Kocis and Whiten (1997) and for the Latin hypercube sampling by Helton and Davis (2003).

The sampling was performed from the corresponding input parameter intervals (Table 1) which results in a θ_{NxM} sample matrix (Feyissa et al., 2012):

$$\begin{bmatrix} \theta_1 \\ \vdots \\ \theta_i \\ \vdots \\ \theta_N \end{bmatrix} = \begin{bmatrix} \theta_{11},\ \theta_{21},\ \theta_{31},\ ...,\ \theta_{M1} \\ \vdots \\ \theta_{1i},\ \theta_{2i},\ \theta_{3i},\ ...,\ \theta_{Mi} \\ \vdots \\ \theta_{1N},\ \theta_{2N},\ \theta_{3N},\ ...,\ \theta_{MN} \end{bmatrix} \tag{8}$$

where θ_i is the sample value of the corresponding uncertain input parameter, M is the total number of uncertain input parameters ($M = 12$ for this study) and N the total number of samples. The sample size in this study (N) was varied from 20 to 1000 samples until it had no further influence on the sensitivity analysis results.

Table 1
Uncertainty ranges for the input parameters.

Parameter	Unit	Nominal value	Source	Range	
				Minimum	Maximum
T_0*	K	277	(a)	275	283
C_0*	kg/kg	0.77	(a)	0.73	0.81
T_{oven}**	K	503	(a)	478	528
h_{eff}***	W/(m^2 K)	40	(a)	34	46
h_{bot}***	W/(m^2 K)	55	(a)	49.5	60.5
C_{air}*	kg/kg	0.05	(a)	0.01	0.1
b***	–	4	(e)	3.4	4.6
ρ_{cm}**	kg/m^3	1050	(b)	997.5	1102.5
$c_{p,cm}$**	J/(kg K)	3591	(b)	3411	3771
k_{cm}**	W/(m K)	0.54	(b)	0.51	0.57
κ	m^2	1×10^{-17}	(c)	1×10^{-18}	1×10^{-16}
D****	m^2/s	3×10^{-10}	(d)	2.1×10^{-10}	3.9×10^{-10}

Source: (a) measured; (b) calculated from Choi and Okos (1986); (c) obtained from Datta (2006) and Feyissa et al. (2013); (d) obtained from Ngadi et al. (2006); (e) obtained from van der Sman (2013).
*Obtained from measurement; ** ± 5% of the nominal value; *** ± 15% of the nominal value; **** ± 30% of the nominal value.

2.4.3. Step 3: model evaluation and statistical analyses

The obtained matrix, θ_{NxM}, with the sampled input parameters was propagated by performing dynamic simulations for N input samples of M input parameters (each row of θ generated one simulation). The coupled governing equations for heat and mass transfer (a system of partial differential equations, PDEs) combined with constitutive equations, as well as the ordinary differential equations (ODE) that describe the texture changes of chicken breast meat were solved. The model output variables were stored in the three-dimensional matrix Y_{GxKxN}. The matrix contained for each time instant G (10 s time steps from $t = 0$ to $t = 600$ s) the predictions of the K output variables (8 outputs) for a total number of N samples (Feyissa et al., 2012).

The results obtained from the model simulations were then analyzed and the mean as well as the 10th and 90th percentile of the output distributions were calculated for each output variables.

2.5. Global sensitivity analysis

The standardized regression coefficients method (SRC) and the Morris screening were used to evaluate the sensitivity of the uncertain input parameters on the model output variables. The simulation output variables (e.g., temperature, moisture content and texture changes) vary with time (dynamic profile). The sensitivity of the input parameters was, therefore, analyzed at two different time points, $t = 4$ min (heating dominant period) and $t = 8$ min (evaporation dominant period), corresponding to the middle and the end of the roasting process, respectively.

2.5.1. Standardized regression coefficients

The method of standardized regression coefficients (SRC) as described by Helton and Davis (2003) and Sin et al. (2009) was used to evaluate the sensitivity of the uncertain input parameters on the model output variables and to rank the parameters. Using the data from the Monte Carlo simulations (see section 2.4), linear regression models were constructed for every model output variable in Y (see section 2.2) using Eq. (9):

$$\frac{sY_{im} - \mu_{sym}}{\sigma_{sym}} = \sum_{j=1}^{M} \beta_{im} \frac{\theta_{ij} - \mu_{\theta j}}{\sigma_{\theta j}} + \varepsilon_{im} \tag{9}$$

where θ is the vector with the input parameters (see section 2.3), m is the index of the output vector sY, i is the index of the Monte Carlo simulations (samples), j is the index of the input parameter vector θ, ε is the error of the linear regression model, β_{im} is the standardized regression coefficient (SRC) and M is the total number of uncertain input parameters. For a linear model the following condition holds for the standardized regression coefficient: $\sum_i (\beta_{im})^2 = 1$. In most cases, $\sum_i (\beta_{im})^2 \leq 1$ and it is equal to the coefficient of determination R^2 (Saltelli et al., 2007; Sin et al., 2011). To apply the SRC method, $\sum_i (\beta_{im})^2$ or R^2 should be above the recommended value of 0.7 to ensure a necessarily linear model (Cariboni et al., 2007).

2.5.2. Morris screening

The Morris screening is a one-step-at-a-time (OAT) sensitivity analysis method, which means that only one input parameter is changed at each simulation run. By repeating these local changes for a predefined number of times, a global sensitivity analysis is achieved (Morris, 1991). The method is relatively simple to implement, and the obtained results can be interpreted easily. Furthermore, it is typically computationally efficient compared to other sensitivity analysis methods (i.e. fewer sample numbers needed) (Campolongo and Saltelli, 1997; Saltelli, 2004).

With the Morris method the distribution of the so-called Elementary Effects (EE) of the input parameters on the model output variables is estimated. The distribution of the effects of the jth model input parameter on the mth model output variable is denoted as F_{jm} (Sin et al.,

2009). The elementary effects EE_{jm} were estimated using Eq. (10) (Morris, 1991):

$$EE_{jm} = \frac{\partial sY_m}{\theta_j} = \frac{sY_m(\theta_1, \theta_2, \theta_j + \Delta, ..., \theta_M) - sY_m(\theta_1, \theta_2, \theta_j, ..., \theta_M)}{\Delta} \quad (10)$$

where $sY_m(\theta_1, \theta_2, \theta_j, \ldots, \theta_M)$ is the model output at the input parameters θ_1 to θ_M and $sY_m(\theta_1, \theta_2, \theta_j + \Delta, \ldots, \theta_M)$ is the model output where θ_j is changed by the predetermined perturbation factor Δ.

The range of the input parameters θ is divided into p levels and each input can only take values from these predefined levels. In this study p was set to 8, corresponding to the 12.5th percentile of the uniform input distributions (Ruano et al., 2011). Thus, the perturbation factor, Δ, had the value of $\Delta = p/(2(p\text{-}1)) = 4/7$. The elementary effects, EE_{jm}, were calculated at randomly sampled points in the input space and the procedure repeated for a number of predefined repetitions, r (Sin et al., 2009). By following this one-factor-at-a-time design (OAT), which was proposed by Morris, a total of $r^*(M+1)$ model simulations are necessary. In this study, the number of repetitions, r, was increased until it had no further influence on the analysis results. A detailed description of the Morris sampling is given by Sin et al. (2009).

Finally, the means (μ) of the distributions of the calculated elementary effects as well as the standard deviations (σ) were estimated. Both sensitivity parameters were then used to rank the input parameters according to their influence on the model output. The model input parameters with low μ and low σ values can be considered as non-influential on the model outputs (Morris, 1991). Furthermore, the graphical approach as proposed by Morris was used to evaluate the input parameters influence. The mean, μ, and the standard deviation, σ_i, are plotted together with two lines which correspond to $\mu_i = \pm 2sem_i$. The standard error of means (sem) is calculated as $sem_i = \sigma_i/\sqrt{r}$ (Morris, 1991).

2.6. Model implementation and solution

COMSOL Multiphysics® 5.3 with MATLAB® was used to solve the coupled PDEs of heat and mass transfer (see section 2.1) as well as the ODEs of the texture kinetics (see section 2.1), and to perform the uncertainty and sensitivity analysis.

3. Results and discussion

3.1. Uncertainty in the model outputs

The results of the uncertainty analysis are presented for the Halton sequence sampling method with a sample size of $N = 500$ samples (see section 3.2). From the raw data obtained by the Monte Carlo simulations, the mean 10th and 90th percentile was calculated for every model output variable at each time point. Figs. 2–4 present the results for the temperature, moisture and texture output variables, respectively. A higher band or spread in the distribution can be related directly to a higher uncertainty in the model prediction.

The temperature profiles at the position A (close to the bottom), T_A, and at position C (close to the surface), T_C, show a similar trend (Fig. 2a and c, respectively). At the start of the cooking process, the uncertainties in the temperature predictions are increasing with time (heating dominant region), while they are decreasing again when the temperature is leveling off around the boiling temperature of water (evaporation dominant region). The heat transfer at the bottom of the chicken meat (in contact with roasting plate) is higher compared to the surface and, consequently, T_A is increasing faster than T_C. Accordingly, the lowest uncertainty for T_A was found after 6 min of roasting, while for T_C the evaporation dominant region is just reached at the end of the process (after 10 min of roasting) (Fig. 2a and c, respectively). The uncertainty of the core temperature predictions (T_{core}), on the contrary,

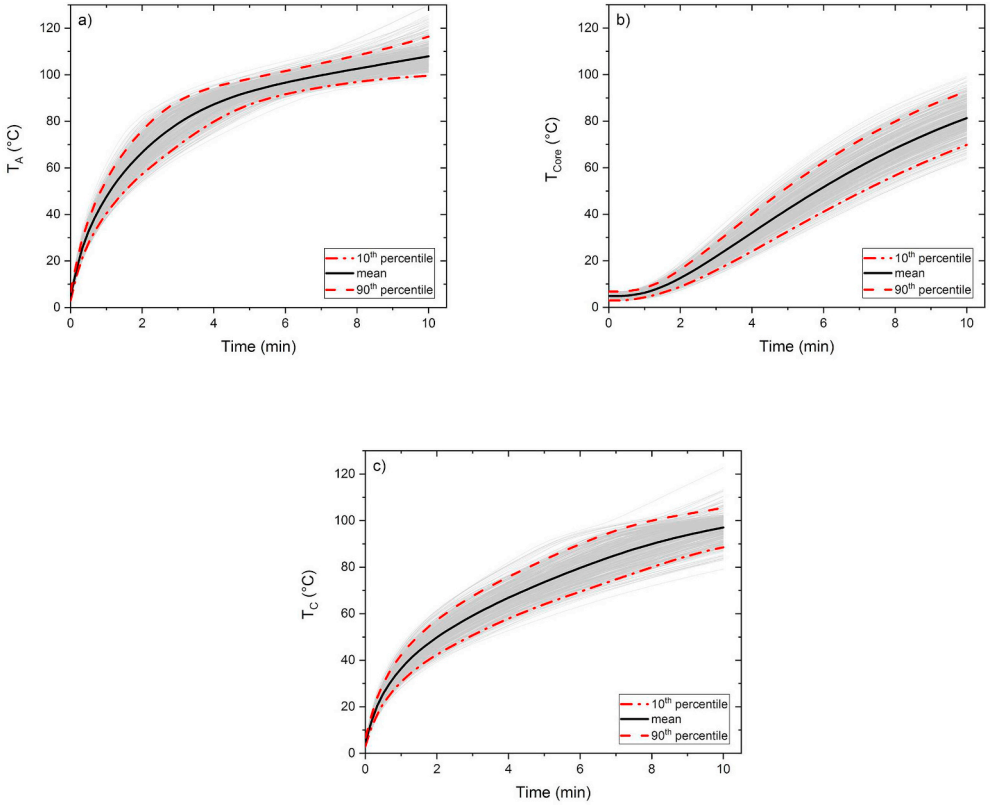

Fig. 2. Uncertainty of the predicted temperature development using mean, 10th and 90th percentile: a) bottom temperature (position A), b) core temperature (position B) and c) surface temperature (position C). The 500 Monte Carlo simulations are shown in grey.

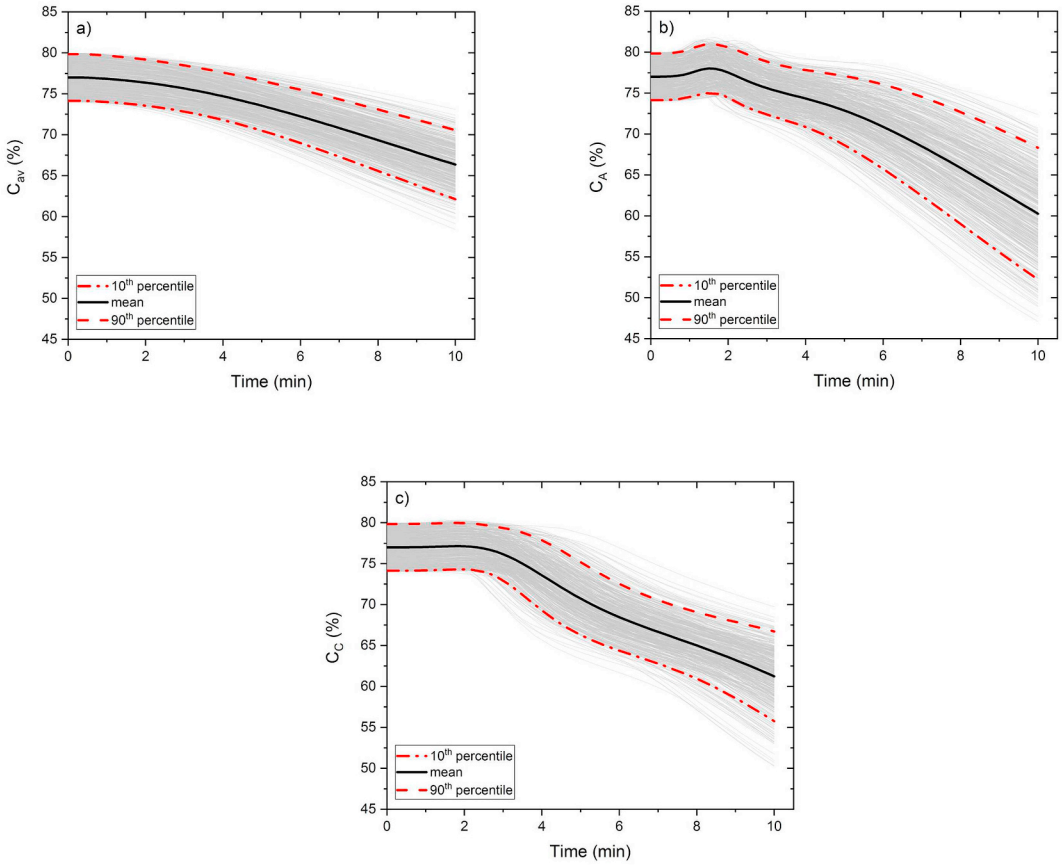

Fig. 3. Uncertainty of the predicted moisture content development using mean, 10th and 90th percentile: a) average moisture content, b) moisture content close to the bottom (position A) and c) moisture content close to the surface (position C). The 500 Monte Carlo simulations are shown in grey.

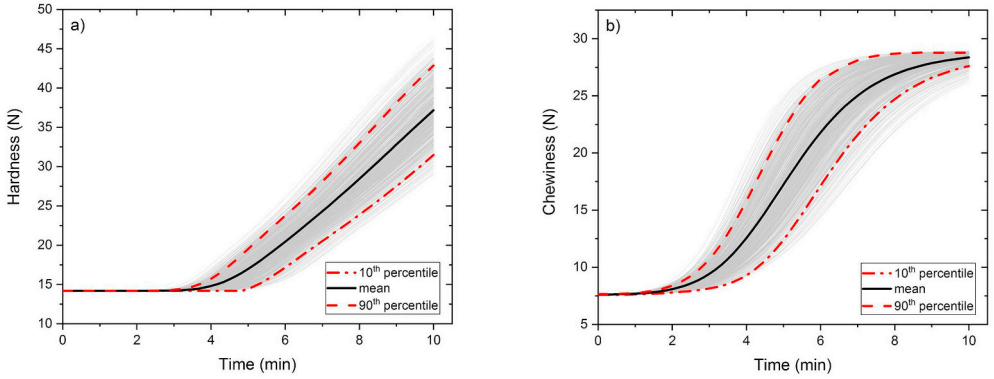

Fig. 4. Uncertainty of the predicted development of the texture parameters a) hardness (*Ha*) and b) chewiness (*Cw*) using mean, 10th and 90th percentile. The 500 Monte Carlo simulations are shown in grey.

is increasing over the whole roasting time, with the highest uncertainty at the end of the process (Fig. 2b).

For the average moisture content of the chicken meat sample (C_{av}) the band for the uncertainty stays constant during the whole roasting process (Fig. 3a). A similar trend was found for the moisture content profile close to the surface (C_C) (Fig. 3c). For the moisture content close to the bottom (C_A) the spread and, consequently, the uncertainty is increasing towards the end of the roasting process (Fig. 3b).

The texture parameters hardness (*Ha*) and chewiness (*Cw*) are a function of the temperature development in the center part of the chicken meat sample (see striped part in Fig. 1). In the beginning of the roasting process the temperature is below the denaturation temperature of the proteins and, therefore, no change of *Cw* and *Ha* can be observed (Fig. 4a and b). With increasing roasting time, the temperature is rising inside the sample and, consequently, the texture parameters are increasing with time. In the beginning of the roasting process, chewiness (*Cw*) is more sensitive to the temperature changes (higher reaction rate (Rabeler and Feyissa, 2018b)) and, therefore, it starts to rise earlier compared to the hardness (*Ha*) (lower reaction rate). The uncertainty for chewiness is first increasing with time where after it is decreasing and levelling off again when the equilibrium value of this texture parameter is reached (Fig. 4b). After the texture parameter hardness starts to rise (approximately after 3.5 min), a constant uncertainty (band) was found along the roasting process (Fig. 4a).

3.2. Standardized regression coefficient (SRC) for global sensitivity analysis

A linear regression model was constructed for each model output variable (sY_i), by using the linear least square method, and the corresponding SRC coefficients were obtained at different time points (t = 4 min and t = 8 min, see section 2.5). As a first step, the influence of the sampling method Latin hypercube sampling, Sobol sequence and Halton sequence (see section 2.4.2)) as well as the sample number (N) on the standardized regression coefficients was studied. For clarity only the influence of the oven temperature (T_{oven}) on the SRC value of the core temperature (T_{core}) at the roasting time of 8 min is reported.

The impact of the sampling method and the sampling size and on the SRC value is shown in Fig. 5. For low sample numbers (20–100) a high discrepancy between the sampling methods can be seen, especially between the Halton and Sobol sequence. However, with increasing sample size the SRC value is reaching a constant value (dashed line in Fig. 5) faster for the Halton and Sobol sequence (N = 500) compared to the Latin hypercube sampling method (N = 1000). This shows that the Halton and Sobol sequence are computationally more efficient and should, therefore, be used instead of the Latin hypercube sampling. Accordingly, the further analyses are presented for the Halton sequence with a sample size of 500.

Tables 2–4 present the results of the SRC method for the temperature, moisture and texture output variables, respectively. Only the first 6 top input parameters that had the highest impact on the model outputs are reported here for clarity.

For all output variables the coefficient of determination, R^2, was found to be higher than 0.92, showing that a necessary degree of linearization was obtained. Therefore, the obtained SRC values can be used to evaluate the impact of the uncertainty in the input parameters (θ) on the output variables (sY) (see section 2.5.1).

The absolute SRC value shows directly the relative impact of the corresponding input parameter on the output variable, while a positive SRC value indicates a positive correlation and a negative SRC value indicates a negative correlation between model input and output.

3.2.1. Chicken meat temperature

After 4 min of roasting the temperatures close to the bottom, T_A, and close to the surface, T_C, are most sensitive to the oven temperature, T_{oven}, and the heat transfer coefficients (fan speeds), h_{bot} and h_{eff} (see Table 2). The positive SRC values indicate that higher oven temperatures and fan speeds lead to an increase of both the surface and the bottom temperature. This is reasonable as with a higher oven temperature and heat transfer coefficient, the heat flux from the surrounding hot air to the chicken meat surface is increasing, leading to the rise of the surface and bottom temperature (see Eq. (4)). Towards the end of the roasting process (t = 8 min) the parameters that are correlated to the moisture transport (κ) and evaporation (b) become more important. At this time point both temperatures reached the boiling temperature of water (around 100 °C, see Fig. 2a and c), and, therefore, the temperature is mainly controlled by the evaporation of the water from the surface of the chicken sample.

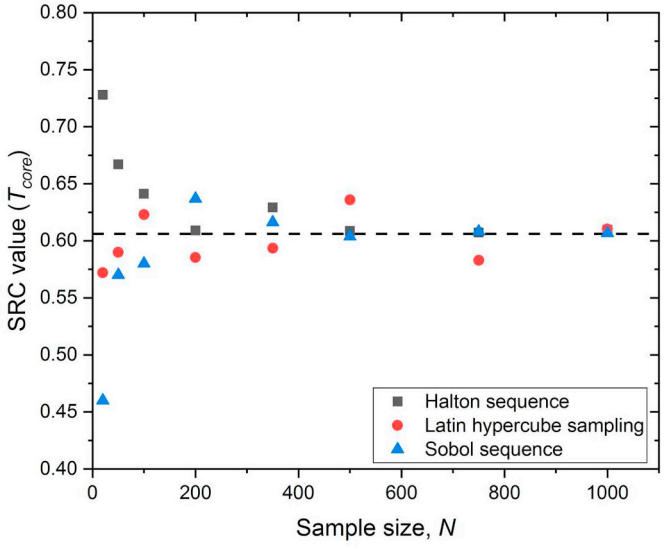

Fig. 5. Influence of the different sampling methods (Latin hypercube sampling, Halton sequence and Sobol sequence) and the sampling size on the resulting SRC value (input parameter: oven temperature T_{oven}; output variable: core temperature T_{core}) at the roasting time of 8 min. The dashed line shows the mean SRC value after 1000 simulations using the Halton sequence.

The core temperature, T_{core}, of the chicken meat sample is also most sensitive to the oven temperature, T_{oven}, with positive SRC values (positive correlation). The thermo-physical properties k_{cm} and $c_{p,cm}$ are ranked on the 2nd and 3rd rank, respectively. The SRC values for the thermal conductivity k_{cm} are positive, indicating the positive correlation between k_{cm} and T_{core}. This is reasonable as the thermal conductivity gives the rate of the heat transfer inside the chicken meat. This means that higher values of k_{cm} lead to a faster heat transfer and, consequently, a faster increase of the core temperature. The specific heat capacity, on the contrary, has a negative impact on the core temperature (negative SRC values). This means, that for lower values of $c_{p,cm}$, less heat is needed to increase the temperature of the chicken sample and, consequently, also the core temperature is rising faster.

3.2.2. Chicken meat moisture content

The ranking of the input parameters according their relative impact on the average moisture content (C_{av}), as well as the moisture contents at the positions A and C (C_A and C_C, respectively) is presented in Table 3 for the two time points of 4 and 8 min.

The average moisture content, C_{av}, is most sensitive to the initial moisture content (C_0) of the sample at both roasting time points. Higher values of C_0 directly result in higher values of C_{av}. The oven temperature (T_{oven}) and fan speed (h_{eff}) are at the second and third position in the ranking, respectively, both having a negative impact on C_{av}. This is reasonable, since increasing values of T_{oven} and h_{eff} lead to an increase in the evaporation of water from the sample surface, which results in the decrease of C_{av}.

After 4 min of roasting, the moisture content close to the top and bottom surface, C_C and C_A, respectively, are most sensitive to the initial moisture content C_0, followed by the permeability κ of the chicken meat, the oven temperature T_{oven} and the heat transfer coefficient (h_{eff} for C_C and h_{bot} for C_A) (Table 3). At 8 min, the moisture content close to the bottom, C_A, is most sensitive to the process parameters T_{oven} and h_{bot}., while the top surface moisture content, C_C, is mainly influenced by the permeability (κ) and the initial moisture content (C_0).

Overall, it becomes clear that the moisture content development is highly influenced by the initial moisture content of the raw chicken breast meat. It is, therefore, necessary to accurately measure the moisture content of the chicken meat sample before the roasting to get an accurate model prediction of the moisture profile during the roasting process. Furthermore, the results show that the permeability of the chicken meat is an important parameter that should be described as accurate as possible. However, for meat products there are no studies available that show the change of the permeability of meat products during the heating process. Therefore, in future works an experimental study is needed that develops the relationship between the permeability changes as function of the process conditions. A possibility could be to describe this relationship with a variable in Eq. (3) (Darcy's law) that is dependent on the local temperature or moisture content. Thus, the denaturation of proteins and the resulting shrinkage of the protein network during the roasting process would be taken into account and a more accurate model prediction could be obtained.

Table 2
Standardized regression coefficients (SRC): ranking of the input parameters according their relative impact on the sample temperatures T_A, T_{core} and T_C for the two time points of 4 and 8 min (only the 6 highest ranked input parameters are presented for clarity).

Rank	T_A		T_{Core}		T_C	
	Time Parameter	**4 min** SRC	Time Parameter	**4 min** SRC	Time Parameter	**4 min** SRC
1	T_{oven}	0.756	T_{oven}	0.541	T_{oven}	0.679
2	h_{bot}	0.461	k_{cm}	0.420	h_{eff}	0.628
3	k_{cm}	−0.196	$c_{p,cm}$	−0.417	k_{cm}	−0.174
4	$c_{p,cm}$	−0.179	T_0	0.331	$c_{p,cm}$	−0.153
5	T_0	0.118	h_{eff}	0.274	b	0.130
6	ρ_{cm}	−0.058	ρ_{cm}	−0.269	T_0	0.119
	R^2	0.958	R^2	0.997	R^2	0.996
	Time Parameter	**8 min** SRC	Time Parameter	**8 min** SRC	Time Parameter	**8 min** SRC
1	T_{oven}	0.648	T_{oven}	0.604	T_{oven}	0.664
2	κ	−0.352	k_{cm}	0.405	h_{eff}	0.511
3	h_{bot}	0.339	$c_{p,cm}$	−0.387	κ	−0.314
4	b	0.239	h_{eff}	0.362	k_{cm}	0.193
5	k_{cm}	0.196	ρ_{cm}	−0.252	b	0.173
6	$c_{p,cm}$	−0.154	h_{bot}	0.140	$c_{p,cm}$	−0.151
	R^2	0.949	R^2	0.995	R^2	0.978

Table 3
Standardized regression coefficients (SRC): ranking of the input parameters according their relative impact on the sample moisture contents C_{av}, C_A and C_C for the two time points of 4 and 8 min (only the 6 highest ranked input parameters are presented for clarity).

Rank	C_{av}		C_A		C_C	
	Time Parameter	**4 min** SRC	Time Parameter	**4 min** SRC	Time Parameter	**4 min** SRC
1	C_0	0.945	C_0	0.757	C_0	0.583
2	T_{oven}	−0.244	κ	−0.456	κ	−0.465
3	h_{eff}	−0.145	T_{oven}	−0.322	T_{oven}	−0.438
4	b	0.072	h_{bot}	−0.174	h_{eff}	−0.363
5	k_{cm}	0.067	k_{cm}	0.054	k_{cm}	0.108
6	κ	−0.066	$c_{p,cm}$	0.048	$c_{p,cm}$	0.092
	R^2	0.998	R^2	0.958	R^2	0.968
	Time Parameter	**8 min** SRC	Time Parameter	**8 min** SRC	Time Parameter	**8 min** SRC
1	C_0	0.680	T_{oven}	−0.713	κ	−0.461
2	T_{oven}	−0.541	h_{bot}	−0.338	C_0	0.417
3	h_{eff}	−0.286	C_0	0.328	T_{oven}	−0.404
4	κ	−0.2510	κ	−0.258	b	0.242
5	k_{cm}	0.146	k_{cm}	0.142	k_{cm}	0.133
6	b	0.133	$c_{p,cm}$	−0.122	$c_{p,cm}$	0.116
	R^2	0.988	R^2	0.974	R^2	0.937

3.2.3. Chicken meat texture

The texture changes inside the chicken meat sample are a result of protein denaturation and, therefore, they are highly dependent on the temperature development with time. This is highlighted in Table 4, where the 3 top ranked input parameters T_{oven}, $c_{p,cm}$ and k_{cm} are the same as for the core temperature, T_{core} (see Table 3). The thermo-physical properties have again a high impact on the output variables of hardness and chewiness. This underlines the fact that both parameters should be defined as accurate as possible to reduce the uncertainty in the model predictions (model refinement, see section 3.3.2).

The results in Table 4 also show, that from the possible oven settings, the oven temperature (T_{oven}) and fan speed (h_{eff}) have the highest impact on the texture of the chicken meat sample. Therefore, these two parameters can be used to optimize the roasting process with the aim of the optimum texture of the final product for the consumer.

Table 4
Standardized regression coefficients (SRC): ranking of the input parameters according their relative impact on the sample texture variables *Ha* and *Chew* for the two time points of 4 and 8 min (only the 6 highest ranking input parameters are presented for clarity).

Rank	*Hardness*		*Chewiness*	
	Time Parameter	**4 min** SRC	Time Parameter	**4 min** SRC
1	T_{oven}	0.565	T_{oven}	0.585
2	$c_{p,cm}$	−0.389	$c_{p,cm}$	−0.401
3	k_{cm}	0.381	k_{cm}	0.399
4	T_0	0.281	h_{eff}	0.285
5	h_{eff}	0.244	T_0	0.279
6	h_{bot}	0.225	ρ_{cm}	−0.233
	R^2	0.924	R^2	0.984
	Time Parameter	**8 min** SRC	Time Parameter	**8 min** SRC
1	T_{oven}	0.614	T_{oven}	0.614
2	k_{cm}	0.396	$c_{p,cm}$	−0.380
3	$c_{p,cm}$	−0.378	h_{eff}	0.366
4	h_{eff}	0.329	k_{cm}	0.357
5	ρ_{cm}	0.242	ρ_{cm}	−0.220
6	T_0	0.206	T_0	0.115
	R^2	0.997	R^2	0.955

3.3. Morris screening for global sensitivity analysis

The number of repetitions, r, was increased from 10 to 50 in order to study its influence on the Elementary Effects, *EE* (see section 2.5.2). We found that 30 repetitions are enough to ensure that it has no further impact on the analysis results. Thus, a total number of 390 simulation runs ($r^*(M+1)$, see section 2.5.2) were necessary. Consequently, the Morris screening needs 110 simulation runs less than the SRC method (500 samples needed, see section 3.2). One simulation run took around 12 min (at the central DTU HPC cluster, with 1 node and 20 cores), which means that the Morris method needed around 1320 min less compared to the SRC method.

The visual results of the Morris method at the roasting time of 8 min are presented in Fig. 6. The two lines in the graphs correspond to $\mu_i = \pm 2sem_i$ (see section 2.5.2). Parameters with a low mean and standard deviation value have a low influence on the corresponding output variable, while high means and standard deviations show a high impact. All parameters have a non-linear effect on the model outputs as none of the input parameters have a zero standard deviation together with a non-zero mean.

The ranking of the first six model input parameters (for clarity) according to their impact on the model outputs after 8 min of roasting ($t = 8$ min) is presented in Table 5. A higher mean value shows a more significant influence of the input parameter on the model output. Furthermore, a positive sign of the mean indicates a positive effect of the input parameter on the output and a negative sign a negative effect.

The ranking of the input parameters according to their impact on the model outputs are mostly in agreement with the results/ranking of the SRC method. However, there are small differences in the exact order of the parameters for nearly all output variables. Only the ranking for the moisture content at position A, C_A, is the same (compare Tables 2–4 and Table 5). For the chicken meat temperatures, for example, the order of the thermal conductivity, k_{cm}, and the specific heat capacity, $c_{p,cm}$,

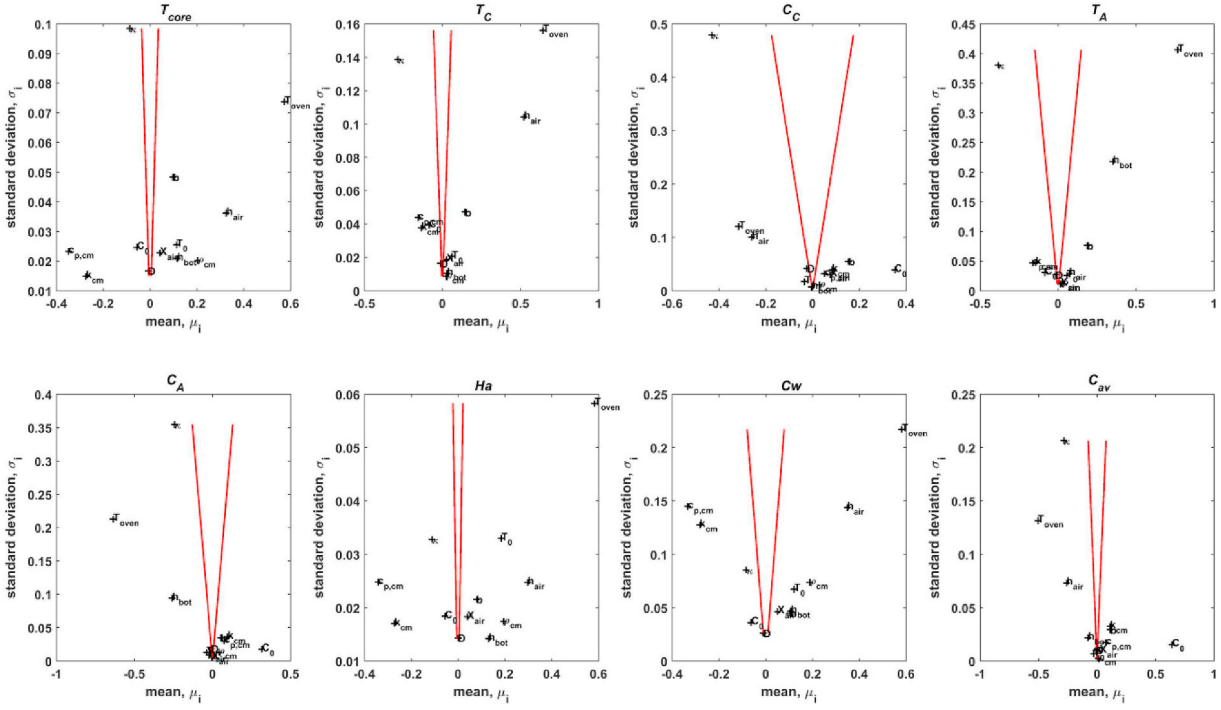

Fig. 6. Mean (μ_i) and standard deviation (σ) of the Elementary Effects distribution of the model input parameters (in total 12 parameters symbolized as crosses with names) on the model outputs. The two lines in each of the plots correspond to $\mu_i = \pm 2sem_i$.

Table 5
Morris screening: ranking of the input parameters according to their estimated means of the Elementary Effects distribution.

Rank	T_A		T_{core}		T_C		C	
	Time Parameter	**8 min** μ_i	Time Parameter	**8 min** μ_i	Time Parameter	**8 min** μ_i	Time Parameter	**8 min** μ_i
1	T_{oven}	0.768	T_{oven}	0.583	T_{oven}	0.641	C_0	0.623
2	h_{bot}	0.384	$c_{p,cm}$	−0.366	h_{eff}	0.535	T_{oven}	−0.486
3	κ	−0.377	h_{eff}	0.353	κ	−0.318	κ	−0.269
4	b	0.206	k_{cm}	0.329	$c_{p,cm}$	−0.162	h_{eff}	−0.264
5	k_{cm}	0.184	ρ_{cm}	0.222	k_{cm}	0.162	k_{cm}	0.115
6	$c_{p,cm}$	−0.183	h_{bot}	0.127	b	0.154	b	0.114
Rank	C_A		C_C		*hardness*		*chewiness*	
	Time Parameter	**8 min** μ_i	Time Parameter	**8 min** μ_i	Time Parameter	**8 min** μ_i	Time Parameter	**8 min** μ_i
1	T_{oven}	−0.596	κ	−0.422	T_{oven}	0.590	T_{oven}	0.585
2	C_0	0.309	C_0	0.340	$c_{p,cm}$	−0.360	h_{eff}	0.370
3	h_{bot}	−0.263	T_{oven}	−0.309	h_{eff}	0.323	$c_{p,cm}$	−0.343
4	κ	−0.246	b	0.151	k_{cm}	0.318	k_{cm}	0.320
5	k_{cm}	0.099	k_{cm}	0.082	ρ_{cm}	−0.210	ρ_{cm}	−0.208
6	$c_{p,cm}$	0.072	$c_{p,cm}$	0.048	T_0	0.197	T_0	0.125

are changed in comparison to the SRC ranking. However, there is only a small difference between their mean and SRC values, indicating/showing that the impact of these two thermo-physical properties on the model outputs is not significantly different. Accordingly, the exact order of the two parameters is not influencing the conclusions of their effect on the model predictions.

All in all, the Morris method showed a mostly similar ranking of the input parameters, confirming the results of the SRC method. In this study less samples were needed for the Morris screening which resulted in lower computational cost compared to the SRC method. However, it should be noticed that with an increasing number of input parameters also the needed number of samples is increasing (see section 2.5.2), while the SRC method is independent of the amount of model inputs (Sin et al., 2009).

3.4. Model refinement and perspective

The results from the sensitivity analysis can be used to refine and strengthen the developed model in order to improve the accuracy of the model predictions.

As shown in Table 2, the temperatures at all presented positions (T_A, T_{core} and T_C) as well as the texture parameters (*hardness* and *chewiness*)

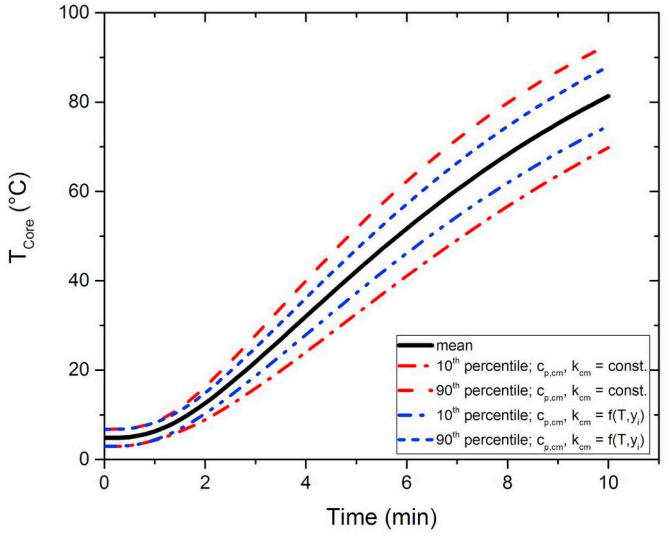

Fig. 7. Uncertainty of the predicted temperature development at the core with fixed values of $c_{p,cm}$ and k_{cm} (red dashed lines) and with $c_{p,cm}$ and k_{cm} as function of temperature and composition (blue dashed lines). (For interpretation of the references to colour in this figure legend, the reader is referred to the Web version of this article.)

are highly sensitive to the thermo-physical properties of chicken breast meat ($c_{p,cm}$ and k_{cm}) at both time steps (4 and 8 min). Therefore, both parameters should be refined to decrease the uncertainty on the output parameters.

From literature it is known that both parameters change with temperature, sample composition and fiber direction (Choi and Okos, 1986). Therefore, one way to refine the model could be to include both parameter as function of temperature and composition instead of fixed values. As it can be seen in Fig. 7, it was possible to reduce the uncertainty of the core temperature development by replacing the fixed values of $c_{p,cm}$ and k_{cm} (red dashed lines in Fig. 7) with expressions as function of temperature and composition (blue dashed lines in Fig. 7).

This shows the strength of the uncertainty and sensitivity analysis, where two parameters were identified as highly sensitive to the model output and consequently the model was refined to decrease the uncertainty in the model predictions.

Furthermore, the moisture content of the sample is highly influenced by the permeability κ of the chicken breast meat (Table 3). Higher values of the permeability describe lower resistance to the water flux through the porous medium and, consequently, also an increased water flux towards the surfaces of the chicken meat sample. On the contrary, the uncertainty in the diffusion coefficient, D, has no significant influence (not shown in Table 3) on the moisture content. This is reasonable as the main moisture transport inside the chicken sample is pressure driven as a result of protein denaturation and the decrease of the water holding capacity (Rabeler and Feyissa, 2018a). The results show that further research is necessary to gain a quantitative knowledge about the change of the permeability with roasting time (i.e. $\kappa(T)$) as already highlighted by different researchers (Feyissa et al., 2013; van der Sman, 2013). On the contrary, for the diffusion coefficient D it is enough to use a constant parameter value (not changing with time) without losing information about the total moisture flux or increasing the uncertainty of the model.

4. Conclusion

In this study, the impact of uncertain input parameters on the model predictions of the mechanistic 3D model of chicken breast roasting was studied and the most important model parameters were identified, using global uncertainty and sensitivity analysis methods.

The Monte Carlo procedure was effectively applied to evaluate the impact of the uncertainty in the input parameters on the model predictions for the temperature, texture and moisture development. It was found that the uncertainty in the model output variables varies with time, but also among the different output variables. By applying the method of standardized regression coefficients (SRC), a global sensitivity analysis technique, the input parameters with relatively high and low impact on the model predictions were identified and ranked, accordingly. We found that the sampling method and the total number of samples had an influence on the SRC method. The ranking of the input parameters then showed that the roasting is mainly influenced by the oven parameters, the thermo-physical properties and the initial properties of the chicken meat.

The SRC method was afterwards compared with the Morris screening, which confirmed the obtained results (mostly similar ranking of the input parameters). However, for the Morris method fewer samples were needed showing that in this study it is computationally more efficient.

Overall, the presented uncertainty and sensitivity analysis methods are strong tools to evaluate mechanistic models. They not only ensure the reliability and accuracy of the developed model but inform the operator/manufacturer about the influence of the process parameters on the safety and quality of the final product.

References

Bird, R.B., Stewart, W.E., Lightfoot, E.N., 2007. Transport Phenomena, Revised 2n. John Wiley & Sons, Inc.
Campolongo, F., Saltelli, A., 1997. Sensitivity analysis of an environmental model : an application of different analysis methods. Reliab. Eng. Syst. Saf. 57, 49–69.
Cariboni, J., Gatelli, D., Liska, R., Saltelli, A., 2007. The role of sensitivity analysis in ecological modelling. Ecol. Model. 203, 167–182. https://doi.org/10.1016/j.ecolmodel.2005.10.045.
Choi, Y., Okos, M.R., 1986. Effects of temperature and composition on the thermal properties of foods. Food Eng. Process Appl. 93–101.
Czitrom, V., 1999. One-Factor-at a Tim versus designed experiments. Am. Stat 53, 126–131. https://doi.org/10.2307/2685731.
Datta, A.K., 2015. Toward computer-aided food engineering: mechanistic frameworks for evolution of product, quality and safety during processing. J. Food Eng. 176, 9–27. https://doi.org/10.1016/j.jfoodeng.2015.10.010.
Datta, A.K., 2006. Hydraulic permeability of food tissues. Int. J. Food Prop. 9, 767–780. https://doi.org/10.1080/10942910600596167.
Dimov, I., Georgieva, R., 2010. Monte Carlo algorithms for evaluating Sobol' sensitivity indices. Math. Comput. Simul 81, 506–514. https://doi.org/10.1016/j.matcom.2009.09.005.
Feyissa, A.H., Gernaey, K.V., Adler-Nissen, J., 2013. 3D modelling of coupled mass and heat transfer of a convection-oven roasting process. Meat Sci. 93, 810–820. https://doi.org/10.1016/j.meatsci.2012.12.003.
Feyissa, A.H., Gernaey, K.V., Adler-Nissen, J., 2012. Uncertainty and sensitivity analysis: mathematical model of coupled heat and mass transfer for a contact baking process. J. Food Eng. 109, 281–290. https://doi.org/10.1016/j.jfoodeng.2011.09.012.
Gargalo, C.L., Cheali, P., Posada, J.A., Gernaey, K.V., Sin, G., 2016. Economic risk assessment of early stage designs for glycerol valorization in biorefinery concepts. Ind. Eng. Chem. Res. https://doi.org/10.1021/acs.iecr.5b04593.
Goñi, S.M., Salvadori, V.O., 2011. Kinetic modelling of colour changes during beef roasting. Procedia Food Sci 1, 1039–1044. https://doi.org/10.1016/j.profoo.2011.09.155.
Gulati, T., Datta, A.K., 2016. Coupled multiphase transport, large deformation and phase transition during rice puffing. Chem. Eng. Sci. 139, 75–98. https://doi.org/10.1016/j.ces.2015.08.057.
Helton, J.C., 1993. Uncertainty and sensitivity analysis techniques for use in performance assessment for radioactive waste disposal. Reliab. Eng. Syst. Saf. 42, 327–367.
Helton, J.C., Davis, F.J., 2003. Latin hypercube sampling and the propagation of uncertainty in analyses of complex systems. Reliab. Eng. Syst. Saf. 81, 23–69. https://doi.org/10.1016/S0951-8320(03)00058-9.
Jha, S.N., 2005. Mathematical simulation of roasting of grain. J. Food Eng. 71, 304–310. https://doi.org/10.1016/j.jfoodeng.2005.03.006.
Kocis, L., Whiten, W.J., 1997. Computational investigations of low- discrepancy sequences. ACM Trans. Math Software 23, 266–294. https://doi.org/10.1145/264029.264064.
Metropolis, N., Source, S.U., 1949. The Monte Carlo method. J. Am. Stat. Assoc. 44.
Morris, M.D., 1991. Factorial Samplig Plans for Preliminary Computational Experiments. Technometrics 33.
Ngadi, M., Dirani, K., Oluka, S., 2006. Mass transfer characteristics of chicken nuggets. Int. J. Food Eng. 2. https://doi.org/10.2202/1556-3758.1071.
Ousegui, A., Moresoli, C., Dostie, M., Marcos, B., 2010. Porous multiphase approach for baking process - Explicit formulation of evaporation rate. J. Food Eng 100, 535–544. https://doi.org/10.1016/j.jfoodeng.2010.05.003.

Purlis, E., Salvadori, V.O., 2009. Bread baking as a moving boundary problem. Part 2: Model validation and numerical simulation. J. Food Eng 91, 434–442. https://doi.org/10.1016/j.jfoodeng.2008.09.038.

Rabeler, F., Feyissa, A.H., 2018a. Modelling the transport phenomena and texture changes of chicken breast meat during the roasting in a convective oven. J. Food Eng. 237, 60–68. https://doi.org/10.1016/j.jfoodeng.2018.05.021.

Rabeler, F., Feyissa, A.H., 2018b. Kinetic modeling of texture and color changes during thermal treatment of chicken breast meat. Food Bioprocess Technol. 1–10. https://doi.org/10.1007/s11947-018-2123-4.

Ruano, M.V., Ribes, J., Ferrer, J., Sin, G., 2011. Application of the Morris method for screening the influential parameters of fuzzy controllers applied to wastewater treatment plants. Water Sci. Technol. 63, 2199–2206. https://doi.org/10.2166/wst.2011.442.

Saltelli, A., 2006. The Critique of Modelling and Sensitivity Analysis in the Scientific Discourse . An Overview of Good Practices. European Commission - Joint Research Center. Office for Official Publications of the European Communities, Luxembourg.

Saltelli, A., 2004. Sensitivity Analysis in Practice: a Guide to Assessing Scientific Models. Google eBook.

Saltelli, A., Ratto, M., Andres, T., Campolongo, F., Cariboni, J., Gatelli, D., Saisana, M., Tarantola, S., 2007. Global Sensitivity Analysis. The Primer. John Wiley & Sons, Ltd, Chichester, UK. https://doi.org/10.1002/9780470725184.

Sin, G., Gernaey, K.V., Lantz, A.E., 2009. Good modeling practice for PAT Applications : propagation of input uncertainty and sensitivity analysis. Biotechnol. Prog. 1–12. https://doi.org/10.1021/bp.166.

Sin, G., Gernaey, K.V., Neumann, M.B., van Loosdrecht, M.C.M., Gujer, W., 2011. Global sensitivity analysis in wastewater treatment plant model applications: prioritizing sources of uncertainty. Water Res. 45, 639–651. https://doi.org/10.1016/j.watres.2010.08.025.

van der Sman, R.G.M., 2013. Modeling cooking of chicken meat in industrial tunnel ovens with the Flory-Rehner theory. Meat Sci. 95, 940–957. https://doi.org/10.1016/j.meatsci.2013.03.027.

van der Sman, R.G.M., 2007. Moisture transport during cooking of meat: an analysis based on Flory-Rehner theory. Meat Sci. 76, 730–738. https://doi.org/10.1016/j.meatsci.2007.02.014.

Publication 4

Rabeler, F., Skytte, J. L., & Feyissa, A. H. (2019). Prediction of thermal induced color changes of chicken breast meat during convective roasting: A combined mechanistic and kinetic modelling approach. *Food Control*, *104*.

DOI: https://doi.org/10.1016/j.foodcont.2019.04.018

Due to merging of files, the inserted publication does not follow the page numbering of the overall document but instead the page numbering of the journal.

Food Control 104 (2019) 42–49

Contents lists available at ScienceDirect

Food Control

journal homepage: www.elsevier.com/locate/foodcont

Prediction of thermal induced color changes of chicken breast meat during convective roasting: A combined mechanistic and kinetic modelling approach

Felix Rabeler, Jacob Lercke Skytte, Aberham Hailu Feyissa*

Food Production Engineering, National Food Institute, Technical University of Denmark (DTU), Denmark

ARTICLE INFO

Keywords:
Heat and mass transfer
Maillard reaction
Mechanistic modelling
Poultry meat
Surface browning
Thermal processing
Quality control

ABSTRACT

Consumers first assess the quality of roasted chicken meat by its appearance. However, studies that evaluate the color changes during thermal processing are lacking. The aim of this work was, therefore, to develop a mathematical model that can predict the lightness (L^*) changes of chicken breast meat during convective roasting.

Chicken breast meat was roasted in a convection oven and the internal as well as surface lightness was measured at different time steps. The lightness of chicken meat increases in the beginning of the process, which shows a whitening due to myoglobin denaturation. When the surface temperature is rising above 88 °C, the lightness starts to decrease again as a result of browning reactions.

We developed a non-isothermal kinetic model that describes the browning (decrease of the lightness) of the surface as function of temperature, water activity and roasting time. The kinetic models for the whitening and browning were then coupled to the validated mechanistic model for chicken meat roasting. This enables the prediction of the internal as well as surface lightness development from the spatial temperature and water activity changes. The validation of the model showed a good agreement between model predictions and experimental values for different roasting conditions.

Overall, the developed model allows the prediction of the spatial lightness distributions with roasting time and advances our understanding of the mechanisms of heat induced color changes. Thus, the model can be applied to control and optimize the roasting of chicken meat to ensure the quality and safety for the consumer.

1. Introduction

The color and appearance of cooked chicken meat are the first quality parameters that are evaluated by the consumers, even before the actual consumption (Guerrero-Legarreta & Hui, 2010). Especially the color of the cooked meat provides information about the quality, flavor and safety of the product (Grunert, Bredahl, & Brunsø, 2004; Pedreschi, León, Mery, & Moyano, 2006). Therefore, the color of cooked chicken breast meat is an important quality parameter in professional kitchens or the food industry that needs to be controlled thoroughly.

In the beginning of the cooking process, the color of chicken breast meat is changing from pink-red to an off-white color. This change is mainly caused by the heat induced denaturation of myoglobin to ferro- and ferrihemochromes, resulting in the color fading (King & Whyte, 2006). The denaturation of myoglobin takes place in the temperature range from 55 to 80 °C, while the rate and amount of denaturation is correlated mainly to the temperature and time of heating (Lawrie & Ledward, 2006; Martens, Stabursvik, & Martens, 1982; Rabeler & Feyissa, 2018a). Moreover, the denaturation of structural proteins, like myofibrillar proteins could result in an increased light scattering from the surface and an optical masking of the hemeproteins. The protein denaturation leads to a reduction of the fiber diameter and larger gabs between the individual fibers. This allows for an increased light scattering and, consequently, the surface and inner regions of the meat product seems lighter (Hughes, Oiseth, Purslow, & Warner, 2014; Martens et al., 1982). However, especially at or close to the sample surface where the temperature is rising fast, the is mainly caused by myoglobin denaturation (Kondjoyan et al., 2014).

When the temperature is further increasing, the surface dries out due to water evaporation which leads to more greyish and darker colors. When the temperature is rising above 85–90 °C, caramelization as well as Maillard reactions take place (Kondjoyan et al., 2014; Nakamura, Mao, Fukuoka, & Sakai, 2011). The latter, also known as

* Corresponding author. Søltofts Plads, 2800, Kgs. Lyngby, Denmark.
E-mail address: abhfe@food.dtu.dk (A.H. Feyissa).

https://doi.org/10.1016/j.foodcont.2019.04.018
Received 11 February 2019; Received in revised form 17 April 2019; Accepted 19 April 2019
Available online 20 April 2019
0956-7135/

non-enzymatic browning is the reaction between reducing sugars and the amino groups of proteins, peptides and free amino acids. This results in the formation of the typical flavor and taste of roasted meat as well as the formation of the typical brown color (Shahidi, Samaranayaka, & Pegg, 2014). The formation of colored compounds (low molecular weight) as well as melanoidins (high molecular weight) during the Maillard reaction is mainly responsible for the browning. Furthermore, reactions in the early stages of the Maillard reaction could lead to the development of brown colors (Ames, Apriyantono, & Arnoldi, 1993; Ledl & Schleicher, 1990; Namiki & Hayashi, 1981). When the surface temperature exceeds 150 °C carbonization reactions are taking place, which results in the formation of dark colors and a burned appearance (Matsuda, Llave, Fukuoka, & Sakai, 2013).

The final color of roasted chicken breast meat is still relying on the cook and a look approach, thus, it depends highly on the skills of the operator or chef. If it is possible to predict the color change during the heating, a better control of the process could be achieved. Kinetic models that describe the change of the color with roasting time can help to understand, predict and control the process to obtain a final high quality product (Haefner, 2005; Van Boekel, 2008).

Kinetic models were developed for the color change of beef (redness, a^*) and chicken breast meat (lightness, L^*) during isothermal heating in water baths (Goñi & Salvadori, 2011 and Rabeler & Feyissa, 2018a, respectively). However, in moist surroundings no browning reactions take place in the studied temperature range (40–100 °C). Thus, the kinetic models are not able to describe the browning at the surface of the meat product during a roasting process. Matsuda et al. (2013) investigated the change of the surface color of fish during grilling and developed kinetics model to describe the development as function of the measured surface temperature. However, the browning of the surface is not only a function of the temperature development but the change of the moisture content or water activity with time (Shahidi et al., 2014).

The accurate measurement of the surface temperature or moisture content is difficult or even not possible (Purlis & Salvadori, 2009; Zanoni, Peri, & Bruno, 1995). Mechanistic models, which are based on principle physical laws, are able to predict the complex change in temperature and moisture content of the product during heating. By combining kinetic models with models of heat and mass transfer (a combined modelling approach) the local quality change (for example texture) can be obtained (Kondjoyan et al., 2014; Rabeler & Feyissa, 2018b). For the baking of bread different researchers have shown that it is possible to predict the change of the surface color by combining kinetic models with mathematical models of heat and mass transfer (Purlis & Salvadori, 2009; Zanoni et al., 1995; Zhang & Datta, 2006).

However, for chicken breast meat no studies are available that describe the color changes during convective roasting. Therefore, the aim of this work is to develop a combined model which allows the prediction of the spatial lightness (L^*) changes as function of the local temperature and water activity development. Our hypothesis is that by combining kinetic models that describe the lightness changes, with the validated mechanistic model of chicken meat roasting it is possible to predict the lightness change as function of roasting time and process settings. Validation trials with an independent data set will then show the accuracy and reliability of the developed combined model.

2. Mathematical models

2.1. Kinetic model to describe the whitening of the chicken meat

The whitening of chicken breast meat during heating was described by Rabeler and Feyissa (2018a) with a modified rate law as function of sample temperature and heating time (Eq. (1)):

$$\frac{\partial L^*_{wh}}{\partial t} = k_{wh}(T)\,(L^*_\infty - L^*_{wh})^n \tag{1}$$

with the lightness L^* at time t, the non-zero equilibrium value L^*_∞, the reaction order n and the reaction rate constant k (min^{-1} $[\text{Q}]^{1-\text{n}}$). The common Arrhenius equation was used to describe the temperature dependency of the reaction rate constant (for details see Rabeler and Feyissa (2018a)). The estimated values for the activation energy (E_a = 101 kJ/mol), pre-exponential factor ($k_0 = 2.65 \times 10^{15}$ min^{-1}), reaction order (n = 1.1) and non-zero equilibrium L^* value ($L_\infty{}^*$ = 87) by Rabeler and Feyissa (2018a) were used in this study.

2.2. Kinetic model for the browning of chicken meat

The browning of the chicken meat depends on the surface temperatures and starts at temperatures greater than 85 °C (Kondjoyan et al., 2014). During the roasting process the surface temperatures are not constant but it is increasing nearly continuously with final temperatures of up to 150 °C. Consequently, the browning of the chicken meat surface is relying on the thermal history during heating.

To address this non-isothermal process and taking the temperature-time history into account, a non-isothermal kinetic was used to model the browning development at the top and bottom surface of the chicken breast meat during the roasting process. The browning reaction was assumed to follow a first order kinetic in the form of Eq. (2):

$$\frac{\partial L^*_b}{\partial t} = -k_b(T,\, a_w)\, L^*_b \tag{2}$$

The browning of the chicken meat surface relies not only on the temperature development but also the change in the water content or water activity at the surface (Eichner & Karel, 1972). Therefore, Purlis and Salvadori (2009) described for bread baking the reaction rate constant k_b as function of the temperatue and water activity. This appraoch was adapted in this study (Eq. (3)):

$$k_b = (p_0 + \frac{p_1}{a_w(t)})\, exp(-(\frac{p_2 + \frac{p_3}{a_w(t)}}{T(t)})) \tag{3}$$

with the water activity a_w, the temperature T (K) and the kinetic parameters p_0, p_1, p_2 and p_3.

If the temperature-time history is neglected during the estimation of the kinetic parameters it is likely that the browning reaction, which is highly temperature dependent, has a larger error (Dolan, 2003). However, the accurate measurement of the surface temperature or water activity during the roasting process is difficult or even not possible (Purlis & Salvadori, 2009). Therefore, we used in this study the validated mechanistic model of chicken breast meat roasting to obtain the change of the surface temperatures and water activities as function of the roasting time (see section 2.3).

The kinetic models for the whitening (see section 2.1) and for the browning of the chicken meat surface were combined with a Heaviside function f which is centered at the start of the browning temperature, T_b (see Eq. (4b)). The function is going from 1 to 0 and it is defined as the transition between the two kinetic models. This enables the estimation of the transition temperature for the surface browning and, additionally, both phenomena can be described with one equation (Eq. (4a)):

$$\frac{\partial L^*}{\partial t} = f\frac{\partial L^*_{wh}}{\partial t} + (1-f)\frac{\partial L^*_b}{\partial t} = f\; k_{wh}(T)\,(L^*_\infty - L^*_{wh})^n + (1-f)\, k_b(T,\, a_w)\, L^*_b \tag{4a}$$

Where f is described as:

$$f = 1 - \frac{1}{1 + \exp(T - T_b)} \tag{4b}$$

2.3. Mechanistic model of chicken breast meat roasting

The validated mechanistic model of chicken breast meat roasting

was used to obtain the development of the surface temperatures and water activities with roasting time. For a detailed description of the mechanistic model we refer the reader to Rabeler and Feyissa (2018b). The governing equation that is describing the heat transfer by convection and conduction is given by Eq. (5). The liquid water transport inside the chicken breast meat by diffusion and convection is described with Eq. (6):

$$\text{Heat transfer:} \quad c_{p,cm}\,\rho_{cm}\,\frac{\partial T}{\partial t} = \nabla(k_{cm}\,\nabla T) - \rho_w\,c_{p,w}\,u_w\,\nabla T \tag{5}$$

$$\text{Mass transfer:} \quad \frac{\partial C}{\partial t} = \nabla(-D\,\nabla C + C\,u_w) \tag{6}$$

with $c_{p,i}$, ρ_i and k_i are the specific heat capacity, density and thermal conductivity, respectively, T is the temperature (K), C is the moisture content (kg of water/kg of sample), D is the moisture diffusion coefficient (m^2/s), u_w is the fluid velocity (m/s) and t the time (s).

The thermal denaturation of proteins results in the shrinkage of the protein network as well as the reduction of the water holding capacity. Thus, a pressure gradient is induced inside the chicken breast meat. Darcy's law gives the relationship between this pressure gradient and the fluid velocity inside the chicken breast meat during the roasting process (Eq. (7)) (Rabeler & Feyissa, 2018b):

$$u_w = \frac{-\kappa}{\mu_w}\nabla p \tag{7}$$

with the swelling pressure $p = G'(C - C_{eq})$, the storage modulus G' (Pa), the water holding capacity C_{eq}, the permeability κ (m^2), and the dynamic viscosity of the fluid μ_w (Pa s).

The heat and mass transfer at the boundaries of the chicken breast meat sample was described with Eq. (8) and Eq. (9), respectively (Rabeler & Feyissa, 2018b):

$$-k_{cm}\nabla T = h\,(T_{oven} - T_{surf}) \tag{8}$$

$$-D\,\nabla C + C\,u_w = \beta_{tot}\,(C_{surf} - C_{oven}) \tag{9}$$

where h is the heat transfer coefficient (W/(m^2 K)) (h_{top} at the top surface and h_{bot} at the bottom surface, see Table 1), T_{oven} and T_{surf} are the oven and surface temperature (K), respectively, β_{tot} is the total mass transfer coefficient (m/s), C_{surf} is the moisture content at the surface of the chicken meat sample (kg/kg) and C_{oven} is the moisture content in the circulated ambient hot air. Table 1 summarizes the model input parameters.

3. Materials and methods

3.1. Raw material and sample preparation

Chicken breast fillets without bones and skins were purchased at a local supermarket the same day as the experiments. The chicken breast fillets were cut into a rectangular shape with a length, width and height of 70, 40 and 20 mm, respectively. The average weight of the sample was 63 g ± 4. The samples were stored at 2 °C in sealed plastic bags until further usage.

3.2. Roasting experiments

The roasting trials were performed in a professional convection oven with dry hot air. The oven was preheated for 30 min before the experiments to ensure steady state conditions. In this study, oven temperatures of 200, 230 and 260 °C were used. The temperature was regulated with the ovens thermostat and it was found to be stable around the setting temperature with ± 3 °C (Rabeler & Feyissa, 2018b). A single chicken meat sample was placed on the roasting tray which was then positioned centrally in the oven. The roasting times in this study were 1, 3, 5, 7, 10, 15 and 20 min. After the specific roasting times, the samples were immediately taken out of the oven, put into plastic bags and placed in ice water. Subsequently the color of the top surface and bottom surface of the sample was measured (see section 3.3).

3.3. Color measurements

For the color measurements a hyper spectral imaging system (VideometerLab 2, Videometer A/S, Denmark) was used. The device was calibrated with a diffuse white and diffuse black (radiometrical calibration) target as well as with a geometrical target (geometrical calibration) (Hansen, 1999).

The colors of the chicken breast samples were evaluated after 1, 3, 5, 7, 10, 15 and 20 min of roasting (see section 3.2). First the color at the top and bottom surface of the roasted chicken meat sample was measured. One sample was placed underneath the camera and an image of the top surface was taken. Afterwards the sample was turned over and another image of the bottom surface was taken. For the internal color measurements, the sample was cut in half (perpendicular to the length axis) and an image was taken from the internal cut surface.

The images were then processed with MATLAB (R2017a, The Mathworks Inc., MA, USA) and the average surface colors of the chicken meat samples were obtained as L^* value (lightness), a^* value (green to red color) and b^* value (yellow to blue color) (Rabeler & Feyissa, 2018a).

Table 1
Model input parameters (Rabeler & Feyissa, 2018b).

Parameter	Symbol	Value	Unit	Source
Density				
chicken meat	ρ_{cm}	1050	kg/m^3	Calculated from (Choi & Okos, 1986)
water	ρ_w	998	kg/m^3	
Diffusion coefficient	D	3×10^{-10}	m^2/s	Ngadi, Dirani, and Oluka (2006)
Permeability	κ	3×10^{-17}	m^2	Datta (2006)
Viscosity water	μ_w	0.988×10^{-3}	Pa s	Rabeler and Feyissa (2018b)
Initial composition				
Water	y_{w0}	0.76	kg/kg	Rabeler and Feyissa (2018b)
Protein	y_{p0}	0.22	kg/kg	Barbanti and Pasquini (2005)
Fat	y_{f0}	0.01	kg/kg	Barbanti and Pasquini (2005)
Ash	y_{a0}	0.01	kg/kg	Barbanti and Pasquini (2005)
Initial meat temperature	T_0	6	°C	Rabeler and Feyissa (2018b)
Initial moisture concentration	C_0	0.76	kg/kg	Rabeler and Feyissa (2018b)
Water vapor concentration in ambient air	C_{air}	0.05	kg/kg	Rabeler and Feyissa (2018b)
Heat transfer coefficient	h_{top}	44	W/(m^2 K)	Rabeler and Feyissa (2018b)
	h_{bot}	59	W/(m^2 K)	

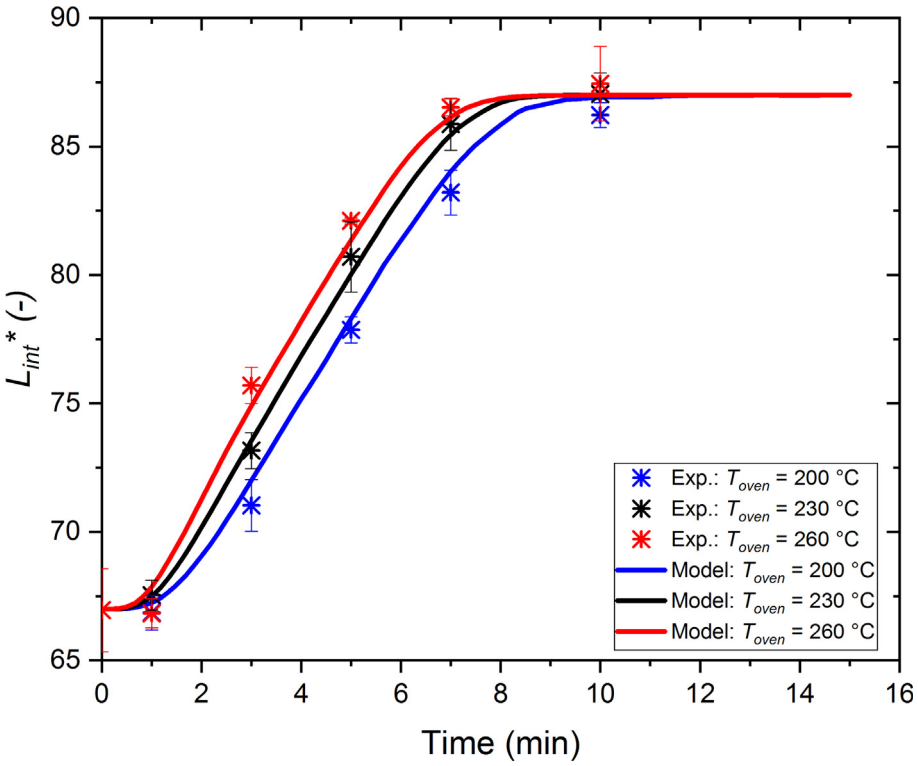

Fig. 1. Comparison between the predicted (solid lines) and measured (symbols) lightness development inside the chicken meat sample during roasting at 200 (blue), 230 (black) and 260 °C (red). Bars indicate the standard deviation (n = 3).

3.4. Model solution and parameter estimation

The commercial finite element (FEM) software COMSOL Multiphysics® 5.3 was used to solve the partial differential equations (PDEs) for the transport phenomena (see section 2.3) and the ordinary differential equations (ODE) that describe the lightness changes of the chicken breast meat (see section 2.1 and 2.2). Mesh sensitivity analysis was conducted, to ensure the quality of the mesh. The mesh size was decreased in a sequence of simulations until the size had no effect on the solution of the model (Kumar & Dilber, 2006; Rabeler & Feyissa, 2018b).

The developed model was calibrated and validated by using experimental data for the change in the surface lightness of the chicken meat sample at different oven temperatures (see section 3.2 and 3.3). The experimental data of the top surface color for an oven temperature of 230 °C was used to estimate the start temperature for browning, T_b (Eq. (4b)), and the kinetic parameters in Eq. (3). COMSOL was coupled with MATLAB (R2017a, The Mathworks Inc., MA, USA) by using the COMSOL LiveLink™. The parameter estimation was done by minimizing the sum of the squared differences between the experimental and the predicted lightness development at the top surface of the chicken meat sample (non-linear least squares, *lsqnonlin* solver in MATLAB) (Feyissa, Gernaey, Ashokkumar, & Adler-Nissen, 2011).

The remaining measurements for the lightness developments at the top and bottom surface of the chicken meat sample were then used to validate the developed model.

3.5. Statistical analysis

Analysis of variance (one-way ANOVA without replication) and Tukey's honestly significant difference procedure was performed to assess the influence of the heating time and oven temperature on the lightness changes of the chicken breast meat during roasting. The significance level for the analysis was set to $P < 0.05$. The estimated parameters and measured values are presented as mean values ± confidence intervals at 95%.

The standard root mean squared error (*RMSE*) was calculated with Eq. (10):

$$RMSE = \sqrt{\frac{\sum_{i=1}^{n} (\hat{\theta}_i - \theta_i)^2}{n}} \quad (10)$$

with $\hat{\theta}$ the predicted value, θ the measured value n is the total number of samples. The *RMSE* together with the randomness and normality of the residuals was used to evaluate the quality of the model predictions.

4. Results and discussion

4.1. Modelling the internal color changes

By combining the kinetic model for the chicken meat whitening (Eq. (1)) with the model of heat and mass transfer (section 2.3) it is possible to predict the internal lightness changes during the roasting process as a function of the local temperature change. The influence of the oven temperature on the internal lightness changes during roasting is shown in Fig. 1. A good agreement between the model predictions (solid lines) and the measured (symbols) lightness changes for all tested temperatures was found. The root mean squared errors (*RMSEs*) between predicted and experimental values are 0.825, 0.773 and 0.848 at 200, 230 and 260 °C, respectively.

The influence of the oven temperature on the internal lightness change was not significant ($P > 0.05$). An increase of the oven temperatures leads to a faster heat up of the sample surface (see Eq. (8)). However, the internal heat transfer from the surface towards the core is slow compared to the external heat transfer ($Bi = 1.1 > 0.1$), which also results in a decreased internal temperature rise (Rabeler & Feyissa, 2018b). Since the internal whitening of the chicken meat is a function of the temperature development with time (see Eq. (1)), it is reasonable that the oven temperature has no significant influence on the internal lightness changes.

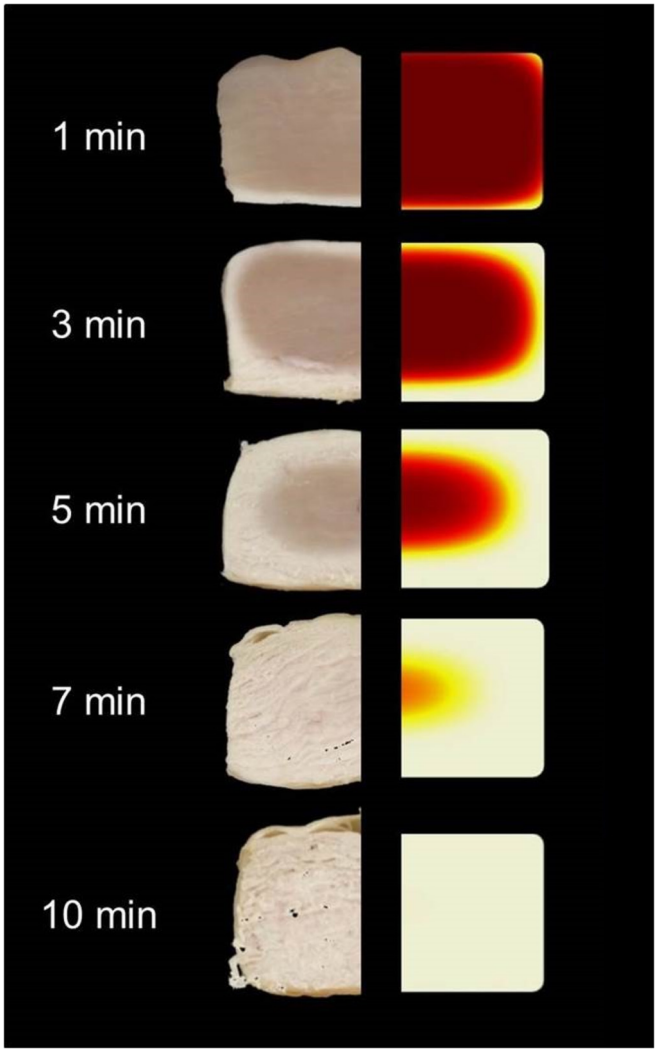

Fig. 2. Visual comparison between the experimental (left side) and predicted (right side) color development inside the chicken meat sample during roasting at 230 °C.

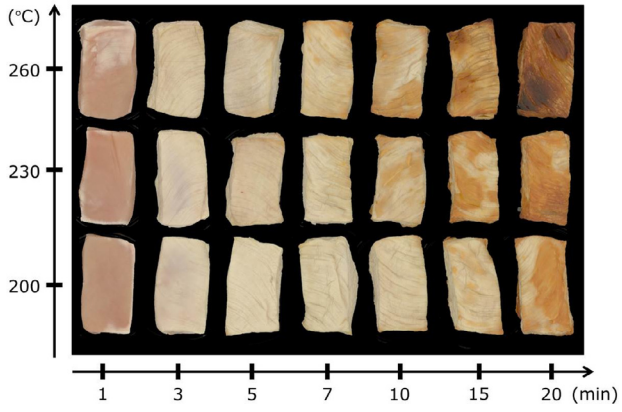

Fig. 3. Color development at the top surface of chicken breast samples roasted at 200, 230 and 260 °C for different roasting times (1, 3, 5, 7, 10, 15, 20 min).

Moreover, a visual comparison between the simulated and measured color change with roasting time for an oven temperature of 230 °C is shown in Fig. 2. First, the surface of the chicken meat which is in contact with the surrounding hot air and roasting plate (only bottom) is getting white. This whitening is caused by the heat induced

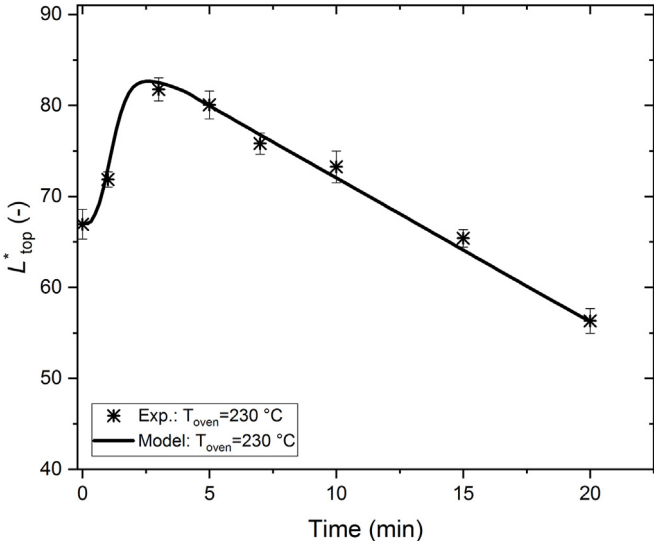

Fig. 4. Measured (symbols) and simulated (solid line) lightness development of the chicken meat top surface (L^*_{top}) with roasting time for an oven temperature of 230 °C. Bars indicate the standard deviation (n = 3).

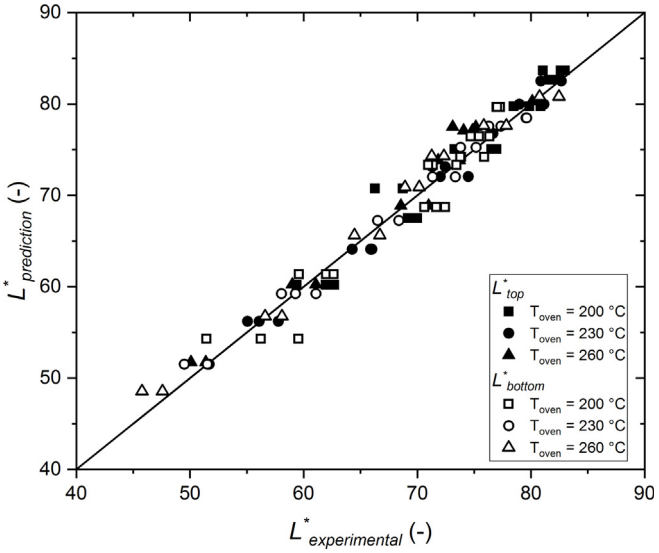

Fig. 5. Comparison between the predicted and experimental lightness values. Filled and unfilled symbols show the top and bottom surface data points, respectively.

denaturation of heme-proteins and the change in structural proteins (Hughes et al., 2014; King & Whyte, 2006). The whitening is faster from the bottom of the sample compared to the top surface. This is due to a higher heat transfer from the roasting plate to the meat that leads to a faster temperature increase at the bottom surface (Rabeler & Feyissa, 2018b). The heat is then transferred inside the chicken meat by convection and conduction which results in the internal whitening of the meat.

After around 7 min of roasting the internal of the chicken breast meat became white (L^*_{int} = 85.9 ± 1) nearly reaching the equilibrium L^* value (L^*_{∞} = 87) (see also Fig. 2). The absence of any pink inside the chicken meat is still used in kitchens to assess the doneness of the meat (cook and a look approach). Chicken meat should be heated to an internal temperature of at least 72 °C to ensure the safety of the product for the consumer. However, after 7 min of roasting at an oven temperature of 230 °C, the core temperature of the chicken meat reaches only 59 °C (Rabeler & Feyissa, 2018b). Thus, the chicken meat is not

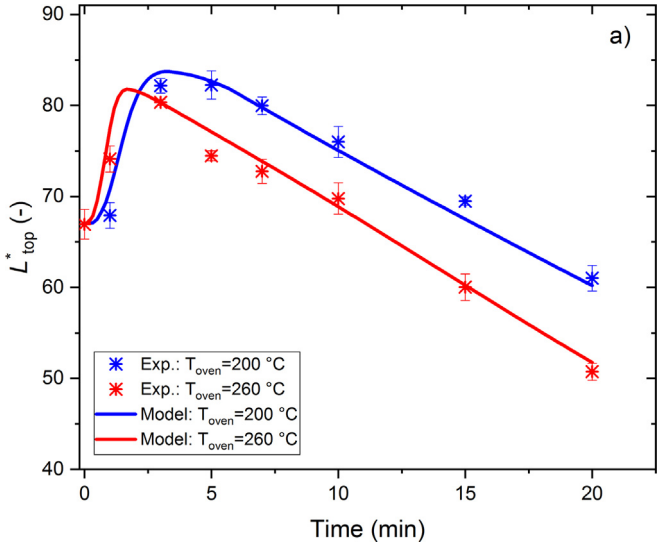

Fig. 6. Measured (symbols) and predicted (solid lines) lightness development at the a) top and b) bottom surface of the chicken breast sample with roasting time. Bars indicate the standard deviation (n = 2).

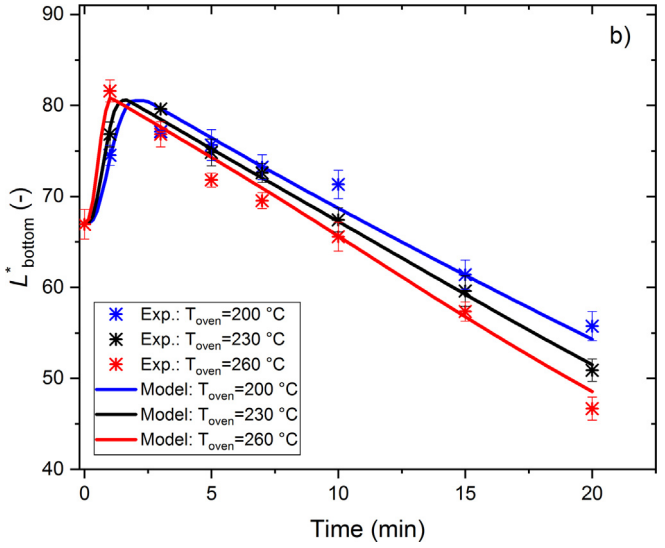

Fig. 6. (*continued*)

safe for the consumer, yet, even though it is already completely white. This shows the advantage of the developed model to ensure the safety of the roasted chicken meat for the consumer independently of the operator or chef.

4.2. Modelling the surface color development

The visual inspection of the roasted chicken meat sample top surfaces shows that two stages of color change can be distinguished (Fig. 3). In the beginning of the roasting process (0 to around 3 min) the surface becomes white mainly due to the thermal denaturation of heme proteins (hemoglobin and myoglobin) and to some degree due to the denaturation of structural proteins (Guidi & Castigliego, 2010; Rabeler & Feyissa, 2018a). Afterwards, the surface of the chicken meat dries out due to the evaporation of water, which leads to a first decrease of the lightness (see for example at 230 °C, 5 min) (Nakamura et al., 2011). When the surface temperature is further rising a browning of the surface can be seen (for example after 5 min at 260 °C, Fig. 3). This can be correlated to non-enzymatic browning reactions (mainly Maillard and caramelization reactions) that take place when the surface temperature is increasing above 85–90 °C (Kondjoyan et al., 2014; Martins, Martins, & Jongen, 2001). Finally, when the surface temperature is rising above 150 °C, carbonization reactions take place, which are resulting in a further darkening and even burning of the sample (see for example after 20 min at 260 °C, Fig. 3) (Nakamura et al., 2011).

4.2.1. Model calibration

For the roasting of chicken breast meat at an oven temperature (T_{oven}) of 230 °C, the two stages of color change (whitening and browning) can be distinguished by following the development of the top surface lightness (L^*_{top}) with roasting time (symbols in Fig. 4). First, the lightness is increasing showing the whitening of the meat surface, followed by a decrease of the L^*_{top} value, which can be associated with the darkening of the sample surface. A similar trend was also reported for the infrared heating (grilling) of fish (Matsuda et al., 2013; Nakamura et al., 2011) or microwave cooking of beef meat (Kondjoyan et al., 2014). We found that the roasting time has a significant influence ($P < 0.01$) on the lightness of the chicken meat surface.

The coupled model for the transport phenomena and lightness changes of chicken breast meat during roasting was calibrated by fitting the experimental data ($L^*_{exp,\ 230\ °C}$) to the corresponding model predictions (see section 2.4). Consequently, the kinetic parameters in Eq. (3) (p_0, p_1, p_2 and p_3) and the start temperature for browning in Eq. (4b), T_b, were estimated.

The parameter estimation showed, that the lightness starts to decrease at surface temperatures around $T_b = 88 \pm 2$ °C (see Eq. (4b)), which corresponds to the start of the surface browning. The identified temperature is in the same range as reported for beef meat (85 °C) or fish products (95 °C) (Kondjoyan et al., 2014 and Matsuda et al., 2013, respectively). The temperature T_b distinguishes between the two mechanisms of whitening (lightness decrease) and browning (lightness increase) (see section 2.2). As it was identified by the parameter estimation, a better insight into the mechanisms of the chicken meat surface browning during heating is obtained. The kinetic parameters p_0, p_1, p_2 and p_3 in Eq. (3) were estimated to be $6.369 \times 10^6 \pm 1.309 \times 10^5$, $1.2943 \times 10^6 \pm 1.488 \times 10^5$, $6.477 \times 10^3 \pm 711.4$ and 929.68 ± 62.49, respectively. The comparison between the predicted and experimental L^*_{top} values shows that the calibrated model is able to predict the development of the top surface lightness during the roasting at 230 °C (filled circles in Fig. 5). The root mean squared error (*RMSE*) between model predictions and experimental values was estimated to be 1.31.

The developed model was then validated against the measured lightness developments for oven temperatures of 200 and 260 °C as well as the lightness developments at the bottom surface of the chicken meat sample (see section 4.2.2).

4.2.2. Validation of the developed model

The validation of the developed model was done by comparing the predicted and measured lightness development at the top and bottom surface of the chicken meat samples for oven temperatures of 200 and 260 °C. A good agreement between the predicted (solid lines) and measured (symbols) lightness changes at the top surface was found for all tested oven temperatures (Fig. 6a). The root mean squared error (*RMSE*) between the predicted and experimental values is 1.61 and 1.8 at 200 and 260 °C, respectively. Additionally, the simulated lightness development at the bottom surface of the chicken meat samples agrees well with the measured values for all oven temperatures (Fig. 6b) with *RMSE* values of 2.29, 1.09 and 1.61 for 200, 230 and 260 °C, respectively. The comparison between the predicted and experimental L^* values for the top (filled symbols) and bottom (unfilled symbols) surfaces is shown in Fig. 5. The results show that the developed model is able to accurately predict the change in surface lightness during the roasting of chicken breast meat.

We found that the oven temperature has a significant influence ($P < 0.05$) on the lightness development at the top surface of the

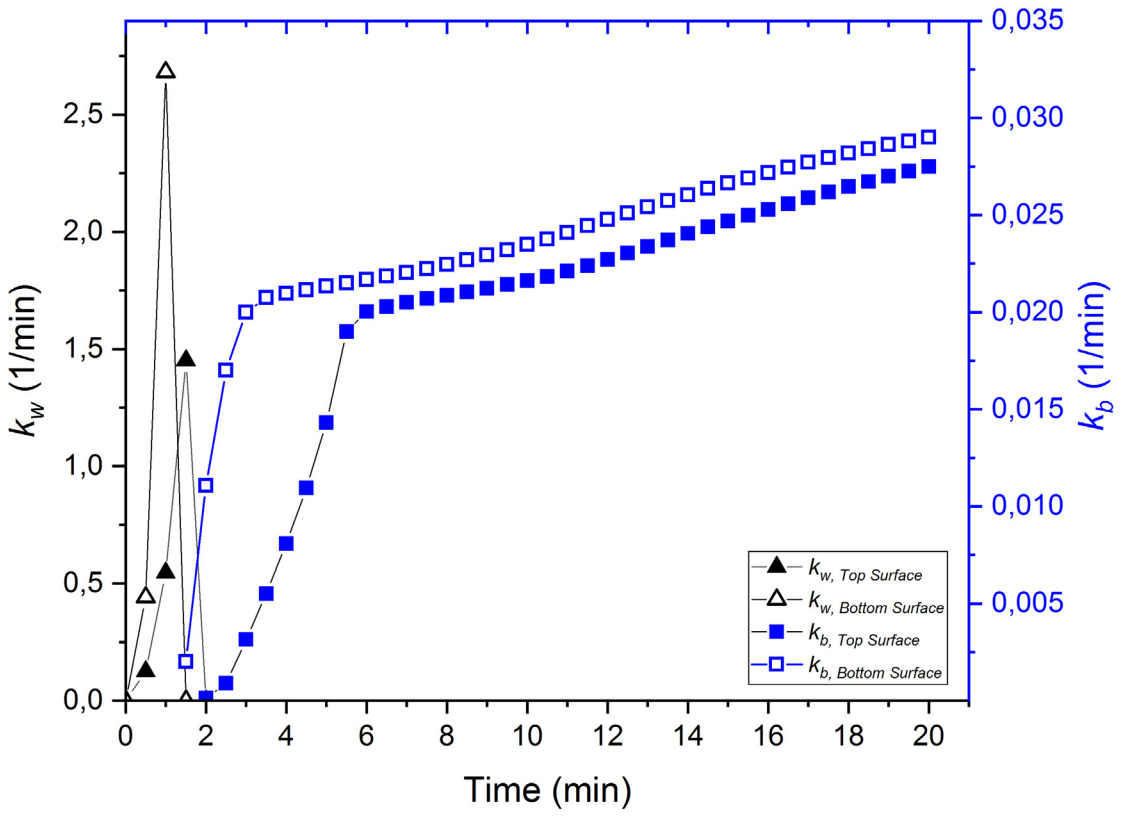

Fig. 7. Predicted development of the reaction rate constants $k_{w,\ Top\ Surface}$, $k_{w,\ Bottom\ Surface}$, $k_{b,\ Top\ Surface}$ and $k_{b,\ Bottom\ Surface}$ with roasting time (T_{oven} = 230 °C).

chicken meat sample (Fig. 6a). An increase of the oven temperature from 200 to 260 °C results in a faster heat up of the sample surface (see Eq. (8)). Subsequently, the heme proteins denature faster which leads to the faster whitening of the sample surface (Lawrie & Ledward, 2006; Martens et al., 1982). Moreover, the transition temperature between whitening and browning (88 °C ± 2, see section 4.2.1) is reached earlier due to the more rapidly heat up. Consequently, an earlier browning of the surface with increasing oven temperature was found. This earlier decrease of the L^*_{top} value also results in darker sample surfaces at all time steps (Fig. 6a).

The temperature at the bottom of the chicken meat sample (in contact with the roasting plate) is increasing faster compared to the top surface due to a higher heat transfer coefficient (conduction) which is also resulting in a higher moisture evaporation rate (Rabeler & Feyissa, 2018b). Thus, the reaction rate constants for the whitening ($(k_w(T)$) and browning ($k_b(T,a_w)$ period (Eq. (4)) are higher for the bottom compared to the top surface. This is clearly illustrated in Fig. 7. Accordingly, the lightness at the bottom is changing faster compared to the top surface (Fig. 6b and a, respectively).

Overall, the results show that the developed model is able to accurately predict the change in the lightness development at the top and bottom surface. The surface lightness is a function of the temperature and moisture content development during roasting. Thus, by adjusting the oven settings it is possible to directly impact the change of the surface lightness. The developed model can be used to control the color change during the roasting process. Furthermore, the acquired knowledge in combination with the developed model can be used to optimize the process of chicken meat roasting to obtain a high quality product for the consumer.

5. Conclusion

In this study, we have focused on the development of a mathematical model to predict the internal as well as surface lightness (L^*) development of chicken breast meat during convective roasting. First a non-isothermal kinetic model was developed to describe the browning of the chicken breast meat surface during roasting as function of the temperature and water activity changes. By combining the kinetic model for browning with the before developed kinetic for the whitening of chicken breast meat the temperature at which browning reactions at the chicken meat surface start was estimated. Thus, a better insight into the mechanisms behind the browning of chicken meat during roasting was achieved. Furthermore, the combination of the two kinetic models enables the prediction of both processes (whitening and browning) with one equation.

The kinetic models were then coupled with the mechanistic model of chicken breast meat roasting which allows the prediction of the internal as well as surface lightness development as function of the local temperature and water activity changes. The validation of the developed model shows that both the internal as well as surface lightness development can be predicted. Furthermore, the influence of changing oven temperatures on the internal and external lightness development was obtained. We found that the oven temperature has a significant influence on the top surface lightness development (L^*_{top}). However, no significant influence of the oven temperature on the bottom (L^*_{bot}) and internal lightness (L^*_{int}) changes was found.

Overall, the developed model is able to predict the lightness changes inside and on the surface of chicken breast meat during convective roasting from the local temperature and water activity changes for different process conditions. Thus, the model can be applied to control the lightness development of the chicken breast meat during convective roasting and at the same time ensure the safety of the final product. Furthermore, the roasting process can be optimized to obtain the product with the highest quality for the consumer.

Nomenclature

a_w	water activity

C	mass concentration (kg/kg)
C_{eq}	Water holding capacity (kg/kg)
c_p	specific heat capacity (J/(kg K))
D	diffusion coefficient (m^2/s)
f	Heaviside function
G'	Storage modulus (Pa)
h	heat transfer coefficient (W/(m^2 K))
k	reaction rate constant (1/min)
k_{cm}	thermal conductivity chicken meat (W/(m K))
L^*	lightness
p	swelling pressure (Pa)
T	temperature (K)
t	time (min)
u	velocity (m/s)
RMSE	Root mean squared error

Greek symbols

β	mass transfer coefficient (m/s)
ρ	Density (kg/m^3)
μ	Viscosity (Pa s)

Subscripts

b	browning
bot	bottom
cm	chicken meat
int	internal
surf	surface
w	water
wh	whitening
∞	equilibrium

References

Ames, J. M., Apriyantono, A., & Arnoldi, A. (1993). Low molecular weight coloured compounds formed in xylose-lysine model systems. *Food Chemistry, 46*, 121–127. https://doi.org/10.1016/0308-8146(93)90023-9.

Barbanti, D., & Pasquini, M. (2005). Influence of cooking conditions on cooking loss and tenderness of raw and marinated chicken breast meat. *Lebensmittel-Wissenschaft und -Technologie- Food Science and Technology, 38*, 895–901. https://doi.org/10.1016/j.lwt.2004.08.017.

Choi, Y., & Okos, M. R. (1986). Effects of temperature and composition on the thermal properties of foods. *Journal of Food Engineering and Process Application,* 93–101.

Datta, A. K. (2006). Hydraulic permeability of food tissues. *International Journal of Food Properties, 9*, 767–780. https://doi.org/10.1080/10942910600596167.

Dolan, K. D. (2003). Estimation of kinetic parameters for nonisothermal food processes. JFS Concise Rev. Hypotheses *Journal of Food Science, 68*https://doi.org/10.1111/j.1365-2621.2003.tb08234.x.

Eichner, K., & Karel, M. (1972). Influence of water content and water activity on the sugar-amino browning reaction in model systems under various conditions. *Journal of Agricultural and Food Chemistry, 20*, 218–223. https://doi.org/10.1021/jf60180a025.

Feyissa, A. H., Gernaey, K. V., Ashokkumar, S., & Adler-Nissen, J. (2011). Modelling of coupled heat and mass transfer during a contact baking process. *Journal of Food Engineering, 106*, 228–235. https://doi.org/10.1016/j.jfoodeng.2011.05.014.

Goñi, S. M., & Salvadori, V. O. (2011). Kinetic modelling of colour changes during beef roasting. *Procedia Food Science, 1*, 1039–1044. https://doi.org/10.1016/j.profoo.2011.09.155.

Grunert, K. G., Bredahl, L., & Brunsø, K. (2004). Consumer perception of meat quality and implications for product development in the meat sector - a review. *Meat Science, 66*, 259–272. https://doi.org/10.1016/S0309-1740(03)00130-X.

Guerrero-Legarreta, I., & Hui, Y. H. (2010). *Handbook of poultry science and technology, Vol. 2*John Wiley & Sons, Inchttps://doi.org/10.1002/9780470504475.

Guidi, A., & Castigliego, L. (2010). Poultry meat color. *Handb. Poult. Sci. Technol: Vol. 2 2*, (pp. 359–388). . https://doi.org/10.1002/9780470504475.ch25.

Haefner, J. W. (2005). *Modeling biological systems: Principles and applications.* New York: Springer-Verlaghttps://doi.org/10.1007/b106568.

Hansen, J. F. (1999). *On chromatic and geometrical calibration.* Technical University of Denmark.

Hughes, J. M., Oiseth, S. K., Purslow, P. P., & Warner, R. D. (2014). A structural approach to understanding the interactions between colour, water-holding capacity and tenderness. *Meat Science, 98*, 520–532. https://doi.org/10.1016/j.meatsci.2014.05.022.

King, N. J., & Whyte, R. (2006). Does it look cooked? A review of factors that influence cooked meat color. *Journal of Food Science, 71*, 31–40. https://doi.org/10.1111/j.1750-3841.2006.00029.x.

Kondjoyan, A., Kohler, A., Realini, C. E., Portanguen, S., Kowalski, R., Clerjon, S., et al. (2014). Towards models for the prediction of beef meat quality during cooking. *Meat Science, 97*, 323–331. https://doi.org/10.1016/j.meatsci.2013.07.032.

Kumar, A., & Dilber, I. (2006). Fluid flow and its modeling using computational fluid dynamics. In S. Sablani, A. Datta, M. Shafiur Rehman, & A. Mujumdar (Eds.). *Handbook of food and bioprocess modeling techniques, food science and technology*CRC Presshttps://doi.org/10.1201/9781420015072.

Lawrie, R. A., & Ledward, D. A. (2006). *Lawrie's meat science*.

Ledl, F., & Schleicher, E. (1990). New aspects of the maillard reaction in foods and in the human body. *Angewandte Chemie International Edition in English, 29*, 565–706. https://doi.org/10.1002/anie.197506551.

Martens, H., Stabursvik, E., & Martens, M. (1982). Texture and color changes in meat during cooking related to thermal-denaturation of muscle proteins. *Journal of Texture Studies, 13*, 291–309.

Martins, S., Martins, S. I. F. S., & Jongen, W. M. F. (2001). A review of Maillard reaction in food and implications to kinetic modelling A review of Maillard reaction in food and implications to kinetic modelling. *Trends in Food Science & Technology, 11*, 364–373. https://doi.org/10.1016/S0924-2244(01)00022-X.

Matsuda, H., Llave, Y., Fukuoka, M., & Sakai, N. (2013). Color changes in fish during grilling-Influences of heat transfer and heating medium on browning color. *Journal of Food Engineering, 116*, 130–137. https://doi.org/10.1016/j.jfoodeng.2012.11.027.

Nakamura, M., Mao, W., Fukuoka, M., & Sakai, N. (2011). Analysis of the color change in fish during the grilling process. *Food Science and Technology Research, 17*, 471–478. https://doi.org/10.3136/fstr.17.471.

Namiki, M., & Hayashi, T. (1981). Formation of novel free radical prodcut in early stage of maillard reaction. *Progress in Food & Nutrition Science, 5*, 81–91.

Ngadi, M., Dirani, K., & Oluka, S. (2006). Mass transfer characteristics of chicken nuggets. *International Journal of Food Engineering, 2*. https://doi.org/10.2202/1556-3758.1071.

Pedreschi, F., León, J., Mery, D., & Moyano, P. (2006). Development of a computer vision system to measure the color of potato chips. *Food Research International, 39*, 1092–1098. https://doi.org/10.1016/j.foodres.2006.03.009.

Purlis, E., & Salvadori, V. O. (2009). Modelling the browning of bread during baking. *Food Research International, 42*, 865–870. https://doi.org/10.1016/j.foodres.2009.03.007.

Rabeler, F., & Feyissa, A. H. (2018a). Kinetic modeling of texture and color changes during thermal treatment of chicken breast meat. *Food and Bioprocess Technology, 1*. https://doi.org/10.1007/s11947-018-2123-4.

Rabeler, F., & Feyissa, A. H. (2018b). Modelling the transport phenomena and texture changes of chicken breast meat during the roasting in a convective oven. *Journal of Food Engineering, 237*, 60–68. https://doi.org/10.1016/j.jfoodeng.2018.05.021.

Shahidi, F., Samaranayaka, A. G. P., & Pegg, R. B. (2014). *Maillard reaction and browning, encyclopedia of meat sciences.* Elsevier Ltdhttps://doi.org/10.1016/B978-0-12-384731-7.00130-6.

Van Boekel, M. A. J. S. (2008). Kinetic modeling of food quality: A critical review. *Comprehensive Reviews in Food Science and Food Safety, 7*, 144–158. https://doi.org/10.1111/j.1541-4337.2007.00036.x.

Zanoni, B., Peri, C., & Bruno, D. (1995). Modelling of browning kinetics of bread crust during baking. *Lebensmittel-Wissenschaft und -Technologie- Food Science and Technology, 28*, 604–609. https://doi.org/10.1016/0023-6438(95)90008-X.

Zhang, J., & Datta, A. K. (2006). Mathematical modeling of bread baking process. *Journal of Food Engineering, 75*, 78–89. https://doi.org/10.1016/j.jfoodeng.2005.03.058.

Publication 5

Rabeler, F., Skytte, J. L., & Feyissa, A.H. (2020). Mechanistic 3D modelling of solid foods with varying shape and size using statistical shape analysis: roasting of whole chicken breast meat. *Submitted to Food Engineering Reviews.*

Mechanistic 3D modelling of solid foods with varying shape and size using statistical shape analysis: roasting of whole chicken breast meat

Felix Rabeler*, Jacob Lercke Skytte, Aberham Hailu Feyissa

Food Production Engineering, National Food Institute, Technical University of Denmark (DTU), Denmark

*Corresponding author:

Søltofts Plads, 2800, Kgs. Lyngby, Denmark

Email address: felra@food.dtu.dk

Keywords: 3D scanning; heat and mass transfer; poultry meat, quality prediction, statistical shape modelling, irregular geometry

---

Abstract

The actual shape of food product is often simplified or neglected in food process models, even though it is crucial for the temperature, moisture and quality predictions. To study the natural shape variation of chicken breast fillets and its impact on the roasting time and quality development, we have developed a landmark-based statistical shape model for chicken breast fillets, which was in the following combined with the mechanistic 3D model of chicken meat roasting. The

first mode of variation, which was mainly associated with the chicken breast fillet size, had the highest impact on the roasting time, with up to 55% longer/ shorter roasting times to reach a safe core temperature compared to the standard chicken breast fillet. The second mode of variation was associated with the global fillet shape, which led to around 23% longer/ shorter roasting times. Moreover, the differences in roasting time due to changes in chicken breast fillet size and shape was found to have a direct influence on the texture and color of the chicken breast fillet with an up to 30% softer texture and 21% darker color, respectively. Overall, our results show that the integration of the actual irregular food geometry is crucial for accurate model predictions and to minimize the simulation error. Thus, we believe the presented approach of combining mechanistic models with statistical shape models is a strong tool for studying the effects that irregular geometries can have on the roasting process.

1. Introduction

Modelling of food processes requires a detailed knowledge about the coupled transport phenomena as well as the transformations the food is undergoing during the heating process (e.g. mechanisms, mathematical formulations). Moreover, the geometry of the food product in the mathematical model is of great importance as its size and shape is influencing the spatial temperature, moisture and pressure gradients (Goñi et al., 2008). The quality changes of food products (for example texture and color) during the heating process are directly linked to the state variables (Goñi et al., 2008; Purlis and Salvadori, 2009a; Rabeler and Feyissa, 2018a). Thus, the internal and surface temperature as well as the moisture distributions have a

direct impact on the spatial quality developments. The actual geometry of the food product should be, therefore, included as accurately as possible, when developing mechanistic models.

However, simple geometries such as cylinders, slabs or spheres are widely used in modelling studies (Blikra et al., 2019; Feyissa et al., 2013; Isleroglu and Kaymak-Ertekin, 2016; Jha, 2005; Liu et al., 2013; Rabeler and Feyissa, 2018b; Sakin-Yilmazer et al., 2012; van der Sman, 2007; Zhu et al., 2015), as most food products have irregular shapes that are difficult to simulate precisely/properly with for instance computer-aided design programs (Goñi et al., 2007). Furthermore, the use of regular geometries enables an easy validation of the developed model, as the points for the temperature measurement or the initial weight of the sample can be controlled more accurately. Finally, regular shapes can be easily implemented or constructed in most commercial available modelling software and its computational time is commonly lower compared to irregular geometries.

Only a few studies have used real food geometries alongside their mathematical models. Fabbri et al. (2011) used 3D scanning to obtain the geometric model of a coffee bean, which was then used in the model of coupled heat and mass transfer. The authors reported a non-uniform surface temperature during the roasting process and showed that the volume of different coffee beans is influencing both the surface and core temperature. Van der Sman (2013) used laser line scanning to obtain 3D geometries of chicken breast fillets, which were then coupled with the model of chicken meat cooking. During the cooking process non-uniform temperature and moisture content profiles were reported with higher temperatures and lower moisture contents at the chicken breast fillet surface compared to the inner parts.

For the roasting of beef meat, Goñi and Salvadori (2010) used a computer vision system to obtain the irregular geometry of the meat samples. These were then implemented into the model of heat and mass transfer during oven roasting and it was claimed that the use of the real, irregular shape decreases the impact of the geometry on the simulation results.

All these studies highlight the need to incorporate irregular geometries of food materials into mathematical models to obtain realistic and comparable results. However, none of these considered the effect of the natural variation in the size and shape of the food product in their models.

But especially for meat products large variations can be observed due to factors like the species, age at slaughter or environmental conditions (Hargin, 1996).

The systematic analysis of the geometrical variations of a given population of shapes can be done by statistical shape analysis (Dryden and Mardia, 1998). In medical imaging research the use of statistical shape models (SSM) is already a common routine for example to reconstruct skulls (Fuessinger et al., 2018) or to model organs like the heart (Bruse et al., 2016) , while only few authors have applied it in the field of food science (Danckaers et al., 2017, 2015). The idea behind using statistical shape models is that the distribution of observed shapes can be modelled. Thus, after model training, new shape instances can be generated, which will all resemble shapes from the training set. This way population extrema can be investigated in a highly controlled way.

However, comprehensive studies that evaluate the natural variation in size and shape of solid foods and their corresponding influence on the cooking process are missing. The aim of this study was, therefore, to combine statistical shape models

with mechanistic models of heat and mass transfer to study the influence of shape and size on the spatial temperature, moisture and quality distribution during a roasting process. A representative population of chicken breast fillets is scanned using laser line 3D scanning and, subsequently, is analyzed using landmark-based shape analysis methods. The obtained shape models are then coupled with the mechanistic model of chicken meat roasting to access the spatial variation in the state variables as well as the surface color and texture of the chicken breast fillets.

2. Mechanistic and statistical shape modelling

2.1. Statistical shape modelling

Statistical shape modelling was used to study the natural shape variation of chicken breast fillets. In order to analyse and model the geometrical variation of the scanned chicken breasts (see section 3.2), pre-processing of the 3D models is critical.

2.1.1. Pre-processing

Each scanned chicken breast 3D model is made up by a triangulated, dense set of points. The number of points is dependent on both the shape and size of the individual chicken breast, and moreover, the point sets are not necessarily oriented similarly in 3D-space. Thus, in order to make a meaningful one-to-one comparisons of the point sets, two steps are required. First, all chicken breast 3D models have to be aligned in 3D space, and secondly point-to-point correspondence throughout the entire population of 3D models has to be enforced.

For the alignment step, Procrustes analysis is carried out, which typically consists of a translation, a rotation, and a scaling of each sample in the population (Dryden and

Mardia, 1998). This ensures that all point sets are centered around the coordinate system origin with a coinciding anatomical orientation, and uniformly scaled to similar size. However, in our specific application we exclude the scaling component, as the size of the chicken breast is important in the subsequent shape analysis.

To obtain point-correspondence between all samples, we apply the approach by Dalal et al. (2007), which is suitable for handling dense, triangulated surfaces. Initially, a single chicken breast model from the data set is selected as the template (preferably an average sample in terms of the entire population), and furthermore the template is down-sampled. We apply the Quadric Edge Collapse Decimation function in MeshLab (Cignoni et al., 2008), which results in a reduction from thousands of points to a few hundred that maintained the overall shape and triangulation of the chicken breast. These resulting points are the template "landmarks".

Finally, corresponding landmarks are found for each of the remaining 49 chicken breast 3D models (denoted targets) (see section 3.2). This is achieved through an optimization scheme, where each corresponding target landmark is placed such that the total non-rigid deformation between the template and the target 3D surface of landmarks is minimized (Dalal et al., 2007).

2.1.2. Point distribution model

From the aligned and landmark correspondent 3D models, a statistical shape model can then be established to investigate the shape variation in the entire data set. We apply the so-called point distribution model introduced by Cootes et al. (1995), which has become a staple within the field of medical image analysis for segmentation and shape analysis tasks.

As each chicken breast model (or shape) consists of *k* landmarks in 3D space, it can be represented as:

$$S = (x_1, y_1, z_1, \dots, x_k, y_k, z_k) \quad (1)$$

Thus, all shapes can be collected in a single n-by-k matrix (Eq. (2)):

$$X = \begin{bmatrix} x_{11} & y_{11} & z_{11} & \cdots & x_{1k} & y_{1k} & z_{1k} \\ x_{21} & & & & & & z_{2k} \\ \vdots & & & & & & \vdots \\ x_{n1} & y_{n1} & z_{n1} & \cdots & x_{nk} & y_{nk} & z_{nk} \end{bmatrix} \quad (2)$$

In this form, the population of shapes exists as a 3n-dimensional cloud of points, from which the shape variation can be investigated using conventional data analysis tools. By principal component analysis (PCA), eigenvectors and eigenvalues are calculated for the covariance matrix of *X*. Assuming the points are normally distributed, this yields the principal axis of the point cloud, and furthermore only the first few directions (also referred to as modes of variation) are required to model the majority in the point cloud. Selecting the top *d* eigenvector a shape model can be written as:

$$X' = \bar{X} + P_1 b_1 + P_2 b_2 + \cdots + P_d b_d \quad (3)$$

where $\bar{X}$ is the mean shape, P_i are the eigenvectors, b_i are scaling values for the eigenvectors.

Typically, the scaling values are varied within the interval $[-2\sqrt{\lambda_i}; 2\sqrt{\lambda_i}]$ (where λ_i are the eigenvalues), which corresponds to two standard deviations (±2σ) of the distribution along each mode of variation. To study a single mode of variation the scaling for this particular mode can be varied, while setting all other scaling values to zero.

2.2. Mechanistic model of chicken meat roasting

The validated mechanistic model for convective chicken meat roasting was used in this study to evaluate the influence of the size and shape of whole chicken breast fillets on the spatial temperature, moisture, texture and color distributions during roasting (a detailed description of the model is found in Rabeler and Feyissa (2018b)).

The heat is transferred by conduction and convection inside the chicken breast meat (i.e. from the surface to the core). The governing equation for the heat transfer is given by Eq. (4) (Bird et al., 2006):

$$c_{p,cm}\,\rho_{cm}\,\frac{\partial T}{\partial t} = \nabla(k_{cm}\,\nabla T) - \rho_w\,c_{p,w}\,u_w\,\nabla T \qquad (4)$$

where $c_{p,i}$ is the specific heat capacity (J/kg/K),k_i is the thermal conductivity (W/m/K), ρ_i is the density (kg/m^3), u_w is the fluid velocity (m/s), t is the time (s) and T is the temperature (K).

The liquid water is transferred inside the chicken breast fillet by diffusion and convection, which is described by Eq. (5) (Bird et al., 2006):

$$\frac{\partial C}{\partial t} = \nabla(-D\,\nabla C + C\,u_w) \qquad (5)$$

where C is the moisture content (kg of water/ kg of sample) and D is the water diffusion coefficient (m^2/s). The pressure induced convective water flux inside the chicken breast fillet is a result of thermal induced muscle fiber shrinkage and the reduction in the water holding capacity (van der Sman, 2007). Darcy's law gives the relationship between the induced pressure and the convective moisture flux (Eq. (6)) (Rabeler and Feyissa, 2018b):

$$u_w = \frac{-\kappa}{\mu_w}\nabla \mathrm{p} = \frac{-\kappa\,G\prime}{\mu_w}\nabla(\mathrm{C} - C_{eq}) \qquad (6)$$

The heat and mass transfer boundary condition are given by Eq. (7) and Eq. (8), respectively (Rabeler and Feyissa, 2018b):

$$-k_{cm}\nabla T = h\,(T_{air} - T_{surf}) \quad (7)$$

$$-D\,\nabla C + C\,u_w = \beta_{tot}\,(C_{surf} - C_{air}) \quad (8)$$

The heat transfer coefficient (*h*) is depending on the geometry and flow, which is described in this study by using a dimensionless correlation (Nusselt (*Nu*), Reynolds (*Re*) and Prandtl number (*Pr*)) for turbulent flow over a flat surface (Chhabra, 2017) (Eq. (9a) to (9d)):

$$Nu = 0.029 Re^{0.8} Pr^{1/3} \quad (9a)$$

$$Nu = \frac{h\,L_c}{k_a} \quad (9b)$$

$$Re = \frac{u_a\,L_c}{\nu_a} \quad (9c)$$

$$Pr = \frac{c_{p,a}\,\mu_a}{k_a} \quad (9d)$$

The total mass transfer coefficient β_{tot} was described in the following form (Eq. (10)) (van der Sman, 2013):

$$\frac{1}{\beta_{tot}} = \frac{1}{\beta_{ext}} + \frac{1}{\beta_{skin}} \quad (10)$$

with β_{ext} the external mass transfer coefficient (m/s), which is calculated with Chilton-Colburn analogy, and $\beta_{skin} = \beta_1\,C^b$ the moisture content dependent mass transfer coefficient (Rabeler and Feyissa, 2018b).

The change of the chicken meat texture parameter hardness (*Hard*) was described as a function of local temperature and roasting time with a modified rate law in the following form (Rabeler and Feyissa, 2018a) (Eq. (11)):

$$\frac{\partial Hard}{\partial t} = k(T)\,(Hard_\infty - Hard)^n \quad (11)$$

with the non-zero equilibrium $Hard_\infty$ (N), the reaction order n and the reaction rate constant k (min^{-1} $[Hard]^{1-n}$), which was described with the common Arrhenius equation (for a detailed description see Rabeler and Feyissa, 2018a).

The thermal induced color changes (a whitening followed by a browning) at the chicken breast surface was described by Rabeler et al. (2019) with a two-step kinetic model (Eq. (12)):

$$\frac{\partial L^*}{\partial t} = f\ k_{wh}(T)\ (L^*_\infty - {L_{wh}}^*)^n + (1-f)\ k_b(T, a_w)\ {L^*}_b \quad (12)$$

where L^* is the lightness at time point t, L_∞ is the non-zero equilibrium value, k_{wh} is the reaction rate constant (min^{-1}) for the whitening, which is described with the common Arrhenius equation, k_b is the reaction rate constant (min^{-1}) for the browning and f is a Heaviside function describing the transition between the surface whitening and browning (for details see Rabeler et al. (2019)). The reaction rate constant for the surface browning (k_b) was described as function of the local temperature and water activity (Rabeler et al., 2019) (Eq. (13)):

$$k_b(T, a_w) = \left(p_0 + \frac{p_1}{a_w(t)}\right)\ exp\left(-\left(\frac{p_2 + \frac{p_3}{a_w(t)}}{T(t)}\right)\right) \quad (13)$$

with a_w the water activity and p_0, p_1, p_2 and p_3 kinetic parameters.

The coupled partial differential equations (PDEs) for the heat and mass transfer as well as the ordinary differential equations (ODEs) for the quality kinetics are solved with the commercial finite element software COMSOL Multiphysics® 5.4. A summary of the model input parameters is given in Table 1.

Table 1: Model input parameters (Rabeler and Feyissa, 2018b)

Parameter	Symbol	Value	Unit	Source
Diffusion coefficient	D	3×10^{-10}	m^2/s	(Ngadi et al., 2006)
Permeability	κ	3×10^{-17}	m^2	(Datta, 2006)
Viscosity water	μ_w	0.988×10^{-3}	Pa s	(Rabeler and Feyissa, 2018b)
Initial composition				
Water	y_{w0}	0.76	kg/kg	(Rabeler and Feyissa, 2018b)
Protein	y_{p0}	0.22	kg/kg	(Barbanti and Pasquini, 2005)
Fat	y_{f0}	0.01	kg/kg	(Barbanti and Pasquini, 2005)
Ash	y_{a0}	0.01	kg/kg	(Barbanti and Pasquini, 2005)
Initial meat temperature	T_0	6	°C	(Rabeler and Feyissa, 2018b)
Initial moisture concentration	C_0	0.76	kg/kg	(Rabeler and Feyissa, 2018b)
Water vapor concentration in ambient air	C_{air}	0.05	kg/kg	(Rabeler and Feyissa, 2018b)

3. Materials and Methods

3.1. Raw material

Skinless and boneless chicken breast fillets were randomly bought at a local supermarket. Any excess fat and skin was trimmed with a knife. Before the 3D scanning (see section 3.2), the surface of the chicken breast fillets was dried with a tissue paper and the breast fillets covered with a thin layer of flour to minimize the reflectance of the laser light.

3.2. 3D scanning

A commercial laser light scanner (3D scanner V1, Matter and Form, Toronto, Canada) was used for the scanning of the chicken breast fillets. Before usage, the scanner was calibrated with the calibration plate to ensure optimal scanner settings. Furthermore, the chicken breast fillets were covered with a thin layer of flour to minimize light reflectance from the surface.

One chicken breast fillet was placed on the turning table and an automatic (chose of optimal settings by the scanner software) scan performed. One scan took around 90 min. MFStudio was afterwards used to clean the obtained point cloud and to mesh the object (setting the detail level to a maximum of 8 in MFStudio). The meshes were finally exported to perform the statistical shape analysis (see section 2.1).

3.3. Roasting experiments

A professional convection oven with dry hot air was used for the roasting experiments in order to validate the mechanistic model (heat and mass transfer) of chicken meat roasting with a whole chicken breast fillet. One chicken breast fillet was scanned as described in section 3.2 to obtain the 3D geometry. The fillet was afterwards placed on the roasting tray, a thermocouple was inserted into the geometrical center and the development of the core temperature measured continuously.

An oven temperature of 230 °C (± 3 °C around the set point) was used for the validation trial (Rabeler and Feyissa, 2018b)). Before the roasting trial, the oven was preheated for at least 30 min to assure steady state conditions at the start of the roasting. The roasting tray with the chicken breast fillet was placed in the oven and it

was roasted for 20 min. Then, the roasted chicken breast fillet was taken out of the oven and its weight was measured. By comparing the weight before and after the roasting trial the cooking loss (*CL*) was calculated (Eq. (14)):

$$CL = \frac{m_0 - m_t}{m_0} * 100\% \quad (14)$$

with m_0 the initial mass (g) and m_t the mass of the sample (g) after the roasting time *t*.

The standard root mean squared error (*RMSE*) was calculated to evaluate the validation of the mechanistic model with Eq. (15):

$$RMSE = \sqrt{\frac{\sum_{i=1}^{n}(\hat{\theta}_i - \theta_i)^2}{n}} \quad (15)$$

where $\hat{\theta}$ is the predicted value, θ is the measured value and *n* is the total number of samples.

4. Results and discussion

4.1. Spatial variations

In order to study the spatial variations of the temperature, moisture content and quality attributes (hardness) a chicken breast sample was scanned, meshed and imported to COMSOL Multiphysics® (see section 3.2). The model predictions for the core temperature development agreed well with the experimentally obtained data (see Fig. 1) with a RMSE value of 1.22 °C. Furthermore, a good agreement between the predicted (16.7 %) and the experimental (16.1%) cooking loss after 20 min of roasting was obtained.

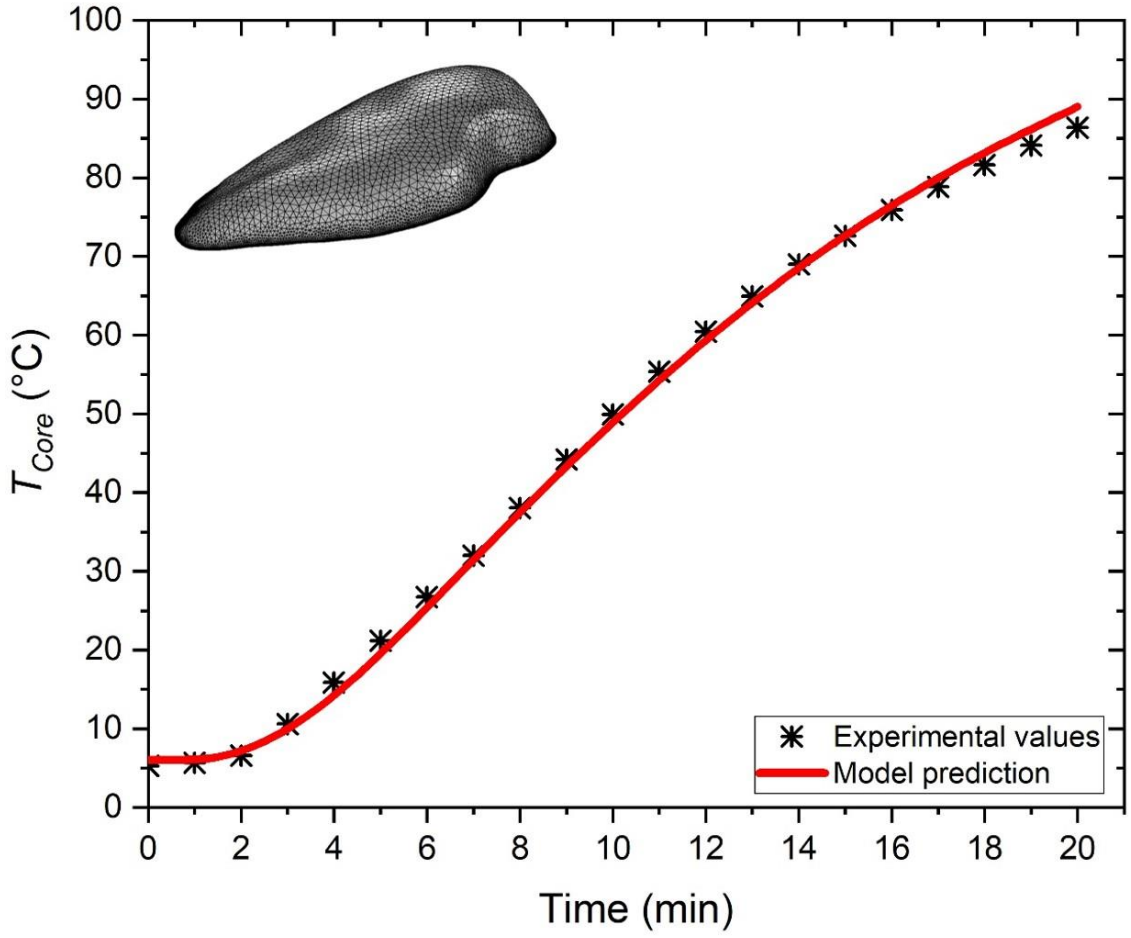

Fig. 1: Comparison between the predicted (red line) and experimental (symbols) core temperature development with roasting time at oven temperatures of T_{oven} = 230 °C.

The simulated spatial temperature, moisture content and texture (hardness) profiles after 7.5 and 15 min of roasting are visualized in Fig. 2. Compared to regular geometries (see for example Blikra et al. (2019) and Rabeler and Feyissa (2018b)), the irregular shape of the chicken breast fillet has an impact on the temperature, moisture and texture distribution. The temperature close to the tip of the chicken breast fillet, is increasing faster compared to the thicker part. This steeper temperature increase leads to a faster evaporation of liquid water and, consequently, to a drying out of the tip and edges. At the thicker part of the chicken breast, the

moisture content is mainly reduced at the surface, while the internal moisture content close to the core is not considerably changing (Fig. 2).

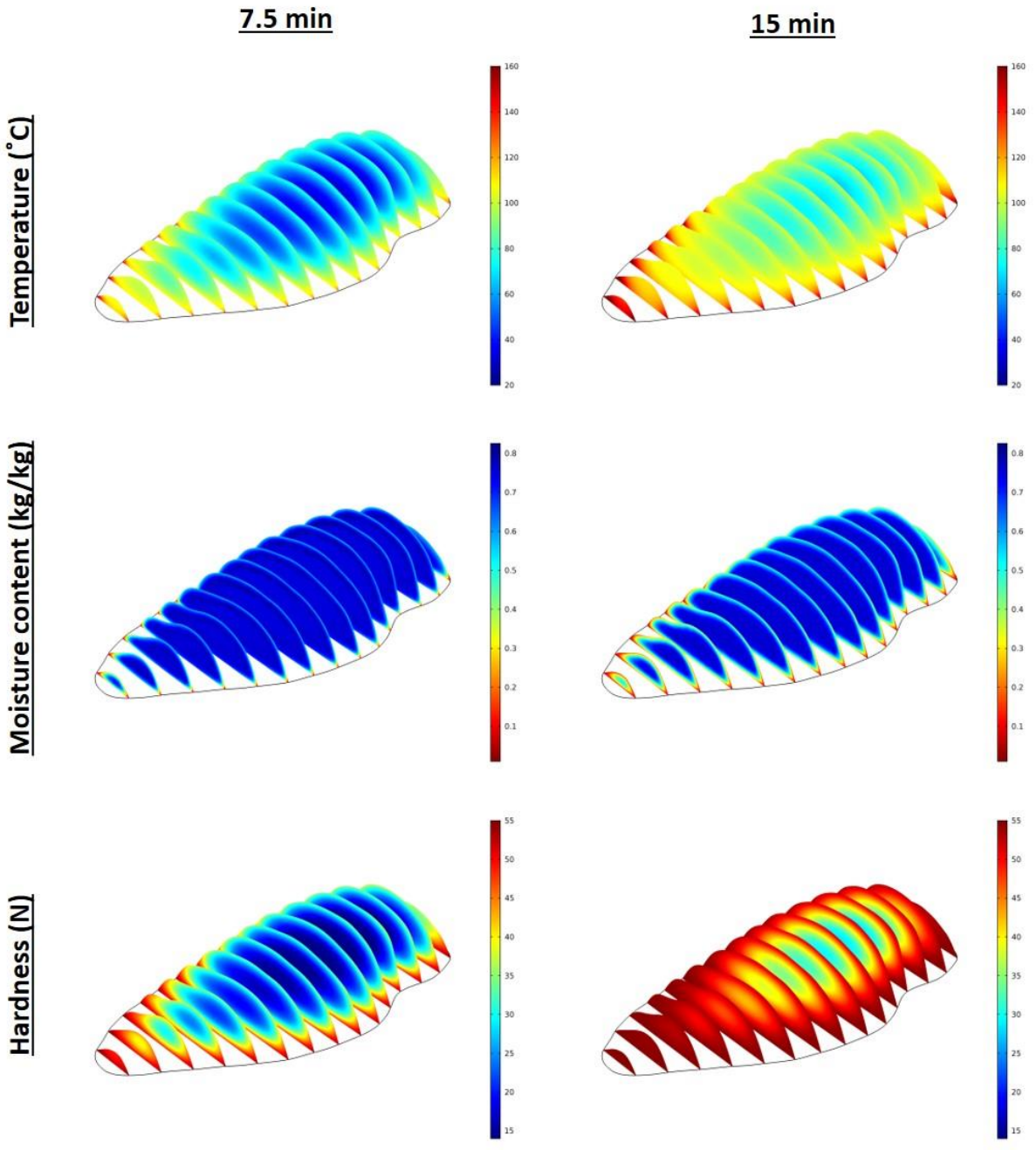

Fig. 2: Visualization of the predicted spatial temperature (°C), moisture (kg/kg) and hardness (N) distribution after 7.5 and 15 min of roasting with hot air at 230 °C.

The texture of the chicken breast fillet is a function of the temperature development during the roasting process (Eq. (11)) (Rabeler and Feyissa, 2018a). Subsequently, a non-uniform texture profile over the chicken breast fillet is achieved, with higher hardness values at the tip compared to the thicker part.

The results show, that the actual shape of the chicken breast fillet has a major impact on the roasting quality of the meat product, which, consequently, influences the acceptance of the consumer. Thus, the actual geometry of the food product should be used when developing mechanistic models to obtain a more detailed prediction, compared to regular/ simplified geometries like rectangular or spheres.

4.2. Natural variation of chicken breast fillets

As shown in section 4.1, the irregular shape of chicken breast fillets has an influence on the spatial temperature, moisture and quality distribution during the roasting process. However, there is a natural variation of the chicken breast size and shape, which could have an effect on the roasting time and quality development (e.g. texture and color). In order to study the natural variation and its impact on the roasting quality, a statistical shape model was developed (see section 2.1).

The first four modes of variation of the chicken fillet shape model are presented in Fig. 3. These are representing over 89% of the total variation in the 3D models. The analysis revealed that 77.4% of the natural chicken breast fillet variation is represented by the first mode (mode 1 in Fig. 3), which is associated with the total size variation of the chicken breast fillet. The second mode represents 6.1% of the total variation and we attributed it to the global chicken breast fillet shape. Mode 3 and mode 4 represent 3.3% and 2.6% of the chicken breast variation, respectively,

which are mainly describing the shape variations near the chicken breast tip (see Fig. 3).

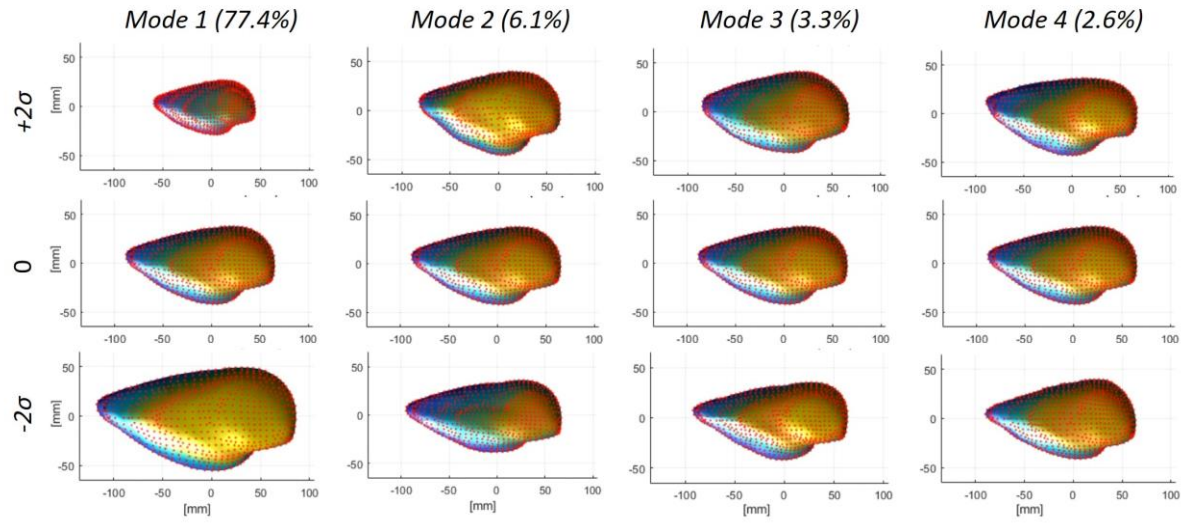

Fig. 3: Top view on the first four modes of variation of the statistical chicken breast model, plus and minus two standard deviations (±2σ). Red points show the landmarks and the color represents the height of the 3D geometry.

The statistical shape analysis showed, that there is a large degree of natural variation in the size and global shape of the chicken breast fillets. The first two modes of variation were selected for the further analysis (roasting time and quality development), as they represent more than 83% of the total variation and collectively accounted for both size (mode 1) and global shape (mode 2). As the first mode is associated with the majority of the total variation, we decided to take 5 different levels (-2σ, -1σ, 0 +1σ, +2σ) into account, while 3 levels were selected for the second mode (-2 σ, 0, +2 σ). Consequently, 15 different geometries, presented in Fig. 4, were generated using the developed statistical shape model. The geometrical

dimensions (max. length, max. width, max. height, volume and surface area) of the obtained geometries are summarized in Table 2.

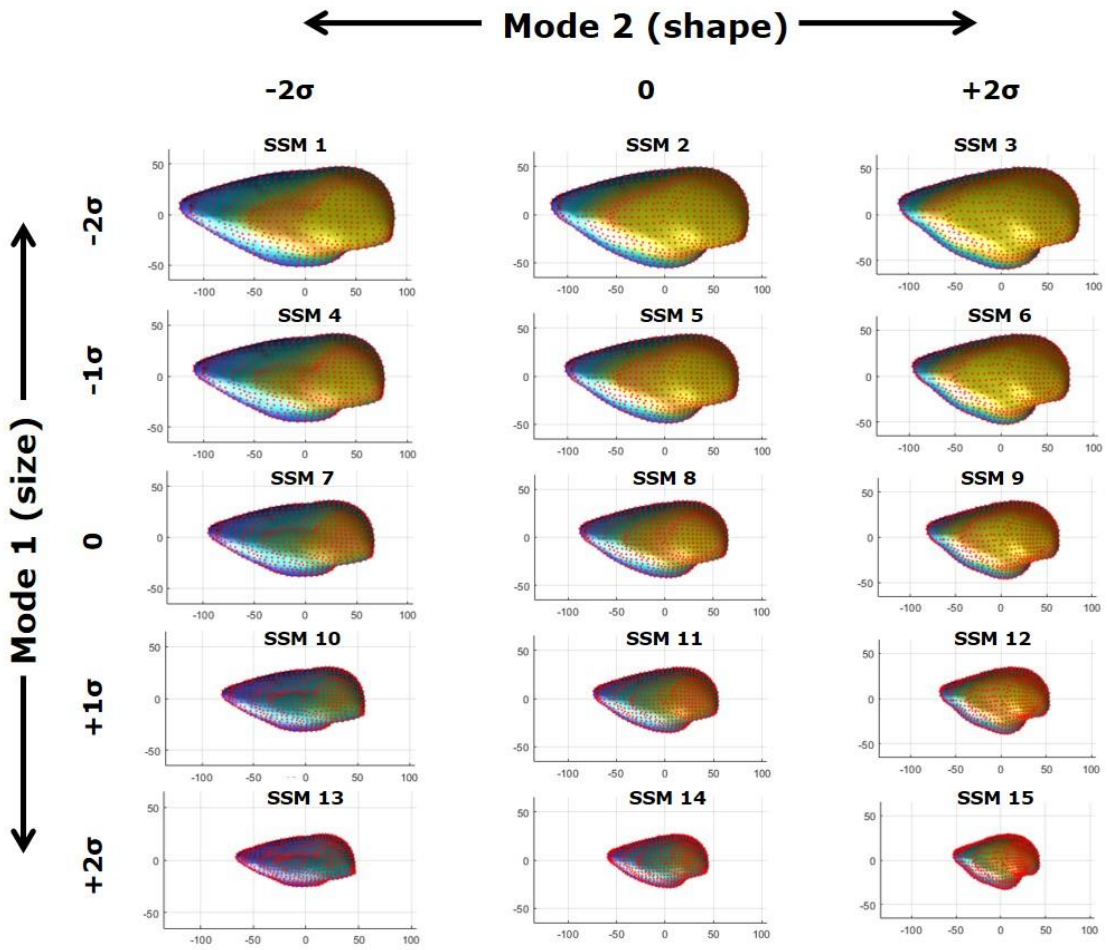

Fig. 4: Top views of the two first modes of variations (mode 1 and mode 2) of the developed chicken breast shape model, plus/ minus one (±1σ) and two standard deviations (±2σ) for the first mode and plus/ minus two standard deviations (±2σ) for the second mode. Red points show the landmarks and the color represents the height of the 3D geometry.

Table 2: Estimated geometric measures of the 15 generated chicken breast fillet geometries, using MeshLab. The max. length and max. width represent the major and minor axis of the chicken breast fillets, respectively.

Sample	Max. Length [mm]	Max. Width [mm]	Max. Height [mm]	Volume [mm^3]	Surface Area [mm^2]
SSM1	210.88	98.88	29.07	2.65E+05	3.55E+04
SSM2	203.99	104.57	34.22	3.34E+05	3.75E+04
SSM3	196.01	110.54	38.69	3.91E+05	3.91E+04
SSM4	181.43	83.96	24.52	1.59E+05	2.57E+04
SSM5	176.48	90.74	28.46	2.05E+05	2.77E+04
SSM6	170.93	98.39	34.60	2.73E+05	3.04E+04
SSM7	160.94	73.95	21.58	1.13E+05	2.03E+04
SSM8	153.90	79.99	26.03	1.48E+05	2.17E+04
SSM9	145.99	86.25	30.51	1.81E+05	2.29E+04
SSM10	136.48	61.76	17.20	6.30E+04	1.42E+04
SSM11	128.85	67.78	21.93	8.88E+04	1.54E+04
SSM12	121.41	74.11	26.43	1.13E+05	1.64E+04
SSM13	112.69	49.75	13.38	3,24E+04	9.35E+03
SSM14	102.37	54.68	15.55	3,79E+04	9.37E+03
SSM15	96.84	61.97	22.38	6.45E+04	1.11E+04

4.3. Influence of the shape modes on the roasting time

By importing the 15 statistical shape geometries (see section 4.2 and Fig. 4) into the mechanistic model of chicken breast meat roasting (see section 2.1), the influence of the first (fillet size) and second (global fillet shape) mode of variation on the roasting time and quality development was studied.

Fig. 5 presents the predicted influence of the chicken breast fillet variations on the roasting time to reach a safe core temperature of 75 °C. For the average chicken breast fillet (SSM 8) it takes around 14 minutes to reach the safe core temperature. The analysis showed, that the first mode of variation (fillet size) has a high impact on the roasting time. The roasting time at one standard deviation (SSM5 and SSM11), is decreasing more than 24% (+1σ) or increasing more than 16% (-1σ) compared to the standard chicken breast fillet. Furthermore, we found that at the two standard deviation (SSM2 and SSM14), the roasting time is even more than 54% shorter (+2σ) or 55% longer (-2σ). But also the second mode of variation (global fillet shape) (SSM7 and SSM9), has a considerable influence on the roasting time with more than 23% shorter (-2σ) or longer roasting times compared to the standard chicken breast fillet to reach the safe 75 °C in the core. The longest roasting time is necessary for the combination of the -2σ level of mode 1 and +2σ level of mode 2 (SSM3) with around 26 minutes, while the opposite combination, +2σ level of mode 1 and -2σ level of mode 2 (SSM13), leads to the shortest time of around 5 minutes. The results indicate the importance of the actual size and global shape of the chicken breast fillet on the roasting time as well as the importance of the irregular geometry in mechanistic models to obtain realistic predictions.

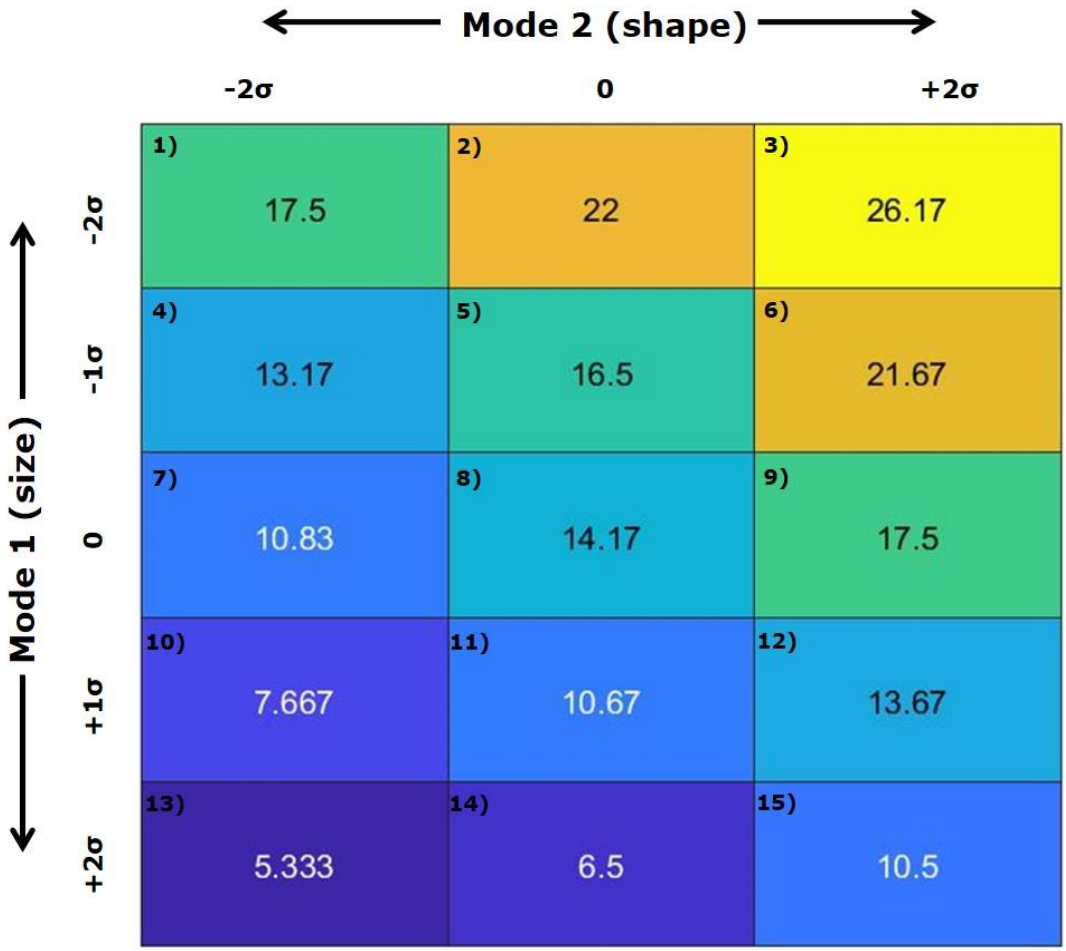

Fig. 5: Influence of the first two modes of variation (mode 1 and mode 2) of the chicken breast shape model on the roasting time (min) to reach 75 °C in the core of the chicken breast sample. T_{oven} = 230 °C.

Further analysis of the results showed that there is an exponential correlation between the roasting times to reach 75 °C in the core and the surface- to-volume ratio of the chicken breast fillets (see Fig. 6). An increase of the surface area (*A*) to volume (*V*) ratio leads to an exponential decrease of the roasting time. In thermal physics the surface-to-volume ratio is an important parameter for the heat transfer. A decrease of the *A/V* ratio leads to a decrease of the heat transfer rate from the ambient air to the chicken breast fillet, which, consequently, resulted in the increased

heating-up time. Furthermore, an increase of the breast fillet volume results in a slower internal heat transfer and also the total mass that needs to be heated up increases. Accordingly, chicken breast fillets with a lower surface-to-volume ratio require longer roasting times compared to fillets with a high A/V ratio.

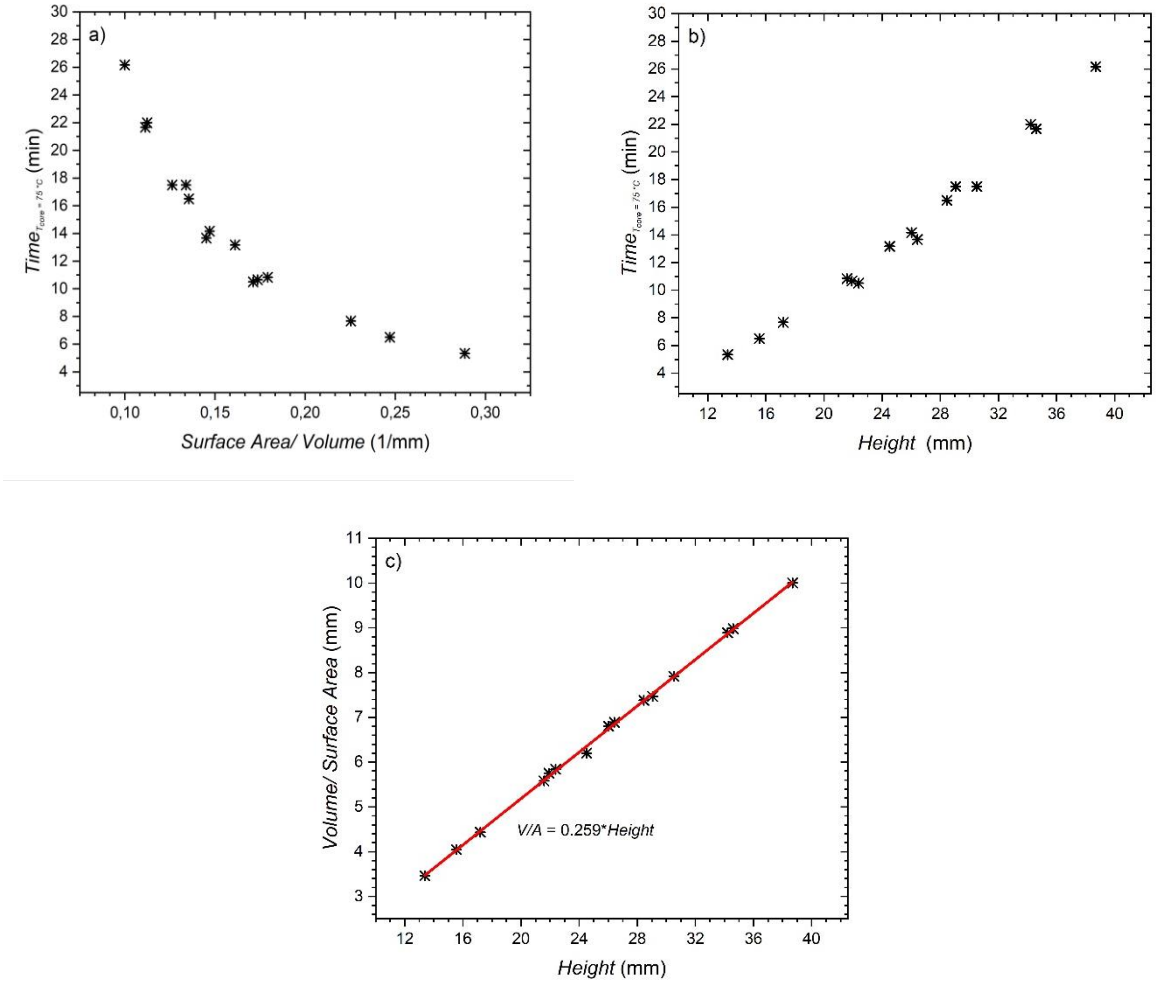

Fig. 6: Influence of different chicken breast dimensions on the roasting time to reach 75 °C in the core: a) change of the roasting time with the surface-to-volume ratio of the chicken breast, b) change of the roasting time with max. chicken breast height, and c) change of the volume-to-surface ratio with the max. chicken breast height.

Moreover, we found that the roasting time to reach 75 °C in the core is directly proportional to the max. height (to the power of 2) of the chicken breast fillet (see Fig. 6b). This obtained relationship could be used by professionals as well as non-trained staff to make a fast prediction of the roasting time to reach a safe product. For dimensionless analysis of the transport phenomena during the roasting process, the characteristic length (L_c) of the system is an important parameter, which is defined as the volume-to-surface ratio (Hahn and Özisik, 2012). Fig. 6c presents the correlation between the V/A ratio and the max. height of the chicken breast fillet and we estimated the characteristic length as: $L_c = 0.259*Height$. This relationship is important for further analyses with dimensionless numbers (for example the Fourier and Biot number) or to simplify the model.

4.4. Influence of the shape modes on the chicken quality

The texture and color of chicken breast meat are two important quality parameters for the acceptance of the consumer (Lawrie and Ledward, 2006). The influence of the two first shape modes (see section 4.2) on the texture parameter hardness is presented in Fig. 7a. The standard chicken breast fillet (SSM8) has an average hardness of around 41 N when reaching a safe core temperature of 75 °C. Similar to the roasting time (see section 4.3) the first mode of variation (mode 1, fillet size) has a higher impact on the hardness compared to the second mode of variation (mode 2, global fillet shape). At the first standard deviation of the first mode (SSM5 and SSM11), up to 11% lower (+1σ) and up to 5% higher (-1σ) hardness values are achieved. At the second standard deviation (SSM2 and SSM14), the hardness of the chicken breast fillet is around 17% lower (+2σ) and up to 8% higher (-2σ), compared

to the standard chicken breast fillet. The change of the texture parameter hardness is a function of the temperature development and roasting time (Rabeler and Feyissa, 2018a) (Eq. (11)). Thus, the longer (16.5 and 22 min) or shorter (10.67 and 6.5 min) roasting times at the first and second standard deviation (±2σ levels at mode 1, Fig. 4) result in a harder or softer texture compared to the standard chicken breast fillet, respectively.

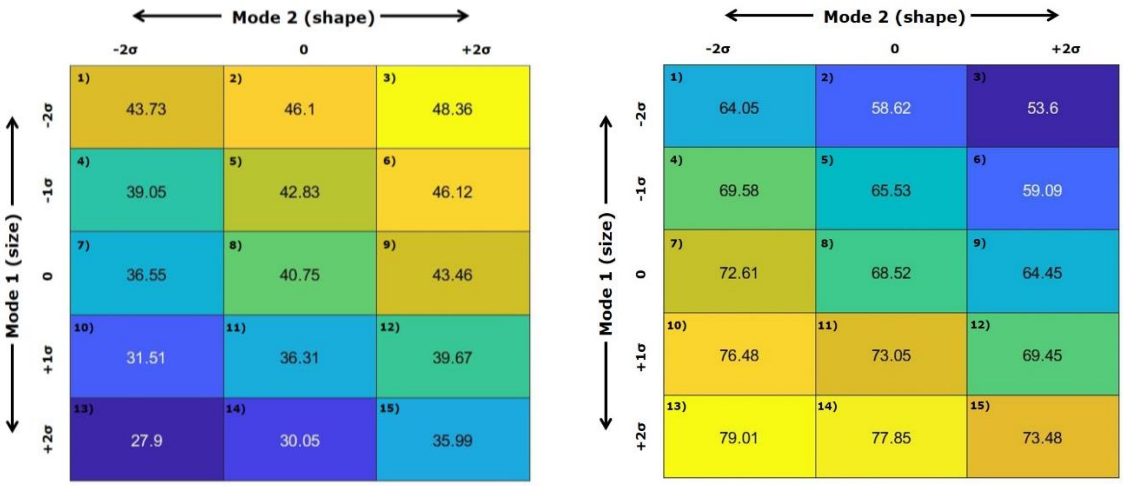

Fig. 7: Effect of the first two modes of variation (mode 1 and mode 2) of the chicken breast shape model on the a) hardness (N) and b) surface lightness of the fillets after reaching 75 °C in the core. T_{oven} = 230 °C.

For the second mode of variation (mode 2, global fillet shape) a hardness decrease of up to 10% (-2σ, SSM7) or hardness increase of up to 7% (+2σ, SSM9) compared to the standard chicken breast fillet was observed (Fig. 7a). These texture differences are a result of the different roasting times for the two different geometries. Consequently, not only the size of the chicken fillet but also its global shape has a considerable impact on the final texture of the chicken breast meat. For the surface color (lightness, *L**) of the chicken breast fillets the first mode of variation (fillet size) has the highest impact with up to 17% darker (-2σ, SSM2) or

14% lighter colors (+2σ, SSM14) compared to the standard chicken breast fillet (see Fig. 7b). For the second mode of variation (mode 2, global fillet shape) around 6% darker (+2σ, SSM9) or lighter (-2σ, SSM7) colors are obtained.

The darkest surface color (L^* = 53.6) was obtained for the combination of the -2σ level of mode 1 and the +2σ level of mode 2 (SSM3), while the combination of the +2σ level of mode 1 and the -2σ level of mode 2 resulted in the highest lightness value (L^*=79.01, SSM13). The roasting time has a direct impact on the surface color of food products (Matsuda et al., 2013; Rabeler et al., 2019) (Eq. (12)). Thus, the prolonged roasting times at the first and second standard deviation (-1σ and -2σ levels at mode 1, Fig. 5) lead to an increase of the surface lightness values compared to the standard chicken breast fillet, while the roasting time decrease (+1σ and +2σ levels at mode 1, Fig. 4) results in a brighter surface color.

Overall, the results show that the variations in the chicken breast fillet size and global shape have a high impact on the quality of the cooked chicken breast meat. Thus, it is crucial to implement the actual shape of the food product into the mechanistic model to obtain an accurate prediction of the quality development with roasting time.

Conclusion

The obtained results of this study show that the actual (i.e. irregular) shape of chicken breast fillets has a major impact on the roasting time and quality development during the roasting process. The actual chicken breast fillet shape led to a spatial variation of the temperature as well as quality attributes (hardness and lightness). This implies that the actual, irregular geometry of the food product should be taken into account when developing mechanistic models.

Moreover, the developed statistical shape model for chicken breast fillets revealed a high degree of natural variation not only in the actual size but also the global shape of chicken breast fillets. The combination of the statistical shape model with the mechanistic model of chicken meat roasting allowed for detailed and systematic analyses of the size and global shape effect on the roasting time and quality development during the roasting process. We found, that the chicken breast fillet size has a major impact on both the roasting time and quality (hardness and lightness) of the cooked chicken meat. Furthermore, the global shape of the chicken breast fillet has a high impact on the roasting time and quality attributes. Thus, a detailed description of the food geometry is important when developing mechanistic models. Not only to minimize the model error due to an over simplified geometry, but also to obtain realistic model predictions that can be used by professionals to optimize the cooking process. Furthermore, the direct correlation between the max. height of the chicken breast fillet and the roasting time to reach a safe core temperature can be used by experts and non-professionals to make fast predictions. The obtained relationships between the geometric measures (for example surface-to-volume ratio and characteristic length) could be used in future work to reconstruct the geometry of chicken breast fillets using simple geometries like trapezoids or triangular. This could enable the use of 2D instead of irregular 3D geometries, resulting in shorter computational times with only slight impacts on the model predictions.

Overall, the presented approach of combining statistical shape models with mechanistic models of heat and mass transfer is a strong tool to obtain a systematic knowledge how the irregular shaped geometry of food products is influencing the

model predictions. Thus, a deeper understanding of the food size and global shape impact on the quality development is obtained.

Nomenclature

A	area (m^2)
a_w	water activity
C	mass concentration (kg/kg)
c_p	specific heat capacity (J/(kg K))
D	diffusion coefficient (m^2/s)
f	Heaviside function
h	heat transfer coefficient ($W/(m^2 K)$)
k	number of landmarks
$k(T, a_w)$	reaction rate constant (1/min)
k_i	thermal conductivity chicken meat (W/(m K))
L_c	characteristic length (m)
L^*	lightness
n	number of scanned samples
P	eigenvector
T	temperature (K)
t	time (min)
u	velocity (m/s)
V	volume (m^3)
$\bar{X}$	mean shape
CL	cooking loss
Nu	Nusselt number
Pr	Prandtl number
Re	Reynolds number
$RMSE$	Root mean squared error

Greek symbols	
β	mass transfer coefficient (m/s)
λ	eigenvalue
ρ	Density (kg/m^3)
σ	standard deviation
Subscripts	
0	initial (t=0)
a	air
b	browning
bot	bottom
cm	chicken meat
int	internal
surf	surface
w	water
wh	whitening
∞	equilibrium

References

Bird, R.B., Stewart, W.E., Lightfoot, E.N., 2006. Transport Phenomena, 2nd Editio. ed. John Wiley & Sons, Inc.

Blikra, M.J., Skipnes, D., Feyissa, A.H., 2019. Model for heat and mass transport during cooking of cod loin in a convection oven. Food Control 102, 29–37. https://doi.org/10.1016/j.foodcont.2019.03.001

Bruse, J.L., McLeod, K., Biglino, G., Ntsinjana, H.N., Capelli, C., Hsia, T.Y., Sermesant, M., Pennec, X., Taylor, A.M., Schievano, S., Taylor, A., Giardini, A., Khambadkone, S., de Leval, M., Bove, E., Dorfman, A., Baker, G.H., Hlavacek, A., Migliavacca, F., Pennati, G., Dubini, G., Marsden, A., Vignon-Clementel, I., Figliola, R., McGregor, J., 2016. A statistical shape modelling framework to extract 3D shape biomarkers from medical imaging data: Assessing arch morphology of repaired coarctation of the aorta. BMC Med. Imaging 16, 1–19. https://doi.org/10.1186/s12880-016-0142-z

Chhabra, R.P., 2017. CRC Handbook of Thermal Engineering Second Edition. CRC Press, Second edition. | Boca Raton : Taylor & Francis, CRC Press, 2017. https://doi.org/10.4324/9781315119717

Cignoni, P., Callieri, M., Corsini, M., Dellepiane, M., Ganovelli, F., Ranzuglia, G., 2008. MeshLab: an Open-Source Mesh Processing Tool, in: Sixth Eurographics Italian Chapter Conference.

Cootes, T.F., Taylor, C.J., Cooper, D.H., Graham, J., 1995. Active Shape Models-Their Training and Application. Comput. Vis. Image Underst. 61, 38–59.

Dalal, P., Munsell, B.C., Wang, S., Tang, J., Oliver, K., Ninomiya, H., Zhou, X., Fujita, H., 2007. A fast 3D correspondence method for statistical shape

modeling. Proc. IEEE Comput. Soc. Conf. Comput. Vis. Pattern Recognit. https://doi.org/10.1109/CVPR.2007.383143

Danckaers, F., Huysmans, T., Dael, M. Van, Verboven, P., Nicolaï, B., Sijbers, J., 2017. Building 3D Statistical Shape Models of Horticultural Products. Food Bioprocess Technol. 10, 2100–2112. https://doi.org/10.1007/s11947-017-1979-z

Danckaers, F., Huysmans, T., Dael, M. Van, Verboven, P., Sijbers, J., 2014. Building a Statistical Shape Model of the Apple from Corresponded Surfaces 44.

Dryden, I.L., Mardia, K. V., 1998. Statistical Shape Analysis. Wiley.

Fabbri, A., Cevoli, C., Alessandrini, L., Romani, S., 2011. Numerical modeling of heat and mass transfer during coffee roasting process. J. Food Eng. 105, 264–269. https://doi.org/10.1016/j.jfoodeng.2011.02.030

Feyissa, A.H., Gernaey, K. V., Adler-Nissen, J., 2013. 3D modelling of coupled mass and heat transfer of a convection-oven roasting process. Meat Sci. 93, 810–820. https://doi.org/10.1016/j.meatsci.2012.12.003

Fuessinger, M.A., Schwarz, S., Cornelius, C.P., Metzger, M.C., Ellis, E., Probst, F., Semper-Hogg, W., Gass, M., Schlager, S., 2018. Planning of skull reconstruction based on a statistical shape model combined with geometric morphometrics. Int. J. Comput. Assist. Radiol. Surg. 13, 519–529. https://doi.org/10.1007/s11548-017-1674-6

Goñi, S.M., Purlis, E., Salvadori, V.O., 2008. Geometry modelling of food materials from magnetic resonance imaging. J. Food Eng. 88, 561–567. https://doi.org/10.1016/j.jfoodeng.2008.03.020

Goñi, S.M., Purlis, E., Salvadori, V.O., 2007. Three-dimensional reconstruction of irregular foodstuffs. J. Food Eng. 82, 536–547. https://doi.org/10.1016/j.jfoodeng.2007.03.021

Goñi, S.M., Salvadori, V.O., 2010. Prediction of cooking times and weight losses during meat roasting. J. Food Eng. 100, 1–11. https://doi.org/10.1016/j.jfoodeng.2010.03.016

Hahn, D.W., Özisik, M.N., 2012. Heat Conduction. John Wiley & Sons.

Hargin, K.D., 1996. Authenticity issues in meat and meat products. Meat Sci. 43, 277–289. https://doi.org/10.1016/0309-1740(96)00072-1

Isleroglu, H., Kaymak-Ertekin, F., 2016. Modelling of heat and mass transfer during cooking in steam-assisted hybrid oven. J. Food Eng. 181, 50–58. https://doi.org/10.1016/j.jfoodeng.2016.02.027

Jha, S.N., 2005. Mathematical simulation of roasting of grain. J. Food Eng. 71, 304–310. https://doi.org/10.1016/j.jfoodeng.2005.03.006

Lawrie, R.A., Ledward, D.A., 2006. Lawrie's meat science. Woodhead Publishing.

Liu, S., Fukuoka, M., Sakai, N., 2013. A finite element model for simulating temperature distributions in rotating food during microwave heating. J. Food Eng. 115, 49–62. https://doi.org/10.1016/j.jfoodeng.2012.09.019

Matsuda, H., Llave, Y., Fukuoka, M., Sakai, N., 2013. Color changes in fish during grilling-Influences of heat transfer and heating medium on browning color. J. Food Eng. 116, 130–137. https://doi.org/10.1016/j.jfoodeng.2012.11.027

Purlis, E., Salvadori, V.O., 2009. Modelling the browning of bread during baking. Food Res. Int. 42, 865–870. https://doi.org/10.1016/j.foodres.2009.03.007

Rabeler, F., Feyissa, A.H., 2018a. Kinetic Modeling of Texture and Color Changes During Thermal Treatment of Chicken Breast Meat. Food Bioprocess Technol. 11, 1495–1504. https://doi.org/10.1007/s11947-018-2123-4

Rabeler, F., Feyissa, A.H., 2018b. Modelling the transport phenomena and texture changes of chicken breast meat during the roasting in a convective oven. J. Food Eng. 237, 60–68. https://doi.org/10.1016/j.jfoodeng.2018.05.021

Rabeler, F., Skytte, J.L., Feyissa, A.H., 2019. Prediction of thermal induced color changes of chicken breast meat during convective roasting: A combined mechanistic and kinetic modelling approach. Food Control 104, 42–49. https://doi.org/10.1016/j.foodcont.2019.04.018

Sakin-Yilmazer, M., Kaymak-Ertekin, F., Ilicali, C., 2012. Modeling of simultaneous heat and mass transfer during convective oven ring cake baking. J. Food Eng. 111, 289–298. https://doi.org/10.1016/j.jfoodeng.2012.02.020

van der Sman, R.G.M., 2013. Modeling cooking of chicken meat in industrial tunnel ovens with the Flory-Rehner theory. Meat Sci. 95, 940–957. https://doi.org/10.1016/j.meatsci.2013.03.027

van der Sman, R.G.M., 2007. Moisture transport during cooking of meat: An analysis based on Flory-Rehner theory. Meat Sci. 76, 730–738. https://doi.org/10.1016/j.meatsci.2007.02.014

Zhu, H., Gulati, T., Datta, A.K., Huang, K., 2015. Microwave drying of spheres: Coupled electromagnetics-multiphase transport modeling with experimentation. Part I: Model development and experimental methodology. Food Bioprod. Process. 96, 314–325. https://doi.org/10.1016/j.fbp.2015.08.003

7 Summary of research results and discussion

As described in **Chapter 5** the aim of my PhD project was to study the possibility of a combined kinetic and mechanistic modelling approach to predict the spatial quality changes of food products, i.e. chicken breast meat in this work, as function of the process parameters.

7.1 The combined kinetic and mechanistic modelling approach

Kinetic models as described in **Chapter 2** allow the prediction of global food quality changes during heating processes. However, to obtain the spatial quality distributions of for example the texture or color, the entire temperature-time-history is needed. Mechanistic models that describe the transport phenomena, i.e. heat and mass transfer, can provide the required spatial temperature and moisture content profiles during the heating process. In my PhD project we developed, therefore, a combined mechanistic and kinetic modelling approach to predict the texture (i.e. hardness, gumminess and chewiness) and color (i.e. lightness) changes of chicken breast meat during convective roasting (Figure 5). Accordingly, we obtained a detailed, quantitative knowledge about the phenomena that lead to the spatial quality changes.

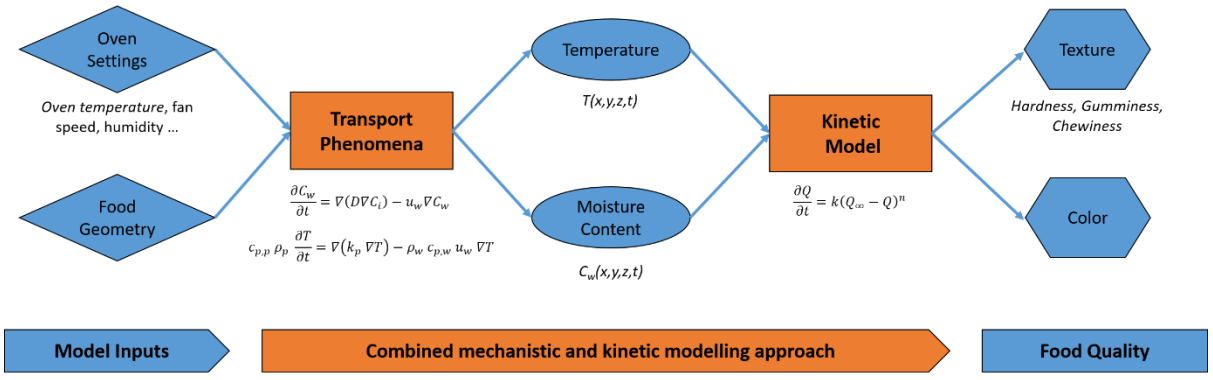

Figure 5: The combined mechanistic and kinetic modelling approach: Correlation between model inputs and the spatial food quality.

In **Section 7.1.1** a summary of the established mechanistic model of chicken breast meat roasting is given. The combination of mechanistic and kinetic models to predict the texture and color changes of chicken breast meat during the roasting process are then discussed in **Section 7.1.2** and **7.1.3,** respectively.

7.1.1 Mechanistic modelling of chicken meat roasting

The roasting of chicken breast meat is a complex process, which involves coupled heat and mass transfer (Figure 6). In **Publication 2**, we established a mechanistic model from first principles that is based on the conservation of mass and energy (see **Chapter 3**). The model includes the external heat transfer by convection towards the chicken breast surface, from which the heat is further transported internally by conduction and convection (Eq. (15)). Moisture migration within the meat towards the surface was modeled with the Flory-Rehner theory (Eq. (23)) combined with Darcy's law (Eq. (22)) (**Section 3.1)**. From the surface, water is then evaporated towards the surrounding hot air (Eq. (24)) (Figure 6).

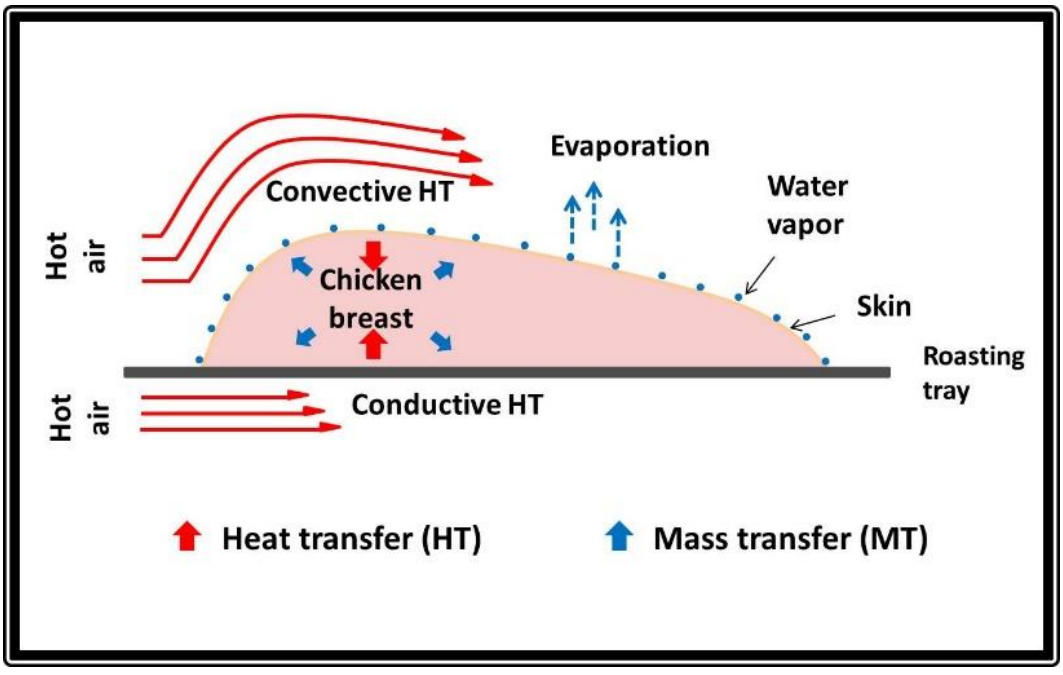

Figure 6: Convective roasting of chicken breast meat: Illustration of main mechanisms (Rabeler and Feyissa, 2018b).

To ensure an accurate description of the internal heat and mass transfer, the model should include a detailed description of the internal physical phenomena. The roasting process is influencing not only the temperature but also the composition (due to the evaporation of water) of the chicken breast meat, which has a direct impact on its thermophysical properties (see **Section 3.1**). We considered this in the developed model by describing the specific heat capacity ($c_{p,cm}$) and thermal conductivity (k_{cm}) of chicken breast meat as function of the temperature and individual component fractions (i.e. water, fat, protein and ash) (Choi and Okos, 1986). We further took the anisotropic structure of the chicken breast meat into account and its influence on the thermal conductivity. We used the parallel model (Eq. (18)) along the chicken meat fiber direction, while we applied the perpendicular model (Eq. (19)) vertical to the fibers (**Publication 3**). By considering these phenomena and its influence on the thermophysical properties, we enabled a detailed description of the internal heat transfer.

The temperature increase inside the chicken breast meat results then in alterations of the microstructure due to the denaturation of proteins. This has a direct impact on the internal moisture transport and, therefore, should be included in the model (Feyissa et al., 2013; Tornberg, 2005). We considered the heat induced dynamic changes in the chicken breast meat microstructure by measuring and describing the storage modulus (G') in Eq. (23) as function of the temperature (**Publication 1**). Similar to meat (Tornberg, 2005) and cod fish (Blikra et al., 2019) the storage modulus of chicken breast meat is increasing when the temperature reaches values between 55 and 80 °C. This increase can be related to protein denaturation, which results in more compact fiber arrangements (Tornberg, 2005). Consequently, the rise of the storage modulus leads to an increase of the swelling pressure (Eq. (23)) and the expulsion of liquid water towards the chicken breast meat surface (Eq. (21)). Above 80 °C the storage modulus reaches an equilibrium value (**Publication 1**), indicating the end of protein denaturation and microstructural changes (Wattanachant et al., 2005).

By carefully considering all these physical phenomena during the roasting of chicken breast meat, we enabled a detailed description of the internal heat and mass transfer. The validation of the established model showed a good agreement between the

measured and predicted core and surface temperature as well as moisture content development. Consequently, we applied the model to study the influence of the process settings on the spatial temperature and moisture content distributions during roasting. The model predictions showed that the convective roasting with hot air leads to a non-uniform temperature and moisture content profile inside the chicken breast meat (see Fig. 4 in **Publication 2**). The surface temperature is increasing faster compared to the core, which leads to the evaporation of liquid water towards the surrounding hot air and finally to the formation of a thin crust. On the contrary, the roasting process does not affect the moisture content at the chicken breast core, which agrees with the findings of Feyissa et al. (2013) who showed, supported by experiments, that the core moisture content of meat is not considerably affected during the roasting process.

However, not all parameters that we needed to build the model were readily available or the reported values came with a certain degree of uncertainty, which has a direct impact on the accuracy and reliability of the model (**Chapter 4**). Therefore, we evaluated the established model in **Publication 3** by using global uncertainty and sensitivity analysis. In details, we applied the Monte Carlo method (see **Section 4.1**) with different sampling techniques (Figure 4) to study the uncertainty in the model predictions. We found that quasi-random sampling (Halton and Sobol sequence) leads to a faster convergence of the following sensitivity analysis and consequently, to shorter computational times compared to the LHS method. The results further showed that the uncertainty in the predicted temperature and moisture content development are not constant but change with roasting time. The standardized regression coefficient (SRC) method, a global sensitivity analysis method, enabled us afterwards to determine the influence of each uncertain input parameter on the model predictions and accordingly, rank them. We found that the oven parameters, such as temperature and fan speed, as well as the thermophysical properties have a high impact on the temperature development during roasting. Therefore, the detailed description of both the thermal conductivity as well as the heat capacity as described above is compulsory to obtain accurate model predictions. Furthermore, we found that the moisture diffusion coefficient has only a minor impact on the moisture content development

during roasting. The result highlights that the dominant moisture transport phenomena during chicken breast meat roasting is not diffusion but the expulsion of liquid water due to the increase of the swelling pressure (Eq. 23). Consequently, it is sufficient to use a simple description of the diffusion coefficient, while the parameters for the pressure driven transport (e.g. storage modulus) should be included as accurately as possible in the model. The results show the strength of the sensitivity analysis to give the user possibilities for a knowledge based refinement or reduction of the developed model to obtain accurate model predictions.

Overall, the established model in this PhD project is able to predict precisely the spatial temperature and moisture content development during the roasting of chicken breast meat. Thus, we obtained a quantitative knowledge about the process parameters influence on the temperature and moisture content changes, which can be used to optimize the roasting process to achieve a more uniform temperature distribution with the least total moisture loss. The results of the uncertainty and sensitivity analysis provide the user then a quantitative, valuable understanding about the reliability of the established model as well as the possibilities for model refinement or reduction. Therefore, it should be a central step during the model development process (Figure 1).

7.1.2 Prediction of texture changes during chicken meat roasting

The texture of chicken breast meat, but generally for most food products, is an essential quality parameter for the consumers' acceptance (Lawrie and Ledward, 2006). In **Publication 1**, we performed texture profile analysis (TPA) to study the changes in the TPA parameters hardness, gumminess as well as chewiness with heating time at different isothermal temperatures (50, 65, 75, 85 and 95 °C). We found that the texture parameters are increasing with heating time until reaching a non-zero equilibrium, showing a toughening of the chicken meat. An increase of the temperature leads thereby to faster texture changes and higher equilibrium values. In order to enable a prediction of the texture changes and to obtain a deeper understanding of the underlying mechanisms, we then developed kinetic models. However, as discussed in **Chapter 2,** a kinetic model that takes the non-zero equilibrium of food

quality attributes into account without the need of preliminary assumptions is missing. Therefore, we established in **Publication 1** a modified rate law that allows for a universal description of food quality changes with or without non-zero equilibrium (Eq. (25) and Eq. (26)):

$$\frac{\partial Q}{\partial t} = -k(Q - Q_\infty)^n \qquad Q_0 \geq Q \geq Q_\infty \tag{25}$$

$$\frac{\partial Q}{\partial t} = k(Q_\infty - Q)^n \qquad Q_0 \leq Q \leq Q_\infty \tag{26}$$

The advantage of the modified rate law is that no assumption of the reaction order is needed. Instead, the reaction order can be estimated together with the rest of the kinetic parameters (e.g. activation energy and pre-factor) and, consequently, it enables a better fit of the experimental data by the model. At the same time, the reliability of the model predictions is increased, as no preliminary assumptions have to be made (see **Chapter 2**). In further own studies (not shown here) we successfully applied the same modified rate law to describe the color changes of bread rolls during the baking process, which shows its usefulness and strength also for other food products.

We applied Eq. (26) combined with the standard Arrhenius equation (Eq. (7)) to describe the changes of the TPA parameters hardness, gumminess and chewiness as function of temperature and time (the equilibrium values (Q_∞) of the texture parameters are larger than the initial values (Q_0)). The analysis with the kinetic models showed that the texture changes can be related directly to the rate as well as degree of protein denaturation and associated microstructural changes. Thus, we obtained a quantitative knowledge about the phenomena that lead to the toughening of chicken breast meat during thermal heating.

In order to predict not only the global but also local or spatial texture changes of chicken breast meat during the roasting process (see Figure 6) the spatial temperature distribution is needed (see **Chapter 2**). Therefore, we combined in **Publication 2** the developed mechanistic model of chicken meat roasting (see **Section 7.1.1**) with the kinetic models for the texture parameters hardness, gumminess and chewiness (see

Figure 5). This enabled us to predict the local texture changes as function of the spatial temperature development during the roasting process. The validation of the developed model showed then a good agreement between the model predictions and experimental values.

Consequently, we applied the established combined model to predict the influence of the process settings (oven temperature and fan speed) on the chicken breast meat texture changes. The global sensitivity analysis conducted in **Publication 3** showed that the process settings are the main factors influencing the texture of the chicken breast meat. Accordingly, an increase of the oven temperature results in a faster change of the texture parameters, due to the increase of the external heat flux towards the chicken meat surface (Eq. (20)). On the contrary, a decrease in the fan speed leads to a slower temperature increase, which leads to a slower texture change (**Publication 2**). The results show, that the control of the oven temperature as well as uniformity of the air velocity inside the oven are highly important for the final texture quality.

Overall, the established combined model of transport phenomena and texture kinetics provide the operator or chef a detailed understanding of the relationship between process settings and the final overall texture of roasted chicken breast meat.

7.1.3 Prediction of color changes during chicken meat roasting

The color of cooked food products is the first quality attribute that consumers evaluate. Thus, it is critical for the acceptance of the consumer (Guerrero-Legarreta and Hui, 2010). During the roasting of chicken breast meat we observed that the meat gets first white (increase of the lightness), while at later stages when the surface temperature is further rising, the color at the surface is changing to brown (decrease of the lightness).

The whitening of the chicken breast meat is caused mainly by the denaturation of heme-proteins, such as myoglobin and hemoglobin (King and Whyte, 2006). In **Publication 1**, we studied the influence of the temperature and heating time on the lightness changes of chicken breast meat. We found that the lightness is rising with

time until leveling off to an equilibrium value, while the temperature affects the rate of the color change. We modeled the temperature and time dependent color changes with the established modified rate law (Eq. (26) in **Section 7.1.2)** combined with the Arrhenius equation (Eq. (7)). Accordingly, we obtained a detail understanding of the relationship between heat induced heme-protein denaturation and the whitening of the chicken breast meat.

In order to predict the local color changes of chicken breast meat during roasting, we coupled in **Publication 4** the developed kinetic model with the mechanistic model of heat and mass transfer (**Section 7.1.1**).This allowed us to predict the spatial lightness development inside the chicken breast meat during the heating process (Figure 7).

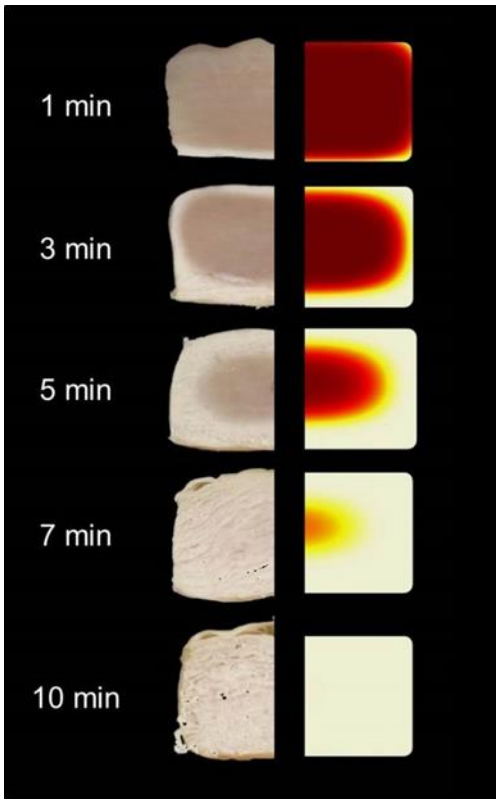

Figure 7: Internal whitening of chicken breast meat during roasting at 230 °C: Visual comparison of the experimental (on the left side) and predicted (on the right side) color changes (Rabeler et al., 2019).

The internal whitening is still used as an indicator for the doneness of the chicken breast meat, especially in private households. However, a visual check does not ensure the safety of the chicken breast meat, as it becomes completely white even before reaching the required safety core temperature of 72 °C (see **Publication 4**). In this manner, the established model is a useful tool to ensure the doneness of the roasted chicken breast meat on a quantitative knowledge instead of the cook and a look approach.

For the surface browning of the chicken breast meat, which is caused by caramelization, Maillard and carbonization reactions (Nakamura et al., 2011), we developed a non-isothermal kinetic model. We applied a first order reaction kinetic model (Eq. (3)) and described the reaction rate constant *k* as function of the local temperature and water activity (Eq. (27)):

$$k_b = \left(a_1 + \frac{a_2}{a_w}\right) exp\left(-\frac{a_3 + \frac{a_4}{T}}{T}\right) \quad (27)$$

where a_1, a_2, a_3 and a_4 are kinetic parameters without a direct physical meaning. We then combined the kinetic model for the whitening and browning, which enabled us to predict both phenomena with one equation. Furthermore, it allowed us to estimate the temperature at which browning reactions start (switch between lightness increase and decrease), and consequently, we obtained a deeper understanding about the mechanisms that result in the surface browning.

In order to predict the surface color changes of chicken breast meat during roasting we coupled then the kinetic models with the mechanistic model of heat and mass transfer (**Publication 4**). Consequently, we estimated the start temperature of the browning reactions as well as the missing kinetic parameters in Eq. (27). The combined model enabled us to study then the impact of the oven temperature and fan speed on the surface color development. A rise of the oven temperature or fan speed results in a faster increase of the surface temperature and decrease of the moisture content (Eq. (20) and Eq. (24), respectively). Consequently, the surface color changing rate increases, which finally results in darker surface colors of the chicken breast meat (**Publication 4**).

Overall, the combined mechanistic and kinetic modelling approach gives the chef or operator the quantitative relationship between the process parameters and the spatial color and texture changes of the chicken breast meat during roasting (Figure 5). Thus, the model can be used to find the optimum process conditions to reach the desired surface color and texture, while guaranteeing the safety of the product for the consumer. By performing what-if scenarios with for example oven temperature and/or fan speed ramps, the degree of the surface browning and meat hardening can be modified, while simultaneously decreasing the amount of total moisture loss. This could lead to an improved overall quality of roasted chicken breast meat, without the need of expensive and time-consuming experiments.

7.2 Sensitivity of the irregular food geometry

The geometry of the food product is an essential part of the mechanistic model as its shape and size has a direct impact on the spatial temperature and moisture content distribution (Goñi and Purlis, 2010). In order to study the influence of the irregular shape of chicken breast meat on the spatial quality development during the roasting process, we performed a geometry sensitivity study in **Publication 5**. We used laser line 3D scanning, as described in **Section 3.2**, to obtain the actual shape of chicken breasts, which was then imported into the established mechanistic model of chicken meat roasting (**Section 7.1.1**). The model predictions showed that the irregular shape of the chicken breast fillet resulted in a non-uniform distribution of the state variables as well as quality attributes, with higher temperatures and texture values at the tip compared to the thicker part (Figure 8).

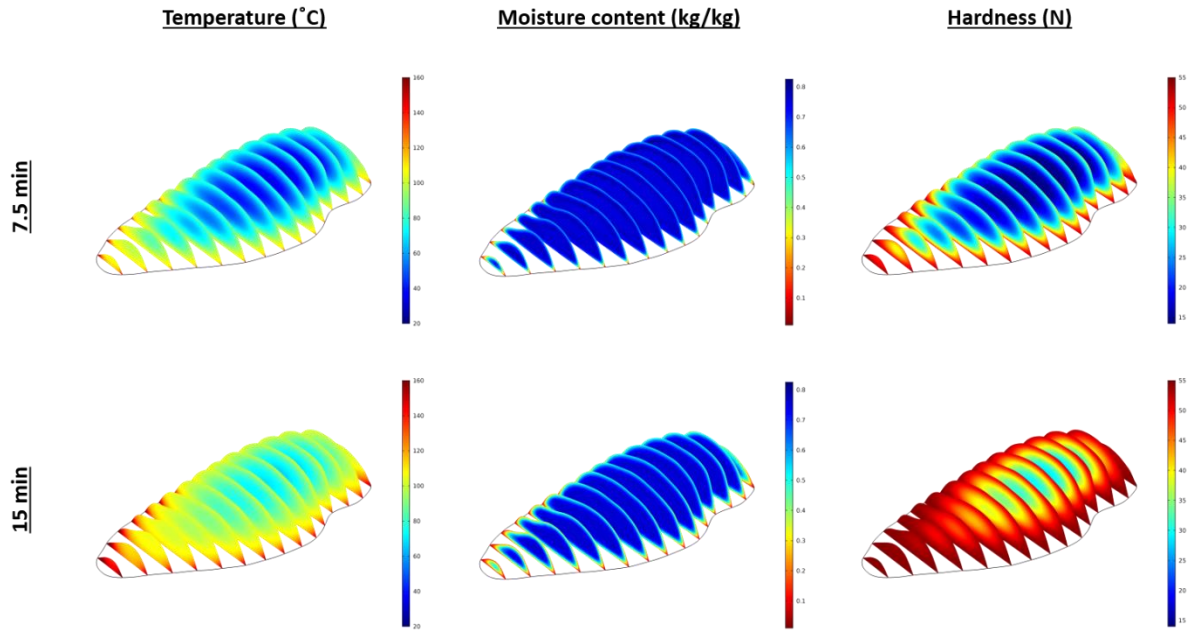

Figure 8: Visualized model predictions of the spatial temperature (°C), moisture (kg/kg) and hardness (N) distribution after 7.5 and 15 min of convective roasting with hot air at 230 °C.

The analysis of a representative population of 50 randomly bought and scanned chicken breast fillets showed a high natural variation in the weight as well as chicken breast fillet dimensions (i.e. length, width and height). In order to assess this natural diversity in a comprehensive way, my colleague Jacob Lercke Skytte developed a landmark-based model statistical shape model (SSM) (**Publication 5)**. The SSM showed that over 77 % of the total variation can be related to the total size variations (mode 1) of the chicken breast fillets, while over 6 % of the total variation can be represented by the global fillet shape (mode 2).

In order to study the influence of the size and total shape variation on the state variables, we created 15 geometries using the SSM, which represent 5 levels of the size variation (±2σ, ±1σ, 0) and 3 levels of the global shape variation (±2σ, 0) (Figure 9). The obtained geometries were then imported into the mechanistic model of chicken meat roasting (**Section 7.1.1**) and the influence of the global shape and size on the spatial temperature, moisture content as well as quality distributions during roasting evaluated.

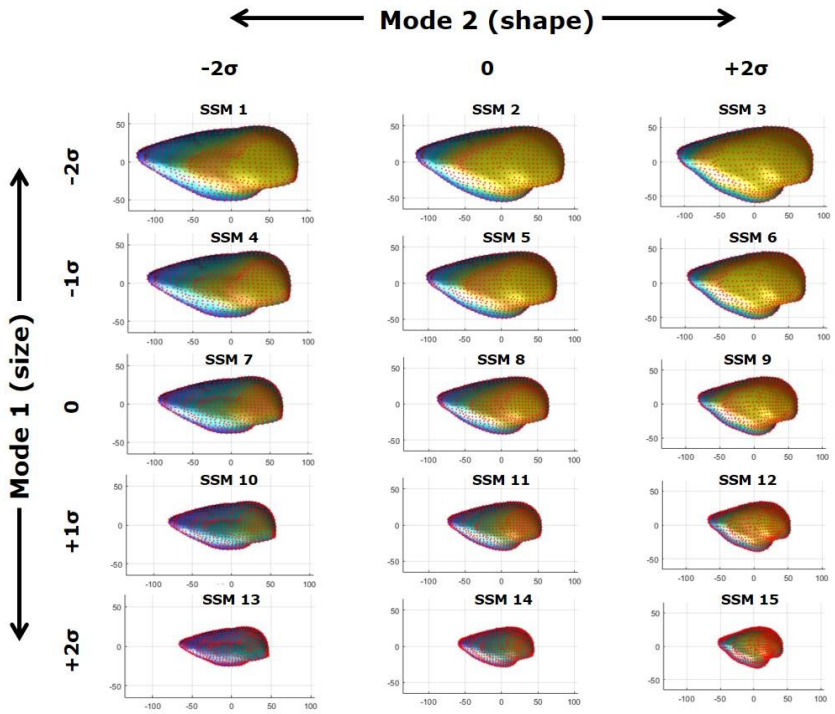

Figure 9: Top views of the two first modes of variations (mode 1 and mode 2) of the developed chicken breast shape model, plus/ minus one (±1σ) and two standard deviations (±2σ) for the first mode and plus/ minus two standard deviations (±2σ) for the second mode. Red points show the landmarks and the color represents the height of the 3D geometry.

We found that both the size and global shape of the chicken breast fillet has a considerable influence on the roasting time to reach 75°C in the core with up to 55% longer or shorter times. Thus, it is crucial for the chef or operator to take the natural variation of chicken breast fillets into account to ensure the safety for the consumer. The combination of the SSM with the mechanistic model showed that it is mainly the height of the chicken breast fillet, which determines the time to reach the safe core temperature. This correlation can be valuable for the user as it gives a direct measurable parameter for fast predictions of the required roasting time.

Moreover, the natural size and global shape variation had a major impact on the texture and color of the roasted chicken breast meat. We found that both the size and global shape variations resulted in up to 30% lower hardness values and, accordingly, a considerable softer texture compared to a standard chicken breast fillet. Moreover, the surface of the chicken breast fillets were up to 21% darker or lighter than the

standard chicken breast fillet which could have a direct impact on the acceptance by the consumer (Guerrero-Legarreta and Hui, 2010).

The result clearly show that the actual irregular geometry of chicken breast meat, but in general of food products, should be implemented in the model development process to obtain accurate, comparable and realistic model predictions. 3D scanning allows a fast and non-destructive acquisition of the irregular food geometry without the need of preliminary training or specific knowledge. Consequently, it can help the modelling community in the development of even more realistic models of food processing. Statistical shape modelling, which is already used widely in other disciplines such as medical image analysis, can then be used to obtain a detailed knowledge about the natural variation of the food geometry. Combined with mechanistic models of heat and mass transfer, it can give the user a quantitative knowledge about impact of the shape and size variations on the final quality of the food product.

8 Conclusions and perspectives

In my PhD project, I have established a combined kinetic and mechanistic modelling approach for the convective roasting of chicken breast meat to study the influence of the heating process on the spatial quality changes. We found that the coupling of kinetic and mechanistic models enables a quantitative understanding of the link between the temperature and moisture content development during heating and the resulting spatial quality changes (i.e. texture or color). The convective roasting of chicken breast meat results in a non-uniform temperature and moisture content distributions. Subsequently, a non-uniform texture and color profile inside the chicken breast is achieved, which could have an influence on the consumer's acceptance. With the combined modelling approach, the direct impact of the process parameters on the non-uniform quality distribution can be assessed. Accordingly, it allows the user to make quantitative decisions for the process settings and optimize them accordingly.

The roasting of chicken breast meat is a complex process, which results in certain uncertainties in the model development process (e.g. input parameters or model formulations). By implementing global uncertainty and sensitivity analysis in the modeling process, we identified the most influential input parameters as well as determined correlations between parameters. Subsequently, an even deeper understanding of the physical phenomena that lead to the quality changes was obtained. Furthermore, we found that the sampling method had a direct impact on the convergence of the Monte Carlo method and, consequently, on the required time for the analysis. The comparison of two sensitivity analysis additionally showed that the Morris screening is more efficient computational wise compared to the standardized regression coefficient method. Thus, the choice of the computationally best sampling and sensitivity analysis method could help to make global uncertainty and sensitivity analysis also applicable for computational even heavier models. This could lead to a better acceptance and application of the analysis methods in the field of food process modelling.

Additionally, our results highlight the importance of the food geometry and its natural diversity on the spatial variations in both the state variables (temperature and moisture

content) as well as quality attributes (texture and color). Thus, geometry sensitivity analysis should be integrated into future model development processes to decrease further the model formulation error (see **Chapter 4**) and to ensure the accuracy of the model predictions.

Overall, the developed model in this PhD project can be used as a decision making tool in order to optimize the heating process of chicken breast meat. Furthermore, the model allows the performance of what-if scenarios, reducing the time that is needed for expensive lab work. This can also speed up the whole product and process development procedure, which could lead to highly intelligent food process systems.

As the model is based on fundamental physical laws it can be extended relatively fast to other meat products. The physical framework as developed for the roasting of chicken breast meat would stay the same and only the property parameters of the corresponding meat product, such as the water holding capacity, storage modulus or initial composition, need to be adopted. Consequently, the overall model development process can be reduced and the application of the established model widened.

However, the established model is not applicable for process control purposes (Figure 1), as the computational time of it is relatively long. Therefore, model reduction is necessary to speed up the model without losing essential information. This could be done by combining the established mechanistic model with machine learning algorithms, such as neutral networks. In this way, the computationally heavy mechanistic model could be used to train the neural network by running different combinations of parameters. Afterwards, the established neural network could be directly applied to control the heating process.

Finally, the following model adjustments are suggested, in order to increase the accuracy of the established model of chicken meat roasting:

1) *Permeability changes during the heating process*

   The permeability of meat products is an important parameter for the moisture transport (see **Publication 3**). During the heating process, protein denaturation as well as moisture loss leads to tremendous microstructural changes, which results in an increase or decrease of the local permeability (Feyissa et al.,

2013). Therefore, the variation of the permeability as function of for example the temperature and/ or moisture content should implemented.

2) *Shrinkage of the chicken breast meat during heating*

The shrinkage of chicken breast meat during the roasting process should be included into the established model. 3D scanning would be one possibility to assess the not only the volume changes, but also the changes in height, width, length or surface are. Preliminary trials showed that chicken breast meat is shrinking in both the width and length, while an increase in height was observed. The coupling of the shrinkage phenomena with the pressure driven flow inside the chicken meat as well as the texture changes could lead to more realistic model predictions and possibly also to a reduction of fitting parameters.

References

Atkins, P., de Paula, J., 2014. Atkins' Physical Chemistry, 10th revis. ed. Oxford University Press.

Balsa-Canto, E., Alonso, A.A., Arias-Méndez, A., García, M.R., López-Núñez, A., Mosquera-Fernández, M., Vázquez, C., Vilas, C., 2016. Modeling and Optimization Techniques with Applications in Food Processes, Bio-processes and Bio-systems, in: Higueras, I., Roldán, T., Torrens, J.J. (Eds.), Numerical Simulation in Physics and Engineering, SEMA SIMAI, Volume 9. Springer International Publishing, pp. 187–216. https://doi.org/10.1007/978-3-319-32146-2_4

Barbanti, D., Pasquini, M., 2005. Influence of cooking conditions on cooking loss and tenderness of raw and marinated chicken breast meat. LWT - Food Sci. Technol. 38, 895–901. https://doi.org/10.1016/j.lwt.2004.08.017

Bernardini, F., Rushmeier, H., 2002. The 3D model acquisition pipeline. Comput. Graph. Forum 21, 149–172. https://doi.org/10.1111/1467-8659.00574

Bird, R.B., Stewart, W.E., Lightfoot, E.N., 2006. Transport Phenomena, 2nd Editio. ed. John Wiley & Sons, Inc.

Blikra, M.J., Skipnes, D., Feyissa, A.H., 2019. Model for heat and mass transport during cooking of cod loin in a convection oven. Food Control 102, 29–37. https://doi.org/10.1016/j.foodcont.2019.03.001

Bourne, M.C., 2002. Food texture and viscosity : concept and measurement, 2nd Editio. ed. Academic Press.

Broyart, B., Trystram, G., Duquenoy, A., 1998. Predicting colour kinetics during cracker baking. J. Food Eng. 35, 351–368. https://doi.org/10.1016/S0260-8774(98)00021-1

Bruse, J.L., McLeod, K., Biglino, G., Ntsinjana, H.N., Capelli, C., Hsia, T.Y., Sermesant, M., Pennec, X., Taylor, A.M., Schievano, S., Taylor, A., Giardini, A., Khambadkone, S., de Leval, M., Bove, E., Dorfman, A., Baker, G.H., Hlavacek,

A., Migliavacca, F., Pennati, G., Dubini, G., Marsden, A., Vignon-Clementel, I., Figliola, R., McGregor, J., 2016. A statistical shape modelling framework to extract 3D shape biomarkers from medical imaging data: Assessing arch morphology of repaired coarctation of the aorta. BMC Med. Imaging 16, 1–19. https://doi.org/10.1186/s12880-016-0142-z

Chaskalovic, J., 2008. Finite Element Methods for Engineering Sciences. Springer Berlin Heidelberg, Berlin, Heidelberg. https://doi.org/10.1007/978-3-540-76343-7

Chhabra, R.P., 2017. CRC Handbook of Thermal Engineering, 2nd Editio. ed. CRC Press, Second edition. | Boca Raton : Taylor & Francis, CRC Press, 2017., CRC Press, 2017. https://doi.org/10.4324/9781315119717

Choi, Y., Okos, M.R., 1986. Effects of temperature and composition on the thermal properties of foods. Food Eng. Process Appl. 93–101.

Cignoni, P., Callieri, M., Corsini, M., Dellepiane, M., Ganovelli, F., Ranzuglia, G., 2008. MeshLab: an Open-Source Mesh Processing Tool, in: Sixth Eurographics Italian Chapter Conference.

Cootes, T.F., Taylor, C.J., Cooper, D.H., Graham, J., 1995. Active Shape Models-Their Training and Application. Comput. Vis. Image Underst. 61, 38–59.

Czitrom, V., 1999. One-Factor-at a Tim Versus Designed Experiments. Am. Stat. 53, 126–131. https://doi.org/10.2307/2685731

Dalal, P., Munsell, B.C., Wang, S., Tang, J., Oliver, K., Ninomiya, H., Zhou, X., Fujita, H., 2007. A fast 3D correspondence method for statistical shape modeling. Proc. IEEE Comput. Soc. Conf. Comput. Vis. Pattern Recognit. https://doi.org/10.1109/CVPR.2007.383143

Danckaers, F., Huysmans, T., Dael, M. Van, Verboven, P., Nicolaï, B., Sijbers, J., 2017. Building 3D Statistical Shape Models of Horticultural Products. Food Bioprocess Technol. 10, 2100–2112. https://doi.org/10.1007/s11947-017-1979-z

Danckaers, F., Huysmans, T., Dael, M. Van, Verboven, P., Sijbers, J., 2015. Building a Statistical Shape Model of the Apple from Corresponded Surfaces. Chem. Eng. Trans. 44.

Datta, A.K., 2015. Toward Computer-Aided Food Engineering: Mechanistic Frameworks for Evolution of Product, Quality and Safety During Processing. J. Food Eng. 176, 9–27. https://doi.org/10.1016/j.jfoodeng.2015.10.010

Datta, A.K., 2008. Status of Physics-Based Models in the Design of Food Products, Processes, and Equipment. Compr. Rev. Food Sci. Food Saf. 7, 121–129. https://doi.org/10.1111/j.1541-4337.2007.00030.x

Datta, A.K., 2006. Hydraulic Permeability of Food Tissues. Int. J. Food Prop. 9, 767–780. https://doi.org/10.1080/10942910600596167

Defraeye, T., Blocken, B., Carmeliet, J., 2013. Influence of uncertainty in heat-moisture transport properties on convective drying of porous materials by numerical modelling. Chem. Eng. Res. Des. 91, 36–42. https://doi.org/10.1016/j.cherd.2012.06.011

Dimov, I., Georgieva, R., 2010. Monte Carlo algorithms for evaluating Sobol' sensitivity indices. Math. Comput. Simul. 81, 506–514. https://doi.org/10.1016/j.matcom.2009.09.005

Dryden, I.L., Mardia, K. V., 1998. Statistical Shape Analysis. John Wiley.

Erdogdu, F., Sarghini, F., Marra, F., 2017. Mathematical Modeling for Virtualization in Food Processing. Food Eng. Rev. 9, 295–313. https://doi.org/10.1007/s12393-017-9161-y

Fabbri, A., Cevoli, C., Alessandrini, L., Romani, S., 2011. Numerical modeling of heat and mass transfer during coffee roasting process. J. Food Eng. 105, 264–269. https://doi.org/10.1016/j.jfoodeng.2011.02.030

Feyissa, A.H., 2011. Robust Modelling of Heat and Mass Transfer in Processing of Solid Foods.

Feyissa, A.H., Gernaey, K. V., Adler-Nissen, J., 2013. 3D modelling of coupled mass and heat transfer of a convection-oven roasting process. Meat Sci. 93, 810–820. https://doi.org/10.1016/j.meatsci.2012.12.003

Feyissa, A.H., Gernaey, K. V., Adler-Nissen, J., 2012. Uncertainty and sensitivity analysis: Mathematical model of coupled heat and mass transfer for a contact

baking process. J. Food Eng. 109, 281–290. https://doi.org/10.1016/j.jfoodeng.2011.09.012

Fuessinger, M.A., Schwarz, S., Cornelius, C.P., Metzger, M.C., Ellis, E., Probst, F., Semper-Hogg, W., Gass, M., Schlager, S., 2018. Planning of skull reconstruction based on a statistical shape model combined with geometric morphometrics. Int. J. Comput. Assist. Radiol. Surg. 13, 519–529. https://doi.org/10.1007/s11548-017-1674-6

Godsalve, E.W., Davis, E.A., Gordon, J., Davis, H.T., 1977. Water Loss Rates and Temperature Profiles of Dry Cooked Bovine Muscle. J. Food Sci. 42, 1038–1045. https://doi.org/10.1111/j.1365-2621.1977.tb12662.x

Goñi, S.M., Purlis, E., 2010. Geometric modelling of heterogeneous and complex foods. J. Food Eng. 97, 547–554. https://doi.org/10.1016/j.jfoodeng.2009.11.017

Goñi, S.M., Purlis, E., Salvadori, V.O., 2008. Geometry modelling of food materials from magnetic resonance imaging. J. Food Eng. 88, 561–567. https://doi.org/10.1016/j.jfoodeng.2008.03.020

Goñi, S.M., Purlis, E., Salvadori, V.O., 2007. Three-dimensional reconstruction of irregular foodstuffs. J. Food Eng. 82, 536–547. https://doi.org/10.1016/j.jfoodeng.2007.03.021

Goñi, S.M., Salvadori, V.O., 2010. Prediction of cooking times and weight losses during meat roasting. J. Food Eng. 100, 1–11. https://doi.org/10.1016/j.jfoodeng.2010.03.016

Guerrero-Legarreta, I., Hui, Y.H., 2010. Handbook of Poultry Science and Technology, Volume 2: ed. John Wiley & Sons, Inc. https://doi.org/10.1002/9780470504475

Gulati, T., Datta, A.K., 2016. Coupled multiphase transport, large deformation and phase transition during rice puffing. Chem. Eng. Sci. 139, 75–98. https://doi.org/10.1016/j.ces.2015.08.057

Gulati, T., Datta, A.K., 2013. Enabling computer-aided food process engineering: Property estimation equations for transport phenomena-based models. J. Food Eng. 116, 483–504. https://doi.org/10.1016/j.jfoodeng.2012.12.016

Haefner, J.W., 2005. Models of Systems, in: Modeling Biological Systems. Springer, Boston, MA, pp. 3–16. https://doi.org/10.1007/0-387-25012-3_1

Hahn, D.W., Özisik, M.N., 2012. Heat Conduction. John Wiley & Sons.

Halder, A., Datta, A.K., Geedipalli, S.S.R., 2007. Uncertainty in thermal process calculations due to variability in first-order and Weibull kinetic parameters. J. Food Sci. 72. https://doi.org/10.1111/j.1750-3841.2007.00329.x

Halder, A., Dhall, A., Datta, A.K., 2011. Modeling Transport in Porous Media With Phase Change: Applications to Food Processing. J. Heat Transfer 133, 031010. https://doi.org/10.1115/1.4002463

Hargin, K.D., 1996. Authenticity issues in meat and meat products. Meat Sci. 43, 277–289. https://doi.org/10.1016/0309-1740(96)00072-1

Helton, J.C., 1993. Uncertainty and sensitivity analysis techniques for use in performance assessment for radioactive waste disposal. Reliab. Eng. Syst. Saf. 42, 327–367.

Helton, J.C., Davis, F.J., 2003. Latin hypercube sampling and the propagation of uncertainty in analyses of complex systems. Reliab. Eng. Syst. Saf. 81, 23–69. https://doi.org/10.1016/S0951-8320(03)00058-9

Isleroglu, H., Kaymak-Ertekin, F., 2016. Modelling of heat and mass transfer during cooking in steam-assisted hybrid oven. J. Food Eng. 181, 50–58. https://doi.org/10.1016/j.jfoodeng.2016.02.027

Ivester, R.W., 2008. Productivity improvement through modeling: An overview of manufacturing experience for the food industry. Compr. Rev. Food Sci. Food Saf. 7, 182–191. https://doi.org/10.1111/j.1541-4337.2007.00035.x

Jancsók, P.T., Clijmans, L., Nicolaï, B.M., De Baerdemaeker, J., 2001. Investigation of the effect of shape on the acoustic response of “conference” pears by finite element modelling. Postharvest Biol. Technol. 23, 1–12. https://doi.org/10.1016/S0925-5214(01)00098-9

Jha, S.N., 2005. Mathematical simulation of roasting of grain. J. Food Eng. 71, 304–310. https://doi.org/10.1016/j.jfoodeng.2005.03.006

Jobe, B., Rattan, N.S., Ramaswamy, H.S., 2016. Kinetics of Quality Attributes of Potato Particulates during Cooking Process. Int. J. Food Eng. 12, 27–35. https://doi.org/10.1515/ijfe-2014-0341

Jousse, F., 2008. Modeling to improve the efficiency of product and process development. Compr. Rev. Food Sci. Food Saf. 7, 175–181. https://doi.org/10.1111/j.1541-4337.2007.00033.x

King, N.J., Whyte, R., 2006. Does it look cooked? A review of factors that influence cooked meat color. J. Food Sci. 71, 31–40. https://doi.org/10.1111/j.1750-3841.2006.00029.x

Kondjoyan, A., Portanguen, S., 2008. Prediction of surface and “under surface” temperatures on poultry muscles and poultry skins subjected to jets of superheated steam. Food Res. Int. 41, 16–30. https://doi.org/10.1016/j.foodres.2007.07.006

Kong, F., Tang, J., Rasco, B., Crapo, C., 2007. Kinetics of salmon quality changes during thermal processing. J. Food Eng. 83, 510–520. https://doi.org/10.1016/j.jfoodeng.2007.04.002

Kumar, C., Joardder, M.U.H., Farrell, T.W., Karim, M.A., 2016. Multiphase porous media model for intermittent microwave convective drying (IMCD) of food. Int. J. Therm. Sci. 104, 304–314. https://doi.org/10.1016/j.ijthermalsci.2016.01.018

Lawrie, R.A., Ledward, D.A., 2006. Lawrie’s meat science, 7th Editio. ed. Woodhead Publishing.

Ling, B., Tang, J., Kong, F., Mitcham, E.J., Wang, S., 2015. Kinetics of Food Quality Changes During Thermal Processing: a Review. Food Bioprocess Technol. 8, 343–358. https://doi.org/10.1007/s11947-014-1398-3

Liu, S., Fukuoka, M., Sakai, N., 2013. A finite element model for simulating temperature distributions in rotating food during microwave heating. J. Food Eng. 115, 49–62. https://doi.org/10.1016/j.jfoodeng.2012.09.019

Llave, Y., Takemori, K., Fukuoka, M., Takemori, T., Tomita, H., Sakai, N., 2016. Mathematical modeling of shrinkage deformation in eggplant undergoing

simultaneous heat and mass transfer during convection-oven roasting. J. Food Eng. 178, 124–136. https://doi.org/10.1016/j.jfoodeng.2016.01.013

Lucas, T., Doursat, C., Grenier, D., Wagner, M., Trystram, G., Flick, D., 2015. Modeling of bread baking with a new, multi-scale formulation of evaporation-condensation-diffusion and evidence of compression in the outskirts of the crumb. J. Food Eng. 149, 24–37. https://doi.org/10.1016/j.jfoodeng.2014.07.020

Mabrouk, S. Ben, Benali, E., Oueslati, H., 2012. Experimental study and numerical modelling of drying characteristics of apple slices. Food Bioprod. Process. 90, 719–728. https://doi.org/10.1016/j.fbp.2012.02.001

Matsuda, H., Llave, Y., Fukuoka, M., Sakai, N., 2013. Color changes in fish during grilling-Influences of heat transfer and heating medium on browning color. J. Food Eng. 116, 130–137. https://doi.org/10.1016/j.jfoodeng.2012.11.027

Metropolis, N., Source, S.U., 1949. The Monte Carlo Method. J. Am. Stat. Assoc. 44.

Mondal, A., Datta, A.K., 2010. Two-dimensional CFD modeling and simulation of crustless bread baking process. J. Food Eng. 99, 166–174. https://doi.org/10.1016/j.jfoodeng.2010.02.015

Morris, M.D., 1991. Factorial Samplig Plans for Preliminary Computational Experiments. Technometrics 33.

Nakamura, M., Mao, W., Fukuoka, M., Sakai, N., 2011. Analysis of the Color Change in Fish during the Grilling Process. Food Sci. Technol. Res. 17, 471–478. https://doi.org/10.3136/fstr.17.471

Ngadi, M., Dirani, K., Oluka, S., 2006. Mass Transfer Characteristics of Chicken Nuggets. Int. J. Food Eng. 2. https://doi.org/10.2202/1556-3758.1071

Nicolas, V., Glouannec, P., Ploteau, J.P., Salagnac, P., Jury, V., 2017. Experiment and multiphysic simulation of dough baking by convection, infrared radiation and direct conduction. Int. J. Therm. Sci. 115, 65–78. https://doi.org/10.1016/j.ijthermalsci.2017.01.018

OECD, 2020. Meat consumption (indicator) [WWW Document]. https://doi.org//10.1787/fa290fd0-en

Ousegui, A., Moresoli, C., Dostie, M., Marcos, B., 2010. Porous multiphase approach for baking process - Explicit formulation of evaporation rate. J. Food Eng. 100, 535–544. https://doi.org/10.1016/j.jfoodeng.2010.05.003

Ovissipour, M., Rasco, B., Tang, J., Sablani, S.S., 2013. Kinetics of quality changes in whole blue mussel (Mytilus edulis) during pasteurization. Food Res. Int. 53, 141–148. https://doi.org/10.1016/j.foodres.2013.04.029

Peleg, M., Engel, R., Gonzalez-Martinez, C., Corradini, M.G., 2002. Non-Arrhenius and non-WLF kinetics in food systems. J. Sci. Food Agric. 82, 1346–1355. https://doi.org/10.1002/jsfa.1175

Purlis, E., Salvadori, V.O., 2009a. Modelling the browning of bread during baking. Food Res. Int. 42, 865–870. https://doi.org/10.1016/j.foodres.2009.03.007

Purlis, E., Salvadori, V.O., 2009b. Bread baking as a moving boundary problem. Part 2: Model validation and numerical simulation. J. Food Eng. 91, 434–442. https://doi.org/10.1016/j.jfoodeng.2008.09.038

Rabeler, F., Feyissa, A.H., 2018a. Kinetic Modeling of Texture and Color Changes During Thermal Treatment of Chicken Breast Meat. Food Bioprocess Technol. 11, 1495–1504. https://doi.org/10.1007/s11947-018-2123-4

Rabeler, F., Feyissa, A.H., 2018b. Modelling the transport phenomena and texture changes of chicken breast meat during the roasting in a convective oven. J. Food Eng. 237, 60–68. https://doi.org/10.1016/j.jfoodeng.2018.05.021

Rabeler, F., Skytte, J.L., Feyissa, A.H., 2019. Prediction of thermal induced color changes of chicken breast meat during convective roasting: A combined mechanistic and kinetic modelling approach. Food Control 104, 42–49. https://doi.org/10.1016/j.foodcont.2019.04.018

Rakesh, V., Datta, A.K., Walton, J.H., Mccarthy, K.L., Mccarthy, M.J., 2012. Microwave Combination Heating : Coupled Electromagnetics- Multiphase Porous Media Modeling and MRI Experimentation 58. https://doi.org/10.1002/aic

Rao, M.A., Rizvi, S.S.H., Datta, A.K., Ahmed, J. (Eds.), 2014. Engineering Properties of Foods, 4th Editio. ed. CRC Press. https://doi.org/10.1201/b16897

Rinaldi, M., Cordioli, M., Barbanti, D., 2017. Investigation on temperature fields in industrial chilling of pork legs for PDO Parma ham production and coupled temperature/microbial growth simulation. J. Food Sci. Technol. 54, 18–25. https://doi.org/10.1007/s13197-016-2397-3

Rizvi, a F., Tong, C.H., 1997. Fractional Conversion for Determining Texture Degradation Kinetics of Vegetables. J. Food Sci. 62, 1–7. https://doi.org/10.1111/j.1365-2621.1997.tb04356.x

Sablani, S.S., 2008. Status of observational models used in design and control of products and processes. Compr. Rev. Food Sci. Food Saf. 7, 130–136. https://doi.org/10.1111/j.1541-4337.2007.00031.x

Saguy, I., Karel, M., 1980. Modeling of quality deterioration during food-processing and storage. Food Technol. 78–85.

Sakin-Yilmazer, M., Kaymak-Ertekin, F., Ilicali, C., 2012. Modeling of simultaneous heat and mass transfer during convective oven ring cake baking. J. Food Eng. 111, 289–298. https://doi.org/10.1016/j.jfoodeng.2012.02.020

Saltelli, A., Annoni, P., Azzini, I., Campolongo, F., Ratto, M., Tarantola, S., 2010. Variance based sensitivity analysis of model output. Design and estimator for the total sensitivity index. Comput. Phys. Commun. 181, 259–270. https://doi.org/10.1016/j.cpc.2009.09.018

Saltelli, A., Ratto, M., Andres, T., Campolongo, F., Cariboni, J., Gatelli, D., Saisana, M., Tarantola, S., 2007. Global Sensitivity Analysis. The Primer. John Wiley & Sons, Ltd, Chichester, UK. https://doi.org/10.1002/9780470725184

Saltelli, A., Tarantola, S., Campolongo, F., 2000. Sensitivity analysis as an ingredient of modeling. Stat. Sci. 15, 377–395. https://doi.org/10.1214/ss/1009213004

Schoeman, L., Williams, P., du Plessis, A., Manley, M., 2016. X-ray micro-computed tomography (μCT) for non-destructive characterisation of food microstructure. Trends Food Sci. Technol. 47, 10–24. https://doi.org/10.1016/j.tifs.2015.10.016

Sin, G., Gernaey, K. V., Lantz, A.E., 2009. Good Modeling Practice for PAT Applications : Propagation of Input Uncertainty and Sensitivity Analysis.

Biotechnol. Prog. 1–12. https://doi.org/10.1021/bp.166

Siripon, K., Tansakul, A., Mittal, G.S., 2007. Heat transfer modeling of chicken cooking in hot water. Food Res. Int. 40, 923–930. https://doi.org/10.1016/j.foodres.2007.03.005

Sobol, I.M., Kucherenko, S., 2009. Derivative based global sensitivity measures and their link with global sensitivity indices. Math. Comput. Simul. 79, 3009–3017. https://doi.org/10.1016/j.matcom.2009.01.023

Tanaka, F., Maeda, Y., Uchino, T., Hamanaka, D., Atungulu, G.G., 2008. Monte Carlo simulation of the collective behavior of food particles in pneumatic drying operation. LWT - Food Sci. Technol. 41, 1567–1574. https://doi.org/10.1016/j.lwt.2007.10.020

Thussu, S., Datta, A.K., 2012. Texture prediction during deep frying: A mechanistic approach. J. Food Eng. 108, 111–121. https://doi.org/10.1016/j.jfoodeng.2011.07.017

Tornberg, E., 2005. Effects of heat on meat proteins - Implications on structure and quality of meat products. Meat Sci. 70, 493–508. https://doi.org/10.1016/j.meatsci.2004.11.021

Trystram, G., 2012. Modelling of food and food processes. J. Food Eng. 110, 269–277. https://doi.org/10.1016/j.jfoodeng.2011.05.001

Uyar, R., Erdoğdu, F., 2009. Potential use of 3-dimensional scanners for food process modeling. J. Food Eng. 93, 337–343. https://doi.org/10.1016/j.jfoodeng.2009.01.034

Van Boekel, M.A.J.S., 2008. Kinetic Modeling of Food Quality: A Critical Review. Compr. Rev. Food Sci. Food Saf. 7, 144–158. https://doi.org/10.1111/j.1541-4337.2007.00036.x

Van Boekel, M.A.J.S., 1996. Statistical aspects of kinetic modeling for food science problems. J. Food Sci. 61, 477–485. https://doi.org/10.1111/j.1365-2621.1996.tb13138.x

van der Sman, R.G.M., 2013. Modeling cooking of chicken meat in industrial tunnel

ovens with the Flory-Rehner theory. Meat Sci. 95, 940–957. https://doi.org/10.1016/j.meatsci.2013.03.027

van der Sman, R.G.M., 2007. Moisture transport during cooking of meat: An analysis based on Flory-Rehner theory. Meat Sci. 76, 730–738. https://doi.org/10.1016/j.meatsci.2007.02.014

van der Sman, R.G.M., Paudel, E., Voda, A., Khalloufi, S., 2013. Hydration properties of vegetable foods explained by Flory-Rehner theory. Food Res. Int. 54, 804–811. https://doi.org/10.1016/j.foodres.2013.08.032

Warning, A., Verboven, P., Nicolaï, B., Van Dalen, G., Datta, A.K., 2014. Computation of mass transport properties of apple and rice from X-ray microtomography images. Innov. Food Sci. Emerg. Technol. 24, 14–27. https://doi.org/10.1016/j.ifset.2013.12.017

Wattanachant, S., Benjakul, S., Ledward, D.A., 2005. Effect of heat treatment on changes in texture, structure and properties of Thai indigenous chicken muscle. Food Chem. 93, 337–348. https://doi.org/10.1016/j.foodchem.2004.09.032

Wedzicha, B., Roberts, C., 2006. Modelling: a new solution to old problems in the food industry. Food Manuf. Effic. 1, 1–7. https://doi.org/10.1616/1750-2683.0001

Zhang, J., Datta, A.K., 2006. Mathematical modeling of bread baking process. J. Food Eng. 75, 78–89. https://doi.org/10.1016/j.jfoodeng.2005.03.058

Zhu, H., Gulati, T., Datta, A.K., Huang, K., 2015. Microwave drying of spheres: Coupled electromagnetics-multiphase transport modeling with experimentation. Part I: Model development and experimental methodology. Food Bioprod. Process. 96, 314–325. https://doi.org/10.1016/j.fbp.2015.08.003

Technical University of Denmark

National Food Institute
Søltofts Plads, Building 227
2800 Kgs. Lyngby

www.food.dtu.dk